MECHANISTIC STUDIES OF REPLICATION FORK REMODELING BY DNA TRANSLOCASES

By

Garrett Mason Warren

Dissertation

Submitted to the Faculty of the

Graduate School of Vanderbilt University

in partial fulfillment of the requirements

for the degree of

DOCTOR OF PHILOSOPHY

In

Biological Sciences

May 31, 2019

Nashville, Tennessee

Approved:

Brandt F. Eichman, Ph.D.

Todd R. Graham, Ph.D.

Lauren Parker Jackson, Ph.D.

Walter J, Chazin, Ph.D.

David Cortez, Ph.D.

For my best friend and wife Lee M. Conell

and for my parents Sarah H. Warren,

Timothy W. Warren, and my sister Erin G. Warren

ACKNOWLEDGEMENTS

This research was made possible in part by the Vanderbilt Training Program in Environmental Toxicology (NIH T32ES07028).

I would like to thank my mentor, Dr. Brandt Eichman, for his mentorship, bike-related banter, and dedication of time to my many musings on PDB files. It was invaluable to have a mentor who listens and allows graduate students to pursue their wild ideas. I would also like to thank my committee members Dr. Todd Graham, Dr. Lauren Jackson, Dr. Walter Chazin, and Dr. David Cortez for your time, ideas, and helping me to develop and mature as a scientist.

To the Eichman lab, I never thought that most of my friends in Nashville would be found in one place day after day. I appreciate the many structural biology, DNA repair, and non-scientific conversations and laughs that have molded my graduate school experience. I think it goes without saying but thank you to Bri and Elwood for your mentorship and putting up with me for all of these years. To all members of the Eichman lab past and present I would like to express my gratitude for the atmosphere that I was fortunate to be a part of.

I would also like to thank my parents Sarah Warren and Timothy Warren. I would not be here without you. You have taught me so much, my love of science and the outdoors stems directly from you. Thank you for always encouraging my independence. Thank you to my sister Erin Warren for your support and your bravery that inspire me.

Most of all I want to express my deepest thanks to my friendship loyalty pact partner, reading partner, reality TV analysis partner, nature observation partner, and wife

Lee M. Conell. Somehow you keep me sane! Your engagement with the world through writing has been such an inspiration to me. May we always squeeze out the toothpaste. We met at a Halloween party in October of 2013 and the party continues everyday. Thank you for supporting me and my anxious, obsessive, time consuming career choice.

TABLE OF CONTENTS

LIST OF TABLES

Table Page

LIST OF FIGURES

LIST OF ABBREVIATIONS

APIM	ALKB homolog 2 PCNA interaction motif
ATM	Ataxia telangiectasia mutated
ATP	Adenosine triphosphate
ATPase	ATP hydrolysis
ATR	Ataxia telangiectasia mutated and Rad3-related
ATRIP	ATR-interacting protein
BER	Base excision repair
BLM	Bloom syndrome protein
CDC25	Cell division cycle 25
CDK	Cyclin dependent kinase
CHK1	Checkpoint kinase 1
CPT	Camptothecin
CRISPR	Clustered regularly interspaced short palindromic repeats
CtIP	CtBP (C-terminal binding protein) interacting protein
DBD	DNA binding domain
DEER	double electron electron resonance
DSB	Double stranded break
DTT	Dithiothreitol
E3	Ubiquitin ligase complex
EDTA	Ethylenediaminetetraacetic acid
EMSA	Electrophorectic mobility shift assay

EPR	Electron paramagnetic resonance
G2	Gap 2 phase
GINS	Go, Ichi, Ni, and San complex
HARP	HepA-related protein
HIRAN	HIP116, RAD5P N-terminal domain
HLTF	Helicase like transcription factor
HNH	Histidine-asparagine-histidine endonuclease domain
HP1	HARP 1 domain
HP2	HARP2 domain
HU	Hydroxyurea
ICL	Interstarnd crosslink
ISWI	Imitation SWI
MCM	Mini-chromosome maintenance
MMS	Methyl-methanesulphonate
MMR	Mismatch repair
MOT1	Modifier of transcription 1
MRD	Mismatch recognition domain
MRN	MRE11-RAD50-NBS1
MTSL	[1-oxy-2,2,5,5-tetramethyl-pyrolline-3-methyl]-methanethiosulfonate
MUS81	MUS81 structure-specific endonuclease subunit
NER	Nucleotide excision repair
NTA	Nitrilotriacetic acid
NZF	NPL4 zinc finger motif

OB	Oligonucleotide/oligosaccharide binding domain
PCNA	Proliferating cell nuclear antigen
PIP box	PCNA interacting protein box motif
POL α-Primase	Polymerase alpha- primase complex
POL δ	Polymerase delta (B-family)
POL ε	Polymerase epsilon (B-family)
RBM	RPA binding motif
RecA	Recombinase A
RecG	Recombination-deficient G
RING	Really interesting new gene
RPA	Replication protein A
SF2	Super family 2
SHPRH	SF2 histone linker PHD RING helicase
SMARCAL1	SWI/SNF related, matrix associated, actin dependent regulator of chromatin, subfamily a-like 1
SNF2	Sucrose non-fermenting 2
SRD	Substrate recognition domain
SSC	Saline sodium citrate
TBE	Tris/Borate/EDTA buffer
TCEP	Tris(2-carboxyethyl)phosphine
TRG	Translocation in RecG
UBC13	Ubiquitin conjugating 13
UV	Ultraviolet radiation

UvsW	UV sensitive W
XPD	Xeroderma pigmentosum, complementation group D, ERCC2
ZRANB3	Zinc finger, RAN-binding domain containing 3

CHAPTER I

INTRODUCTION

The complete and accurate duplication of genetic information is required for the survival of all living organisms. The replisome, a multi-protein complex, replicates DNA at the replication fork to produce two new daughter molecules of DNA from a single original parental DNA molecule. The two new daughter DNA molecules are then propagated to two new daughter cells upon cell division. DNA replication in both prokaryotes and eukaryotes (**Figure 1.1**) requires several essential activities. A DNA helicase separates the parental DNA molecule. DNA primase synthesizes short oligo-ribonucleotide primers for initiating the discontinuous synthesis of Okazaki fragments on the lagging strand and less frequently for initiation of leading strand synthesis. DNA polymerases access the DNA template for leading and lagging strand synthesis. Single stranded DNA binding proteins are required to protect the exposed parental ssDNA and recruit other proteins to the replication fork. During eukaryotic replication histones are removed ahead of the replisome and replaced behind the replisome. The genome is stable when all of these activities are working in concert and there is no exogenous or endogenous damage, blockage, or mis-incorporation.

When the replisome encounters various forms of DNA replication stress it can lead to genome instability or cell death. Genome instability results from inaccurate replication of the parental DNA, over-replication, incomplete replication, or genome rearrangements and consequently can lead to carcinogenesis. To alleviate genome instability and prevent

carcinogenesis and cell death there are multiple pathways to preserve genome stability during replication. Furthermore, nucleotide excision repair (NER), base excision repair (BER), and DNA mismatch repair (MMR) pathways survey the genome to remove and repair DNA damage as it occurs, however, there are still scenarios where the replisome experiences DNA replication stress.

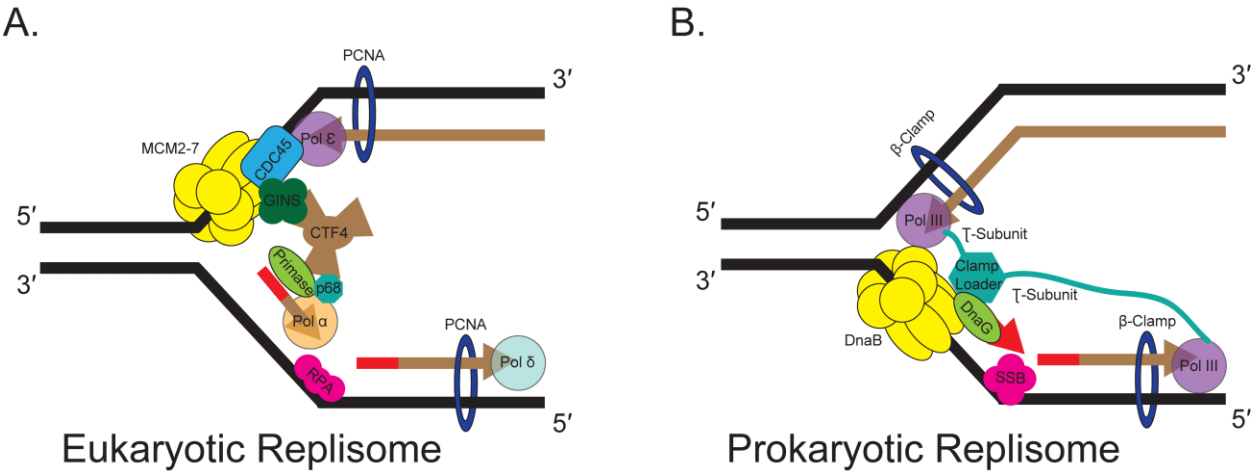

Figure 1.1 Replisome components in eukaryotes and prokaryotes. A. Schematic of replisome proteins for eukaryotic DNA replication. **B.** Schematic of replisome proteins in prokaryotic replication.

Types of DNA Replication Stress

During DNA replication the replisome encounters myriad forms of stress inducing agents ranging from modified DNA bases, collisions with transcription, tightly bound proteins, cross-links, and depleted nucleotide pools (**Figure 1.2**). Encounters with DNA replication stress causing agents can lead to replication fork slowing, stalling, or even collapse of the replication fork. Familiarity with the various forms of DNA replication stress is essential to understanding the necessity and context of the multiple pathways available to restoring DNA replication.

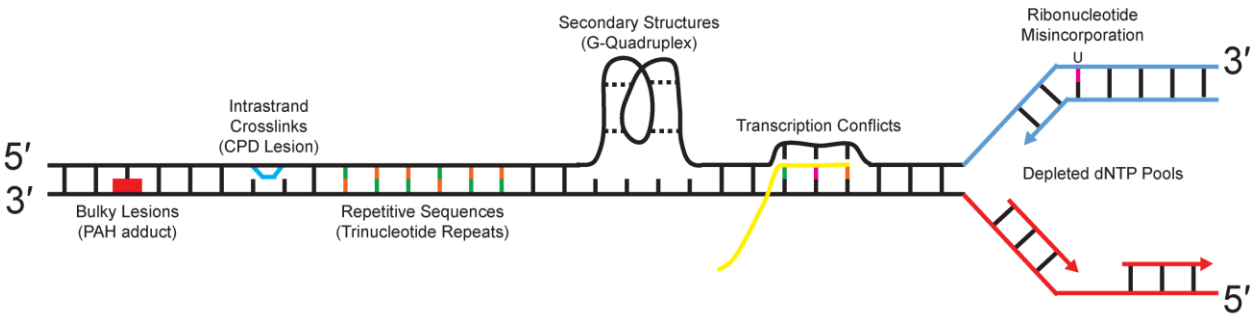

Figure 1.2 Agents of replication stress. Replication stress is caused by various impediments to DNA replication as illustrated. Adapted from (Zeman & Cimprich, 2014).

DNA Damage

DNA damage is extremely common, and all domains of life rely on multiple repair mechanisms to clear DNA damage from the genome. DNA damage can occur from both exogenous and endogenous sources. Endogenously generated DNA damage stems from oxidation, deamination, methylation, and the most commonly occurring depurination. Depurination in DNA results in approximately 10,000 apurinic/apyrimidinic (AP) sites per cell per day (Ciccia & Elledge, 2010, Lindahl & Barnes, 2000). External DNA damage results from exposure to sunlight, combustion byproducts, medical imaging, and more recently discovered small molecules produced by plants, fungi, and bacteria. Pyrimidine dimers caused by UV exposure can cause approximately 100,000 lesions per cell per day at peak hour sunlight (Ciccia & Elledge, 2010). Aside from the amount of damage that a cell might encounter, the variety of DNA damage size and effect on DNA sequence and secondary structure vary greatly and so multiple pathways have evolved to preserve genome stability.

Misincorporation

Although the fidelity of DNA polymerases is impressive there is room for error and misincorporation of the incorrect base and even ribonucleotides occurs *in vivo*. In eukaryotes on the lagging strand Pol δ incorporates 1 ribonucleotide per 5000 bases and on the leading strand Pol ε incorporates 1 ribonucleotide per 1250 bases (Dalgaard, 2012). Pol α is involved in extending RNA primers synthesized *de novo* by primase to initiate replication on the leading and lagging strand and incorporates 1 ribonucleotide per 650 bases. These rates of misincorporation are likely caused by the overabundance of ribonucleotides to deoxyribonucleotides in the nucleus as well as the varying degrees of 3′-5′ exonuclease activity of the replicative polymerases. Misincorporation of rNTPs stalls the replicative polymerases and requires the activity of RNaseH2 to remove and repair ribonucleotide misincorporation (Lazzaro, Novarina et al., 2012, Nick McElhinny, Kumar et al., 2010, Sparks, Chon et al., 2012).

Transcription Conflicts

Work from both prokaryotic and eukaryotic systems has demonstrated that collisions between DNA replication and transcription complexes can lead to replication stress especially if the two processes are in a head-on orientation (Bermejo, Lai et al., 2012, Helmrich, Ballarino et al., 2013). Replication stress caused by transcription might also be caused by RNA:DNA hybrids, R-loops, that arise from base pairing of the nascent RNA transcript to the DNA template behind the RNA polymerase (Aguilera & Garcia-Muse, 2012). RNA:DNA hybrids are more thermo-stable than DNA duplexes *in vitro* and might produce a form of replication stress if left unresolved by RNaseH, RNA:DNA

helicases, or other RNA processing enzymes (Alzu, Bermejo et al., 2012, Huertas & Aguilera, 2003, Yuce & West, 2013).

Difficult to Replicate Sequences and Heterochromatin

Secondary structures found naturally in DNA such as G-quadruplexes and repetitive sequences such as trinucleotide repeats are both forms of replication stress caused by the DNA template (Bochman, Paeschke et al., 2012, McMurray, 2010, Paeschke, Bochman et al., 2013). Trinucleotide repeats can lead to replication stress that when improperly replicated can lead to expansions or deletions in the DNA that result in human disease (Kim & Mirkin, 2013). Even transcriptionally repressed regions of the genome such as heterochromatin have been observed to induce replication stress and this is part of the natural chromatin environment (Jiang, Lucas et al., 2009, Lambert & Carr, 2013).

Depleted Nucleotide Pools and Replication Components

During replication it is critical that replication origin firing and replication speeds are appropriately regulated to prevent depleted nucleotide pools and avoid replication stress (Beck, Nahse-Kumpf et al., 2012, Sorensen & Syljuasen, 2012). Replication stress also results if there is a lack of necessary components for replication such as replisome proteins, histones, or chromatin remodelers associated with replication (Prado & Aguilera, 2005, Tanaka & Diffley, 2002, Ye, Franco et al., 2003).

Consequences of Stalled or Collapsed DNA Replication Forks

In eukaryotes replication stress has many different outcomes. However, replication stress induced by a stalled replication fork generally manifests in generation of excess ssDNA. Continued DNA unwinding by the replicative helicase and polymerase stalling and uncoupling at sites of replication stress produces excessive ssDNA at the replication fork that is coated by Replication Protein A (RPA) (Byun, Pacek et al., 2005). RPA coated ssDNA on the leading template strand of the replication fork presents a platform for the replication stress response that is largely orchestrated by ATR kinase (Nam & Cortez, 2011, Zou & Elledge, 2003). ATR itself is phosphorylated and thus activated by TOPBP1 and ETAA1 at stalled replication forks to then phosphorylate hundreds of downstream target proteins (Bass, Luzwick et al., 2016, Kumagai, Lee et al., 2006). Targets of ATR phosphorylation are involved in DNA replication, homologous recombination (HR), NER, and inter-strand crosslink (ICL) repair as previously reviewed (Cimprich & Cortez, 2008, Zeman & Cimprich, 2014). In addition to insuring the successful protection and even restoration of stalled replication forks, ATR activation by replication stress regulates the S/G2 phase transition (Saldivar, Hamperl et al., 2018).

While ATR phosphorylates many of its targets at stalled replication forks, ATR phosphorylation of CHK1 subsequently amplifies the replication stress response to the rest of the nucleus (Cimprich & Cortez, 2008, Liu, Guntuku et al., 2000, Lopez-Girona, Tanaka et al., 2001, Walworth & Bernards, 1996). CHK1 regulates the cell cycle, specifically the G2/M checkpoint, by phosphorylation of CDC25 (Furnari, Rhind et al., 1997, Peng, Graves et al., 1997). CDC25 phosphorylation by CHK1 blocks activation of CDK thus preventing entry into mitosis (Boutros, Dozier et al., 2006, Sanchez, Wong et

al., 1997). Slowing of new origin firing during replication stress might also be regulated by the CHK1-CDC25 pathway with and without the presence of exogenous replication stress (Dimitrova & Gilbert, 2000, Merrick, Jackson et al., 2004, Tercero & Diffley, 2001).

Interestingly, upon replication stress induced fork stalling in eukaryotes, replisome components remain bound to the replication fork with or without the replication stress response (De Piccoli, Katou et al., 2012, Dungrawala, Rose et al., 2015). The replication stress response protects and stabilizes stalled replication forks, however, under certain conditions replication fork collapse occurs when the replisome is unloaded, a DSB occurs, or replication can no longer restart (Cortez, 2015). Estimates of fork collapse frequency in bacteria lacking functional PriA replication restart protein suggest that fork collapse occurs once per cell per generation (Cox, Goodman et al., 2000). In eukaryotes an estimate of fork collapse frequency is more elusive, however, evidence of recombination induced crossover products that are replication dependent suggests that fork collapse occurs more than once per cell since these crossover products are selected against by BLM, Topoisomerase IIIα, RMI1 and RMI2 dissolvase (Bizard & Hickson, 2014). However, both bacterial and eukaryotic cells are prepared to protect stalled replication forks and fork protection pathways minimize the event of fork collapse (Bhat & Cortez, 2018).

DNA Replication Fork Reversal

When replication forks stall there are many pathways to restore DNA replication, protect the replication fork, or even repair the cause of replication stress. Aside from lesion skipping and translesion synthesis pathways (**Figure 1.3**) one of the many pathways

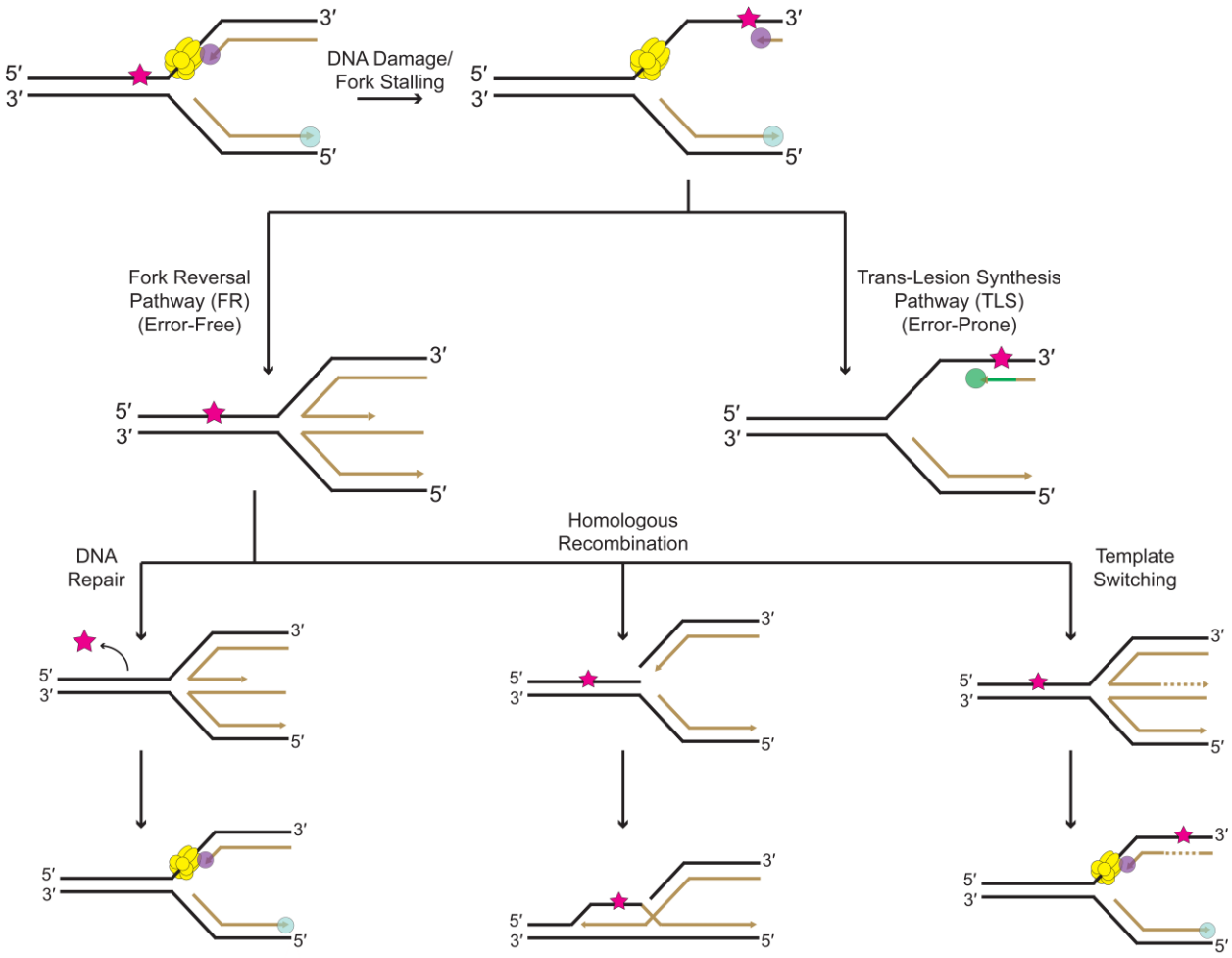

Figure 1.3 The translesion synthesis pathway and fork reversal pathway allow for bypass of DNA damage during replication. Schematic demonstrating the possible pathways available to a stalled replication fork to bypass DNA damage. DNA damage (magenta star) can stall polymerases (purple) and uncouple the leading strand polymerase and helicase (yellow). Error-free pathways for DNA damage bypass are possible through the fork reversal pathway (left). Reversed forks can then be repaired through several potential pathways (DNA repair, Homologous recombination, and template switching). Translesion synthesis (TLS) is an error-prone pathway where specific polymerases are recruited to bypass (green nascent strand) the DNA damage to resume replication albeit error-prone.

available to a stalled replication fork is replication fork reversal. Replication fork reversal occurs when the template DNA strands are re-annealed in the opposing direction of

replisome progression thus causing the pairing of the nascent leading and nascent lagging DNA strands to form a four stranded DNA structure also referred to as a chicken foot structure or Holliday junction. Replication fork reversal can protect a stalled replication fork from further damage or fork collapse until replication is resumed or an adjacent replisome replicates through the stalled replication fork (Bhat & Cortez, 2018, Courcelle, Donaldson et al., 2003). Originally, fork reversal was proposed as a pathway to bypass damage during replication (Fujiwara & Tatsumi, 1976, Higgins, Kato et al., 1976). However, levels of fork reversal observed in the two original studies were higher than those found when DNA psoralen cross-linking was performed in vivo rather than after DNA extraction (Tatsumi & Strauss, 1978). More recent work from the Lopes lab has demonstrated that a variety of DNA damaging agents cause increased replication fork reversal in Eukaryotes ranging from yeast to humans (Sogo, Lopes et al., 2002, Zellweger, Dalcher et al., 2015).

Multiple studies have shown RAD51 to be essential for fork reversal and that BRCA2 stabilizes RAD51 fork reversal intermediates (Hashimoto, Ray Chaudhuri et al., 2010, Schlacher, Christ et al., 2011, Zellweger et al., 2015). Although RAD51 is required to observe fork reversal *in vivo* RAD51 alone cannot reverse a stalled replication fork *in vitro*. Several proteins including SMARCAL1, ZRANB3, HLTF, BLM, WRN, FANCM, and FBH1 are capable of mediating fork reversal *in vitro* (Achar, Balogh et al., 2011, Betous, Couch et al., 2013, Betous, Mason et al., 2012, Ciccia, Nimonkar et al., 2012, Fugger, Mistrik et al., 2015, Gari, Decaillet et al., 2008a, Gari, Decaillet et al., 2008b, Machwe, Karale et al., 2011, Machwe, Xiao et al., 2006, Opresko, Sowd et al., 2009). Recently ATPase dependent fork reversal, quantified by electron microscopy, has been observed

for both ZRANB3 and SMARCAL1 in human cells under replication stress caused by DNA damaging agents (Kolinjivadi, Sannino et al., 2017, Taglialatela, Alvarez et al., 2017, Vujanovic, Krietsch et al., 2017). MRE11-dependent nascent DNA degradation is dependent on HLTF in BRCA1-deficient cells suggesting that HLTF generates a substrate for MRE11 (Taglialatela et al., 2017). These recent studies implicate all three of the SNF2 fork remodeling enzymes in the replication fork reversal pathway *in vivo* under replication stress conditions. Now that fork reversal activity by SNF2-family fork remodelers has been observed in cells it will be important to further characterize the temporal distribution of each fork remodeler at a stalled replication fork. Investigating the specific substrates each SNF2-family fork remodeler recognizes, mechanisms of fork remodeling, and whether the activity of each fork remodeler is stimulated by a particular form of replication stress will be essential to our understanding of fork reversal and fork protection in disease.

DNA replication in prokaryotes requires a more simplified replisome than that of eukaryotes (**Figure 1.1**) and lacks the requirement of chromatin remodeling. Having a more simplified replisome also impacts the regulation of fork reversal pathways. The first observations of fork reversal in *E. coli* were made using 2-D gel electrophoresis or Brewer-Fangman gels to identify replication intermediates indicative of replication fork reversal in cells exposed to UV radiation (Courcelle et al., 2003). This work by the Courcelle lab demonstrated that RecA, RecF, RecO, and RecR are all essential for efficient fork reversal and fork protection at stalled replication forks in *E. coli*. Although RecA and the RecF pathway proteins are required for replication fork reversal and fork protection in *E. coli* it remains that *in vitro* RecA fork reversal activity is inhibited by SSB and the branch migration proteins RecG and RuvAB are able to reverse a replication fork

stalled at a CPD lesion in a reconstituted *E. coli* replication system with the replisome still bound (Gupta, Yeeles et al., 2014a).

Fork Protection by Fork Reversal

In eukaryotes the SNF2-family fork remodeler SMARCAL1 has been a front-runner in the search for proteins implicated in the replication fork reversal pathway. SMARCAL1 has both fork reversal and fork restoration activities *in vitro* and biallelic loss of function of SMARCAL1 results in the human disease Schimke Immunoosseous Dysplasia (SIOD). Cells lacking functional SMARCAL1 have higher frequencies of DSBs and genome instability.

SMARCAL1 is recruited to stalled replication forks by its interaction with the single stranded DNA binding protein RPA (**Figure 1.4**). RPA binds ssDNA with affinities in the low nM range and has multiple domains that allow for transient modes of interaction with ssDNA and other proteins (Gibb, Ye et al., 2014, Kim, Paulus et al., 1994, Pokhrel, Caldwell et al., 2019). RPA has two protein recruitment domains, 70N and 32C, that recognize short motifs found in DNA repair and homologous recombination proteins (Ball, Myers et al., 2005, Bansbach, Betous et al., 2009, Bass et al., 2016, Bochkareva, Kaustov et al., 2005, Ciccia, Bredemeyer et al., 2009, Guilliam, Brissett et al., 2017, Mer, Bochkarev et al., 2000, Theriot, Hegde et al., 2010, Xu, Vaithiyalingam et al., 2008, Zhao, Vaithiyalingam et al., 2015, Zou & Elledge, 2003).

The RPA binding motif (RBM) found in SMARCAL1 is essential for localization to sites of replication stress (Bansbach et al., 2009, Ciccia et al., 2009). Fork reversal intermediates induced by high concentrations of aphidicolin in BRCA2-deficient cells are

reduced by depletion of SMARCAL1 (Kolinjivadi et al., 2017). Addition of WT SMARCAL1 to SMARCAL1-depleted BRCA2-deficient cells restored levels of fork reversal intermediates observed in BRCA2-deficient cells, however, addition of SMARCAL1 that lacks ATPase activity or the RBM motif does not restore levels of fork reversal. This data suggests that at least in BRCA2-deficient cells functional SMARCAL1 is required for the generation of reversed replication fork intermediates. Fork reversal is also dependent on RAD51, however, a simultaneous loss of RAD51 and SMARCAL1 results in even fewer reversed fork intermediates. Fork reversal replication intermediates are also greatly reduced in MCF10a cells treated with hydroxyurea (HU) and depleted of SMARCAL1 when compared to control cells (Taglialatela et al., 2017). The visualization of replication intermediates by electron microscopy demonstrates that SMARCAL1 generates reversed replication forks that require both ATPase activity and recruitment by RPA. SMARCAL1 fork reversal activity is enhanced when RPA is bound to the leading strand emulating the environment present during replication stress (**Figure 1.4**) (Betous et al., 2013, Bhat, Betous et al., 2015). The regulated fork reversal activity of SMARCAL1 by RPA is able to create transiently reversed forks caused by short bursts of fork reversal activity, 400 bp per annealing event (Betous et al., 2013). The short bursts of fork reversal activity by SMARCAL1 might be important to prevent extensive and prolonged reversal, which is also known to be deleterious to genome stability. ATR phosphorylation of SMARCAL1 inhibits SMARCAL1 mediated fork reversal further suggesting that fork reversal is a highly regulated process that is beneficial within some range of activity (Couch, Bansbach et al., 2013).

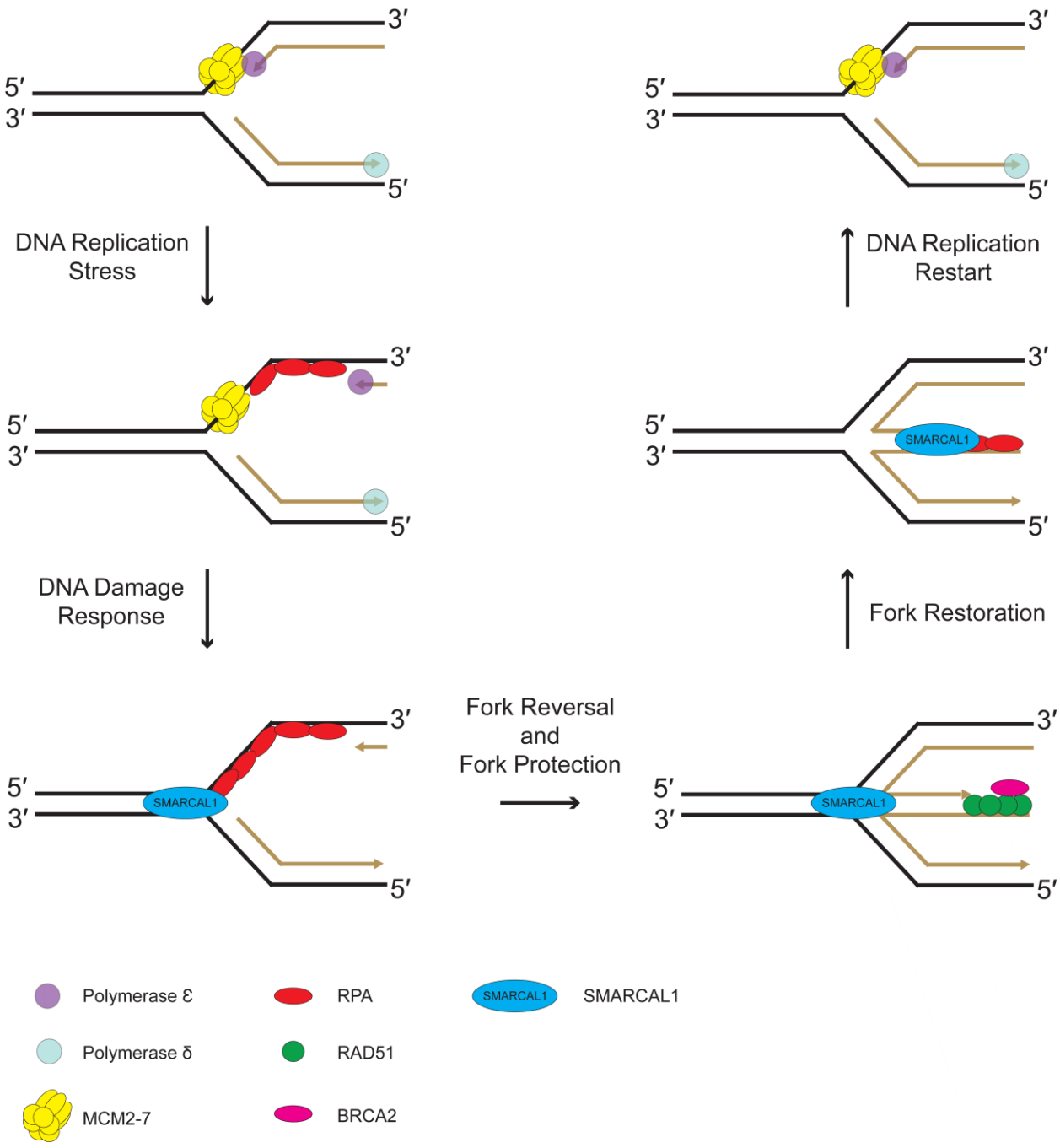

Figure 1.4 Fork reversal and fork protection in eukaryotes. Schematic of DNA replication fork reversal, fork protection, and DNA replication fork restoration and restart. Proteins required for DNA replication fork reversal and fork protection are colored and depicted as in the figure legend.

The recombination protein RAD51 is implicated in stabilizing fork reversal intermediates along with the BRCA2 protein (**Figure 1.4**), which stabilizes RAD51-ssDNA filaments (Hilario, Amitani et al., 2009, Kowalczykowski, 2015). Without appropriate levels of RAD51, fork reversal is not observed *in vivo* (Zellweger et al., 2015). Overexpression of RAD51 causes genome instability and increased DSBs mediated by MUS81 endonuclease activity (Klein, 2008, Richardson, Stark et al., 2004). RAD51 cannot catalyze fork reversal on its own but stimulates known fork reversal proteins (Bugreev, Rossi et al., 2011). All of this information suggests that RAD51 is important for regulating the fork reversal and fork protection pathway. RADX is a newly discovered protein composed of three OB-folds that is antagonistic to RAD51 ssDNA binding and plays a role in regulating levels of fork reversal, fork protection, and homologous recombination (Bhat & Cortez, 2018, Bhat, Krishnamoorthy et al., 2018). RADX functions to regulate RAD51 mediated fork reversal and fork protection and so it is unsurprising that loss of RADX leads to increased MUS81 endonuclease activity and DSBs (Dungrawala, Bhat et al., 2017).

Many parallels to fork reversal and fork protection pathways in eukaryotes exist in prokaryotes (Courcelle et al., 2003). In *E. coli* the homologous recombination protein RecA, an ortholog of Rad51, is also capable of forming ssDNA-RecA filaments as well as dsDNA-RecA filaments (Stasiak & Egelman, 1994). At stalled replication forks in prokaryotes the RecG fork reversal protein is stimulated by single stranded binding protein (SSB) when bound to the leading parental strand of a replication fork. The stimulation of RecG by SSB is similar to the regulation of SMARCAL1 by RPA. Although RecG is a functional homolog of SMARCAL1 and is capable of efficient fork reversal *in*

vitro, the only direct observations *in vivo* of proteins responsible for replication fork reversal in *E. coli* are the homologous recombination proteins RecA and RuvAB (Michel & Sandler, 2017). There is no direct evidence of RecG mediated fork reversal at a stalled replication fork *in vivo*. What we do know is that RecG prevents over-replication during termination of replication, regulates PriA mediated replication restart, and appears to limit replication intiation to OriC and sites of replication restart. All of the aforementioned functions require an active RecG protein to reverse and maintain a stalled fork-like substrate.

Superfamily 2 ATPases

The focus of this dissertation is on the molecular mechanisms of fork remodeling enzymes that translocate on duplex DNA. The fork remodeling enzymes examined in this work (RecG, SMARCAL1, ZRANB3, and HLTF) are all superfamily 2 ATPases. DNA-dependent and RNA-dependent ATPases are categorized into six superfamilies (**Figure 1.6**) (Singleton, Dillingham et al., 2007). Superfamily 1 (SF1) and superfamily 2 (SF2) ATPases are characterized by tandem RecA domains tethered by a flexible linker (Fairman-Williams, Guenther et al., 2010). The RecA domain is named based on structural similarity to the fold of the RecA protein that promotes homologous recombination. The RecA fold is a parallel β-sheet surrounded by α-helices. The superfamilies 3-6 (SF3-SF6) are all toroidal ATPases meaning that they form a ring. SF3-SF6 ATPases form homo-hexamers or heterohexamers and contain a single RecA fold.

The largest superfamily of DNA-dependent and RNA-dependent ATPases is SF2. A diverse range of cellular functions are carried out by SF2 ATPases and most are RNA

helicases, however, the SNF2 and RecQ families are also quite large (Beyer and Spies 2012 textbook chapter). A majority of the SF2 ATPases translocate with 3′-5′ polarity with the exception of the Rad3/XPD family that translocate with 5′-3′ polarity (Cheng & Wigley, 2018, Saikrishnan, Powell et al., 2009, Sung, Prakash et al., 1987). Most of the SF2 ATPases translocate on single stranded DNA primarily through contacts to the phosphodiester backbone, however, a subset of the SF2 ATPases, particularly the SNF2 family, require dsDNA for translocation.

SF2 ATPases bind DNA or RNA to stimulate hydrolysis of ATP. Eleven conserved motifs are located throughout the two RecA folds of all SF2 ATPases. There are up to 14 conserved motifs in some of the SF2 families. The eleven conserved motifs that identify SF2 ATPases are motifs (Q, I, Ia, Ib, II, III, IV, IVa, V, Va, and VI). These conserved motifs are critical for binding ATP (motifs Q, I, II, and VI) and interaction with a nucleic acid substrate (motifs Ia, Ic, IV, and V) (**Figure 1.5**).

Although many of the SF2 ATPases are RNA helicases the focus of this work is on a smaller subset of SF2 ATPases that are capable of dsDNA translocation. The dsDNA translocases have largely been identified using a triplex displacement assay, preferential ATPase stimulation by dsDNA over ssDNA, or using fork reversal assays with substrates containing regions of reverse polarity (Fairman, Maroney et al., 2004, Firman & Szczelkun, 2000, Jaskelioff, Van Komen et al., 2003, Levy, Ptacin et al., 2005, McGlynn & Lloyd, 2001, Stanley, Seidel et al., 2006, Whitehouse, Stockdale et al., 2003). The SNF2 family (**Figure 1.6**) is the largest family of dsDNA translocases within SF2 and almost all of the proteins are only found in eukaryotes (Flaus, Martin et al., 2006). In contrast the RecG-like family within SF2 contains prokaryotic proteins that are also

dsDNA translocases. The remainder of the introduction will expand upon the SF2 dsDNA translocases that catalyze fork reversal and what is known regarding substrate preference, mechanisms of dsDNA translocation, and translocation polarity.

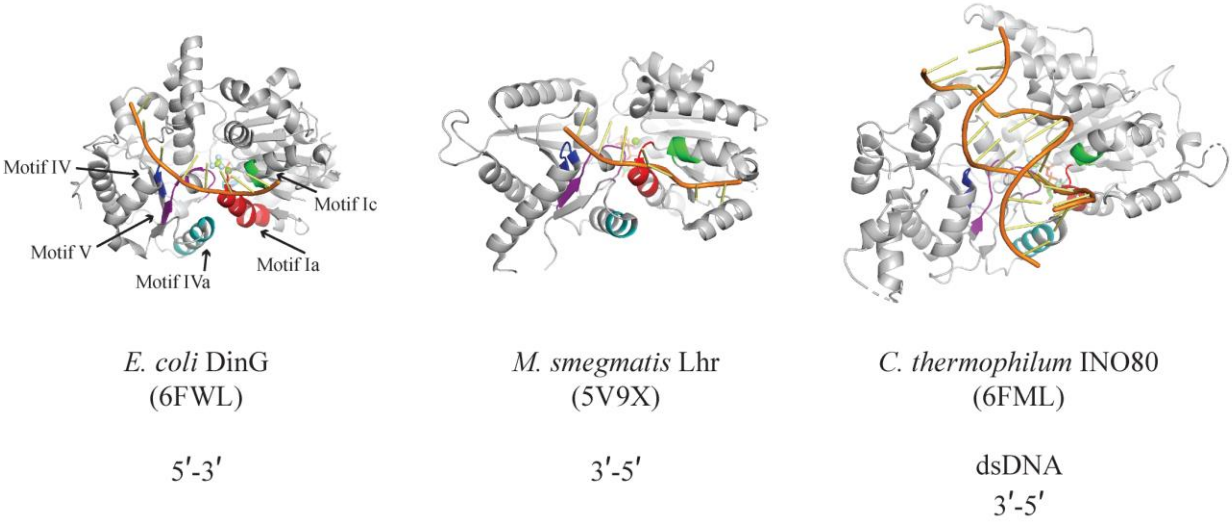

Figure 1.5 SF2 ATPases contact nucleic acids through conserved motifs. Crystal structures of SF2 ATPases bound to nucleic acid substrates with different translocation polarities DinG (PDB ID: 6FWL) and Lhr (PDB ID: 5V9X). Cryo-EM reconstruction of INO80 bound to dsDNA (PDB ID: 6FML).

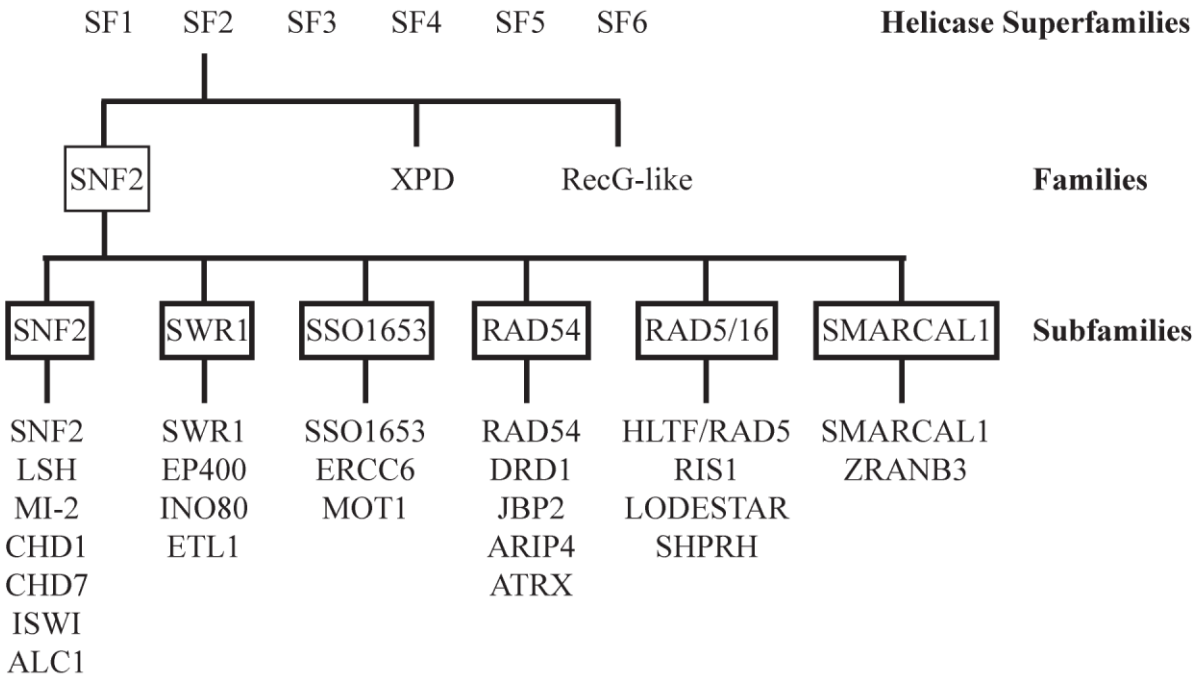

Figure 1.6 Subfamilies of the SNF2 family of proteins. Schematic of SNF2 subfamily organization based on sequence conservation. Adapted from (Flaus et al., 2006).

RecG-like Family

The RecG-like family of SF2 ATPases includes the bacterial dsDNA translocase proteins RecG and Mfd (Fairman-Williams et al., 2010). RecG is required for maintaining genome stability and preventing over-replication of the terminus region. The dsDNA translocase activity of RecG promotes reversal of stalled DNA fork junctions. Mfd is required for efficient transcription-coupled repair and functions to rescue transcription complexes stalled by DNA damage. The dsDNA translocase activity of Mfd promotes the removal of stalled RNA polymerases and recruitment of the nucleotide excision repair (NER) proteins. Both RecG and Mfd use the dsDNA translocase activity provided by the SF2 ATPase domains to maintain genome stability in bacteria by interacting with DNA structures or other proteins through an auxiliary domain.

Interestingly all of the RecG-like family proteins contain a helical hairpin motif called the Translocation in RecG (TRG) motif located between the two ATPase domains (Chambers, Smith et al., 2003, Deaconescu, Chambers et al., 2006, Mahdi, Briggs et al., 2003). This dissertation is focused on the mechanisms of fork remodeling enzymes and so I will expand on the structure and function of the RecG protein.

RecG

The RecG protein has been studied in great detail by the Lloyd, Wigley, Bianco, and Marians labs and has a known role to promote genome stability in bacteria. The bacterial fork reversal enzyme RecG was first characterized in *E. coli* by the Lloyd lab (Mahdi & Lloyd, 1989). The RecG gene was discovered originally during a screen for recombination deficient mutants in *E. coli* (Storm, Hoekstra et al., 1971). Almost all bacteria contain RecG (Rocha 2005) and even some plant mitochondria and chloroplasts contain homologues (Odahara 2015, Wallet 2015). No animal or fungal species contain RecG although a functional homologue with a different domain organization has recently been identified in Yeast mitochondria (Gaidutsik, Sedman et al., 2016). Loss of RecG function causes a sensitivity to treatment with UV radiation, mitomycin C, and irradiation (Lloyd, 1991, Lloyd & Buckman, 1991). RecG loss of function also exhibits a 2-3 fold reduction in recovery during conjugational (Hfr x F-) recombination screens and sensitivity to UV radiation that is exacerbated by a loss of RuvAB.

A singular functional role of RecG is difficult to pinpoint since RecG null cells have a pleiotropic phenotype and may play several roles in DNA metabolism. RecG is implicated in DNA replication fork reversal, regulation of DNA replication fork restart, DNA

replication termination, homologous recombination, and naïve adaptation in CRISPR-CAS immunity (Lloyd & Rudolph, 2016). Recent studies regarding the role of RecG in DNA replication termination and past studies of RecG and PriA deficient E. coli would suggest that RecG regulates the replication restart activity of PriA and prevents OriC-independent replication and over replication of the terminal region (Midgley-Smith, Dimude et al., 2018a, Tanaka & Masai, 2006). As stated in recent reviews from both Marians and Lloyd labs the role of RecG in DNA replication fork reversal will remain speculative until techniques allow the resolution of identifying component proteins at a stalled replication fork (Lloyd & Rudolph, 2016, Marians, 2018).

RecG is active on stalled fork substrates *in vitro* and requires homologous sequences to pair the parental strands back together and dsDNA to stimulate ATPase activity and translocate. These substrate requirements make RecG an excellent candidate for replication fork reversal activity *in vivo*, however the lack of direct evidence for RecG mediated fork reversal and fork protection in *E. coli* is interesting. In an *in vitro* reconstituted *E. coli* replication system RecG reverses stalled replication forks caused by CPD lesions with the replisome bound (Gupta et al., 2014a). The replication intermediates generated by RecG fork reversal are cleaved preferentially by the resolvase RuvC over those generated by the fork reversal activity of the homologous recombination protein RuvAB. Furthermore, RecG fork reversal activity is stimulated by the presence of SSB on the leading parental DNA of a model replication fork while RecA, which has been implicated in replication fork reversal *in vivo*, is inhibited by the presence of SSB (Gupta, Yeeles et al., 2014b).

Single-molecule studies and biochemical assays with RecG have demonstrated that it translocates on dsDNA to catalyze fork reversal and that reverse polarity substrates on the 3′-5′ parental lagging strand are more inhibitory to translocation and fork reversal activity than the same impediment placed in the 5′-3′ leading parental strand (Manosas, Perumal et al., 2013, McGlynn & Lloyd, 2001). The single molecule studies demonstrate that the dsDNA translocase RecG tracks primarily on the lagging parental strand in the 3′-5′ direction. The first crystal structure of a dsDNA translocase bound to DNA was determined by the Wigley lab and demonstrated that RecG binds to DNA junctions through a substrate recognition domain (**Figure 1.7**) (Singleton, Scaife et al., 2001). Unfortunately the crystal structure of RecG did not reveal how the ATPase domain binds dsDNA. Therefore, there are still many questions left unanswered over 18 years later about a mechanism of double stranded DNA translocation. Characterizing the fork reversal mechanism of RecG, a monomeric fork remodeling protein, enhances our general understanding of fork reversal by the eukaryotic SNF2-family fork remodelers that reverse stalled replication forks *in vivo* and are important for maintaining genome stability. Recent work from our lab discussed in chapter II suggests that a conserved loop within the aforementioned TRG motif of RecG is necessary for conformational changes observed in the ATPase motor induced by DNA binding and that these conformational changes are essential for ATPase and fork reversal activity.

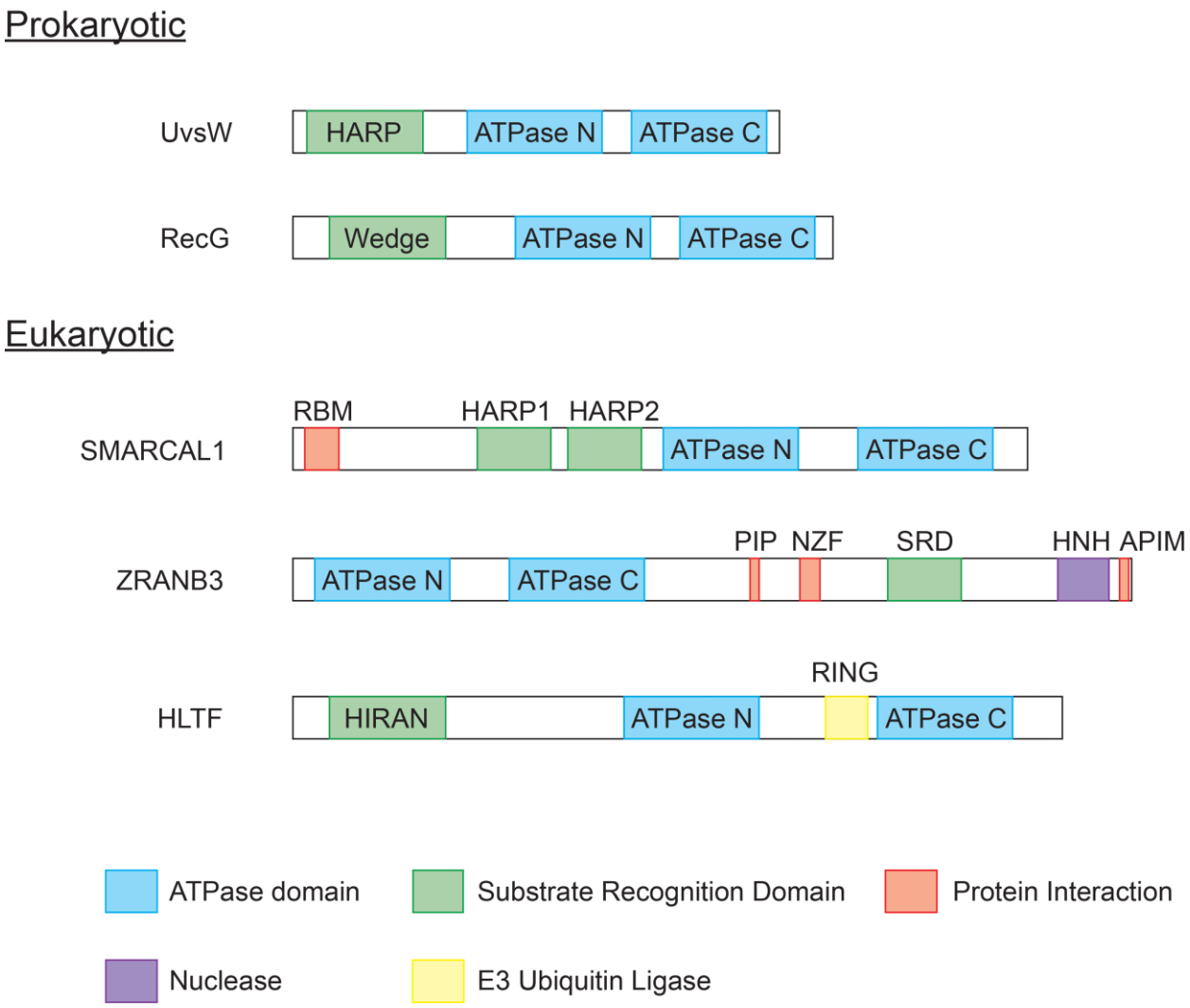

Figure 1.7 Domain organization of fork remodeling enzymes. Protein domain organization of fork remodeling enzymes with ATPase domains (purple) and substrate recognition domains (yellow). Eukaryotic fork remodeling enzymes SMARCAL1, ZRANB3, and HLTF with accessory domains for protein interaction (red), nuclease activity (blue), ubiquitin ligase activity (green).

SNF2 Family

The SNF2 family of SF2 ATPases have diverse cellular functions in chromatin remodeling, homologous recombination, DNA replication fork reversal, telomere maintenance, nucleotide excision repair, and transcriptional regulation. SNF2 family members translocate on dsDNA in an ATP-dependent manner to remodel nucleic acids and nucleic acid bound proteins. Recent cryo-EM reconstructions of the chromatin remodelers CHD1, INO80, ISWI, SNF2, and SWR1 have demonstrated that dsDNA is bound between the RecA domains. Interestingly, these new cryo-EM models are in agreement with previous crystallographic data for the N-terminal domain of Rad54 bound to dsDNA and the path of ssDNA bound to SF2 helicases.

While there are many well studied chromatin remodeling SNF2 proteins there are also three fork reversal proteins within the family that use dsDNA translocation to remodel stalled DNA replication forks. It will be important to further understand the mechanisms of fork reversal and dsDNA translocation by the three fork reversal proteins SMARCAL1, HLTF, and ZRANB3 because of the diverse roles each has been demonstrated to play in maintaining genome stability.

HLTF

Helicase like transcription factor (HLTF) is a 1009 amino acid protein that migrates with the replication fork (Kile, Chavez et al., 2015). HLTF is silenced in colorectal cancers and therefore HLTF has been implicated as a potential tumor suppressor. However, deletion of HLTF does not result in a genome instability phenotype unless introduced to DNA replication stress such as UV radiation, MMS, or HU. In BRCA1-deficient cells

treated with HU, active HLTF with the HIRAN domain was required to observe MRE11-dependent nuclease activity caused by fork reversal. So far the function of HLTF *in vivo* appears to be regulation of polyubiquitinated PCNA and some role in fork reversal upon replication stress.

HLTF binds ssDNA alone presumably through the HIRAN domain, which recognizes a 3′ OH and whose structure has been determined (Hishiki, Hara et al., 2015, Kile et al., 2015). However, HLTF binds model replication forks with a much higher affinity than ssDNA or dsDNA alone and the DNA and ATP-dependent motor domain is active even without the HIRAN substrate recognition domain (SRD) (Chavez, Greer et al., 2018). The fork reversal activity of HLTF is similar to SMARCAL1 since it can reverse a fork with RPA bound whereas ZRANB3 cannot perform fork reversal when RPA is bound to the leading parental strand (Achar et al., 2011). Unlike SMARCAL1 and ZRANB3 HLTF contains an E3 ubiquitin ligase domain between the two ATPase domains of the SNF2 motor domain (**Figure 1.7**).

Beyond fork reversal activity, HLTF polyubiquitinates mono-ubiquitinated PCNA to shift the balance between translesion synthesis pathways and template switching pathways towards the latter (Lin, Zeman et al., 2011, Motegi, Liaw et al., 2008, Unk, Hajdu et al., 2008). HTLF contains a conserved E3 RING domain located between the N-terminal ATPase domain and C-terminal ATPase domain. HLTF acts as an E3 ligase to polyubiquitinate PCNA in conjunction with Mms2-Ubc13 and Rad6-Rad18 (Motegi et al., 2008). Polyubiquitinated PCNA has been demonstrated to control a number of activities at a stalled replication fork including regulation of the DNA damage tolerance pathways

or recruitment of other proteins required for genome stability under replication stress like ZRANB3 (Ciccia et al., 2012, Saugar, Ortiz-Bazan et al., 2014).

SMARCAL1

SMARCAL1 and ZRANB3 are distantly related to the other SNF2 proteins (**Figure 1.6**) (Flaus et al., 2006). SMARCAL1 is a 954 amino acid protein that is essential for genome stability. Biallelic mutations in SMARCAL1 result in the disease Shimke immuno-osseus dysplasia (SIOD) (Boerkoel, Takashima et al., 2002). SIOD is characterized by short stature, spondyloepiphysial dysplasia, nephropathy, and T-cell deficiency. Current *in vitr*o and *in vivo* data for SMARCAL1 suggests that it is involved in DNA replication fork reversal and is important for preventing DSBs and fork collapse caused by both DNA damage as well as endogenous sources (Bansbach et al., 2009, Betous et al., 2012, Kolinjivadi et al., 2017). Therefore there is some disconnect between work on the SMARCAL1 protein and our understanding of the plieotropic phenotype of patients with biallelic pathogenic variants of SMARCAL1.

Several groups have proposed models for the multisystemic disease observed in SIOD patients. Renal biopsies of SIOD patients have an increase in DNA fragmentation suggesting that genome instability due to a lack of active SMARCAL1 leads to defects in fetal kidney development (Sarin, Javidan et al., 2015). Work in Zebrafish also observed an increase in apoptosis during development when SMARCAL1 is depleted (Huang, Gu et al., 2010). Other studies have highlighted the possibility that SMARCAL1 might transcriptionally regulate several important genes that are implicated in renal disease and T-cell deficiency (Morimoto, Choi et al., 2016, Morimoto, Myung et al., 2016, Morimoto,

Yu et al., 2012, Sanyal, Morimoto et al., 2015, Sharma, Bansal et al., 2015). Similarly another model suggests chromatin remodeling alters transcription and is effected by loss of SMARCAL1 activity and that these changes are also susceptible to genetic, epigenetic, and environmental influences (Baradaran-Heravi, Cho et al., 2012). This last model would help to explain the poor genotype-phenotype correlation (Clewing, Antalfy et al., 2007, Dekel, Metsuyanim et al., 2008, Lama, Marrone et al., 1995, Lou, Lamfers et al., 2002, Lucke, Billing et al., 2005). It is still unclear what the direct relationship is between loss of active SMARCAL1, a fork remodeling protein, and the multisystemic disease of SIOD. It is clear that loss of SMARCAL1 function leads to an increased number of double strand breaks (DSB) in undamaged cells and a hypersensitivity to the DNA damaging agents hydroxyurea (HU), aphidicolin, mitomycin C, ionizing radiation, topoisomerase inhibitors, and evidently endogenous sources of replication stress (Poole & Cortez, 2017).

SMARCAL1 is enriched at replication forks and localizes to sites of replication stress through its interaction with the ssDNA binding protein Replication Protein A (RPA) (Bansbach et al., 2009, Ciccia et al., 2009). RPA enhances SMARCAL1 fork reversal activity on leading strand gap fork substrates and inhibits the activity on lagging strand gap fork substrates (Betous et al., 2013, Bhat et al., 2015). Regulation of SMARCAL1 fork reversal activity by RPA is logical since a leading strand block generates excess ssDNA at the leading strand that is rapidly bound by RPA to then also act as a platform for ATR activation.

Currently there are no *in vitro* studies to characterize the mechanism of SMARCAL1 mediated fork reversal when encountering different types of DNA damage. In future studies it will be important to define the mechanisms of SMARCAL1-mediated

fork reversal activity since SMARCAL1 deficiency causes SIOD and clearly plays some role in fork protection under both replication stress as well as in untreated cells.

ZRANB3

ZRANB3 is closely related to SMARCAL1 within the context of the SNF2-family fork remodelers, however, the domain organization of ZRANB3 is inverted (**Figure 1.7**). The SNF2 ATPase domains of ZRANB3 are located on the N-terminal portion of the protein, opposite that of SMARCAL1 and HLTF, and the SRD and other accessory domains are located on the C-terminal portion of ZRANB3. The SRD of ZRANB3 was identified by the Cortez lab and demonstrated an affinity for ss/dsDNA junctions (Badu-Nkansah, Mason et al., 2016). Like the tumor supressor HLTF, loss of ZRANB3 function has not been implicated in human disease, however ZRANB3 is essential for genome stability and ZRANB3 deficiency has been identified in endometrial cancers (Lawrence, Stojanov et al., 2014).

The accessory domains of ZRANB3 include both APIM, PIP and NZF motifs used to bind polyubiquitanted PCNA which is essential for ZRANB3 activity and localization at replication forks *in vivo* (Ciccia et al., 2012, Taglialatela et al., 2017, Vujanovic et al., 2017). Yet another accessory domain found in ZRANB3 is the HNH endonuclease whose role in vivo remains elusive. The endonuclease activity of ZRANB3 targets ss/dsDNA junctions that cannot be reversed and incises precisely 2 base pairs into the leading strand side of the parental duplex (Badu-Nkansah et al., 2016, Sebesta, Cooper et al., 2017, Weston, Peeters et al., 2012). Interestingly, ZRANB3 endonuclease does not

appear to be critical for ZRANB3-mediated replication fork slowing or fork reversal activity in vivo (Vujanovic et al., 2017).

As in the case of HLTF, ZRANB3 is not implicated in human disease but rather as a tumor suppressor. The role of HLTF and ZRANB3 in regulating replication speed during replication stress to prevent genome instability suggests that understanding the mechanisms of fork reversal under differing types of potential replication stress will be essential to understanding the cellular context of each protein in replication fork reversal and fork protection pathways.

Translocation Polarity

To date all SNF2 dsDNA translocases that have been tested for translocation polarity or structurally characterized in complex with dsDNA demonstrate a 3′-5′ polarity. Thanks to structural, biochemical, and biophysical studies on SF1 helicases, from both the Spies and Wigley labs, we know that the ATPase motor binds the DNA strand in the same orientation regardless of translocation polarity. That work demonstrated that the order of substrate binding and release, upon ATP binding and hydrolysis, dictate the polarity of the enzyme (**Figure 1.8**). It appears from recent X-ray crystal structures of the the XPD homolog, DinG, that SF2 helicases also bind to ssDNA with the same orientation regardless of the translocation polarity of the enzyme.

However, the question of translocation polarity remains unanswered for the SF2 dsDNA translocases since all dsDNA translocases have demonstrated a requirement for both DNA strands and the mechanism of translocation is likely dependent on contacts to the entire DNA duplex. The recent plethora of Cryo-EM structures of SNF2 motor proteins

bound to nucleosomes and dsDNA demonstrate that there is likely a tracking strand and a guide strand where one strand is more important for the protein's mechanism of translocation.

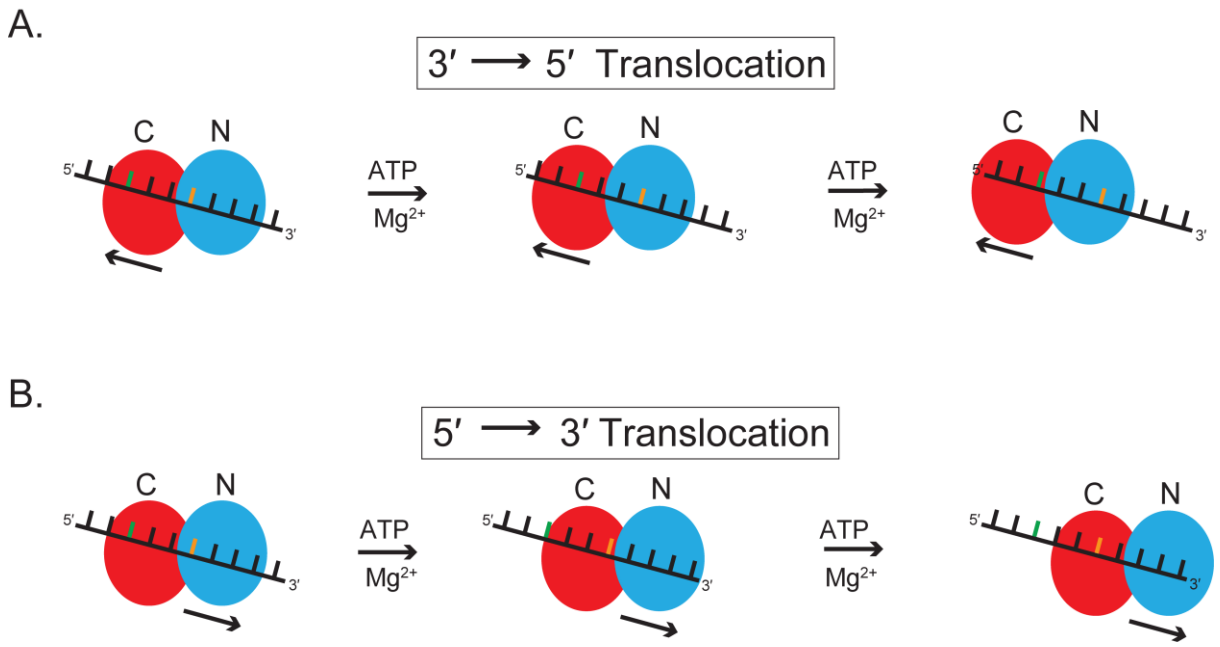

Figure 1.8 Translocation polarity in SF2 ATPases is determined by domain release after ATP hydrolysis. The N-terminal ATPase domain (blue) and C-terminal ATPase domain (red) of SF2 ATPases bind DNA (black) with the same orientation regardless of translocation polarity. **A.** 3′-5′ translocation polarity requires that the C-terminal domain release after ATP hydrolysis while the N-terminal domain stays bound leading to an overall shift in the ATPase domain binding to the left as the colored bases move across the ATPase domain surface to the right. Binding the next ATP molecule leads to a ratchet motion caused by closure of the two domains. **B.** 5′-3′ translocation polarity is the opposite and requires that the N-terminal domain release after ATP hydrolysis while the C-terminal domain stays bound leading to an overall shift in the ATPase domain binding to the right.

Scope of this Work

This dissertation presents work characterizing the fork reversal activity of proteins ranging from the prokaryotic fork remodeler RecG to the eukaryotic SNF2-family fork remodelers SMARCAL1, ZRANB3, and HLTF. The work explores how dsDNA translocases that reverse stalled forks are activated by DNA binding and cope with various perturbations to carry out the reversal of stalled replication forks. Chapter II characterizes both a mechanism for DNA substrate binding and activation of the archetypal fork reversal protein RecG using both biophysical and biochemical approaches. The contents of chapter II were published in (Warren, Stein et al., 2018). Chapter III determines the consequences of DNA modifications that might present a block to fork reversal and translocation activities of the SNF2-family fork reversal proteins SMARCAL1, ZRANB3, and HLTF using a biochemical approach. Chapter IV discusses the implications of this work, the ongoing work to characterize a mechanism of fork reversal by dsDNA translocases, and the specific substrate preferences of the SNF2 fork remodelers. This work has expanded on both our knowledge of RecG mediated fork reversal activity and the substrate preferences of the SNF2-family fork remodelers.

CHAPTER II

MOVEMENT OF THE *THERMOTOGA MARITIMA* RECG MOTOR DOMAIN UPON BINDING DNA IS REQUIRED FOR EFFICIENT FORK REVERSAL

Abstract

RecG catalyzes reversal of stalled replication forks in response to replication stress in bacteria. The protein contains a fork recognition ("wedge") domain that binds branched DNA and a superfamily II (SF2) ATPase motor that drives translocation on double-stranded (ds)DNA. The mechanism by which the wedge and motor domains collaborate to catalyze fork reversal in RecG and analogous eukaryotic fork remodelers is unknown. Here, we used electron paramagnetic resonance (EPR) spectroscopy to probe conformational changes between the wedge and ATPase domains in response to fork DNA binding by *Thermotoga maritima* RecG. Upon binding DNA, the ATPase-C lobe moves away from both the wedge and ATPase-N domains. This conformational change is consistent with a model of RecG fully engaged with a DNA fork substrate constructed from a crystal structure of RecG bound to a DNA junction together with recent cryo-EM structures of chromatin remodelers in complex with dsDNA. We show by mutational analysis that a conserved loop within the translocation in RecG (TRG) motif that was unstructured in the RecG crystal structure is essential for fork reversal and DNA-dependent conformational changes. Together, this work helps provide a more coherent

---

*The work in this chapter was published in Warren GM, Stein RA, McHaourab HS, Eichman BF (2018) Movement of the RecG Motor Domain upon DNA Binding Is Required for Efficient Fork Reversal. *Int J Mol Sci* 19

model of fork binding and remodeling by RecG and related eukaryotic enzymes**.**

Introduction

Faithful DNA replication at every round of cell division is critical for transmission of genetic information. Replisomes assembled at progressing replication forks regularly encounter a number of impediments including DNA damage, aberrant DNA structures, difficult to replicate nucleotide sequences, and transcription complexes (Zeman & Cimprich, 2014). Stalled replication forks can lead to replisome disassembly, strand breaks and other pathogenic DNA structures, and are a potential source of genome instability associated with a number of diseases (Cortez, 2015, Zeman & Cimprich, 2014). To ensure complete genome duplication, a number of pathways operate to mitigate fork stalling or to restart replication through reassembly of the replication fork in an origin independent manner (Berti & Vindigni, 2016, Marians, 2018). One important mechanism for stabilizing and/or restarting stalled forks is fork reversal (or fork regression), in which specialized motor proteins push the fork backward to convert the three-way fork into a four-way junction (**Figure 2.1**) (Atkinson & McGlynn, 2009, Fujiwara & Tatsumi, 1976, Higgins et al., 1976, Neelsen & Lopes, 2015). The Holliday junction like structure serves as an important intermediate for recombination-coupled repair and can also promote template switching to enable DNA synthesis from an unhindered nascent strand template (Marians, 2018). Fork reversal may also promote excision repair of fork-stalling DNA lesions by sequestering them away from the fork and back into the context of dsDNA.

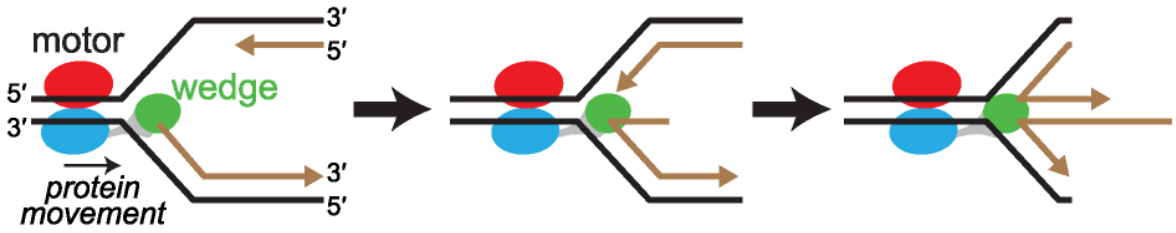

Figure 2.1 RecG catalyzes replication fork reversal. Schematic of fork reversal. Template DNA strands are black and nascent strands are brown. RecG is colored according to domains: ATPase-N and -C lobes are blue and red, respectively, and the wedge domain is green.

Fork reversal mechanisms are operative in both prokaryotes and eukaryotes (Atkinson & McGlynn, 2009, Marians, 2018, Neelsen & Lopes, 2015). In bacteria, the dsDNA translocase RecG is a key player in this process and is important for maintenance of genome stability via DNA repair and recombination (Bianco, 2015, Lloyd & Rudolph, 2016, McGlynn & Lloyd, 2002). Inactivation of RecG sensitizes cells to the interstrand crosslinking agent mitomycin C and to UV and ionizing radiation (Lloyd, 1991, Lloyd & Buckman, 1991), and leads to over-replication of the terminus region in circular DNA (Rudolph, Upton et al., 2009, Rudolph, Upton et al., 2013). The molecular rationale for these phenotypes remains under debate (Courcelle & Hanawalt, 2003), but may result from the generation of DNA structures necessary for origin-independent replication restart by PriA (Gregg, McGlynn et al., 2002, Lloyd & Rudolph, 2016, McGlynn & Lloyd, 2002, Rudolph, Upton et al., 2010) or recombination repair by RecA/BCD or RuvABC machinery (Kowalczykowski, 2000, Lloyd & Rudolph, 2016, West, 1997).

In vitro, RecG catalyzes regression of replication forks and branch migration of Holliday junctions (Lloyd & Sharples, 1993, Whitby, Ryder et al., 1993), even in the presence of stalled replisome components (Gupta et al., 2014a), and also unwinds D-loops and R-loops (Azeroglu & Leach, 2017, Azeroglu, Mawer et al., 2016, Midgley-Smith, Dimude et al., 2018b). These remodeling activities rely on ATP-dependent dsDNA translocation catalyzed by a superfamily 2 (SF2) helicase motor comprised of two RecA-like ATPase lobes (Fairman-Williams et al., 2010). RecG preferentially binds Holliday junctions and model replication forks that contain ssDNA on the leading strand and dsDNA on the lagging strand (Abd Wahab, Choi et al., 2013, McGlynn & Lloyd, 2001). The basis for RecG's preference for branched structures was illustrated by a crystal structure of the *Thermotoga maritima* enzyme bound to a model replication fork, which revealed an N-terminal oligonucleotide/oligosaccharide (OB)-fold ("wedge") domain that engaged both leading and lagging template strands at the branch point, and that is connected to the motor by a helical linker (**Figure 2.2**) (Singleton et al., 2001). DNA remodeling is presumably catalyzed by dsDNA translocation by the motor tracking with 3′→5′ polarity on the lagging strand of the parental duplex toward the fork (Manosas et al., 2013, McGlynn & Lloyd, 2001), while the wedge domain aids unwinding of parental-nascent duplexes and possibly annealing of nascent strands to form the 4-way Holliday junction (Briggs, Mahdi et al., 2005, Singleton et al., 2001) (**Figure 2.1**).

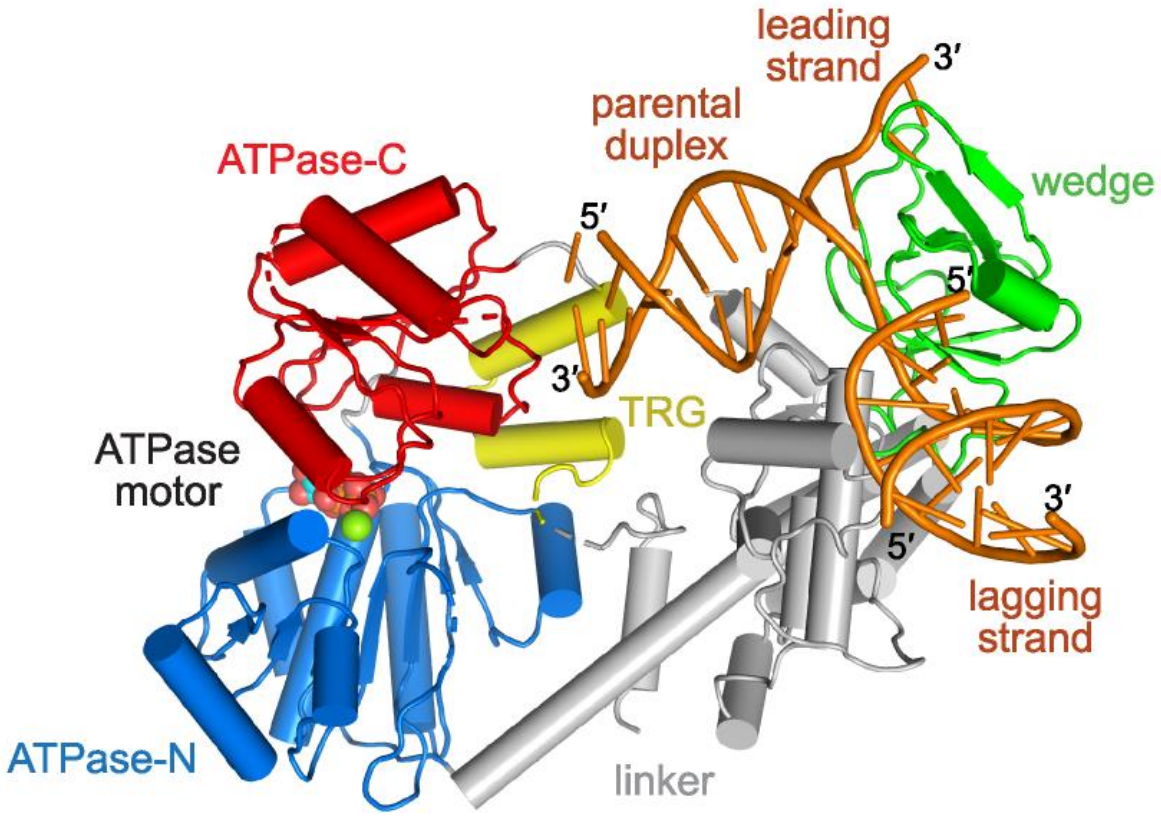

Figure 2.2 Crystal structure of RecG bound to fork DNA. Protein Data Bank (PDB) ID 1GM5. The protein is colored as in Figure 3.1, with the translocation in RecG (TRG) motif yellow and DNA orange.

How the motor domain engages DNA and how translocation is coupled to fork stabilization by the wedge domain to remodel a branched nucleic acid substrate is not entirely clear, in part because the DNA corresponding to the parental duplex template in the structure was too short to contact the ATPase motor (**Figure 2.2**). One clue for DNA translocation was provided by the identification of a conserved helical hairpin—the TRG (translocation in RecG) motif—in RecG and TRCF/Mfd (transcription-repair coupling factor), a bacterial SF2 helicase that translocates on dsDNA to terminate transcription (Chambers et al., 2003, Deaconescu et al., 2006, Mahdi et al., 2003, Park, Marr et al.,

2002). Mutagenesis of the TRG motif impaired fork reversal by RecG and displacement of RNA polymerase from DNA by TRCF/Mfd, and thus this motif is essential for DNA translocase activities in both proteins (Chambers et al., 2003, Mahdi et al., 2003). In RecG, the TRG motif is centrally located between the wedge and motor domains, but the TRG region predicted to lie in the path of the DNA was disordered in the crystal structure, and thus how it enables DNA translocation remains speculative (Deaconescu et al., 2006, Deaconescu, Savery et al., 2007, Mahdi et al., 2003, Savery, 2007).

In this study, we aimed to understand the role of the TRG motif and how the RecG motor engages parental DNA in the context of a fork. Using a combination of EPR spectroscopy and mutagenesis, we found that *T. maritima* RecG undergoes a conformational change in the ATPase motor relative to the wedge domain upon binding a model DNA replication fork. DNA binding is required to activate the ATPase activity and fork reversal activity, and therefore our EPR distance distributions provide insight into the operation of a DNA fork remodeling enzyme fully bound to a relevant DNA substrate in solution. In addition, we expanded on the previous TRG analysis (Mahdi et al., 2003) by showing that the conserved loop region C-terminal to the TRG motif is critical for ATP hydrolysis and fork reversal activity, and that mutations in the loop attenuate conformational changes induced by DNA binding. Our data support a model whereby the TRG loop is required for stabilizing the DNA-bound motor in an active conformation.

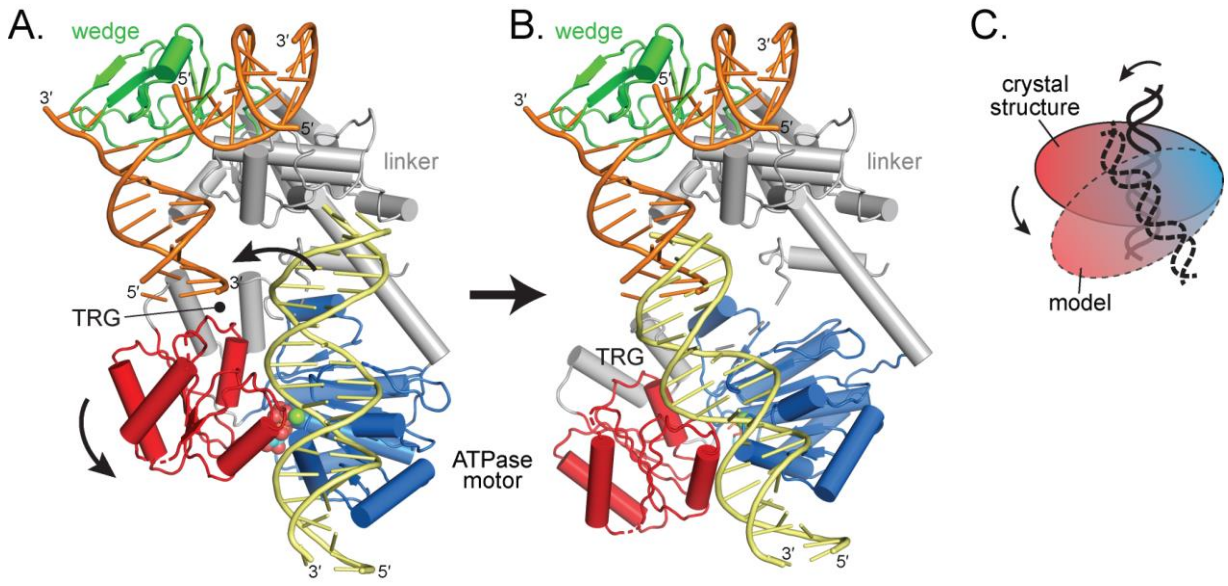

Figure 2.3 Reorientation of the RecG motor domain to accommodate parental DNA. **A.** The RecG/DNA crystal structure (PDB ID 1GM5), rotated 90° with respect to the view shown in Figure 3.2. The wedge domain is colored green, the linker domain is grey, and the ATPase motor is blue (N-lobe) and red (C-lobe). Parental DNA (yellow) was modeled by superposition of the XPB-ATPase and its bound DNA from the TFIIH complex (PDB ID 5IY9) onto the RecG-ATPase domain. The curved black arrow denotes the rotation of the motor domain necessary to align the helical axis of the modeled DNA to that of the crystal structure. **B.** Model of RecG bound to parental DNA after 30° rotation of the RecG motor and its accompanying DNA. **C.** Schematic of the rotation of the motor domain needed to bring parental duplex into alignment with the fork.

Results

Reorientation of the RecG Motor Domain to Accommodate the Parental DNA Duplex.

The RecG crystal structure illustrated how the wedge domain engages the branch point of a DNA fork (Singleton et al., 2001), but did not address the interaction of the motor domain with DNA or its relative conformation in the DNA bound state because the 10 base pairs (bps) of parental duplex used in the structure did not reach the motor domain (**Figure 2.2**). The structure predicts that at least 25 bps are necessary to fully engage the motor, consistent with DNase I footprinting showing that RecG protects a significant portion of the parental DNA duplex (Tanaka & Masai, 2006). To gain insight

into how the motor and wedge domains might collaborate in a fully bound DNA complex, we constructed a model of DNA bound to the motor domain using available structures of SF2 ATPase motors bound to dsDNA (**Figure 2.3a, Figure 2.6**). Recent cryo-EM structures of chromatin remodeling complexes CHD1, SNF2, INO80 bound to nucleosomes (Ayala, Willhoft et al., 2018, Eustermann, Schall et al., 2018, Farnung, Vos et al., 2017, He, Yan et al., 2016, Liu, Li et al., 2017) and of XPB helicase within the TFIIH component of the transcription pre-initiation complex (He et al., 2016) showed a conserved path of DNA across the N- and C-terminal lobes of the ATPase in a manner predicted from an archaeal Rad54 homolog bound to DNA in an open conformation (Durr, Korner et al., 2005). Superposition of the DNA from these structures onto RecG using the motor domain as a guide shows that the modeled and crystallized DNA duplexes are misaligned (**Figure 2.3a**). Alignment of these two DNA segments into a continuous parental duplex requires either a 25-40° bend in the DNA helical axis or rotation of the motor domain in which the ATPase-C lobe swings away from the wedge domain (**Figure 2.3b,c**).

To determine if DNA binding causes a conformational change within the protein, we used electron paramagnetic resonance (EPR) to determine the distances between domains upon addition of DNA. The four-pulse, double electron-electron resonance (DEER) technique provides probability distributions of the distances between spin-labeled residue pairs (McHaourab, Steed et al., 2011). Our experimental design was to place spin-labels in three domains—the linker that connects the wedge to the ATPase motor, the ATPase N-lobe connected to the linker, and the ATPase C-lobe (**Figure 2.4a**). The linker region is predicted to be relatively inflexible based on the network of centrally

located α-helices, whereas the C-lobe is likely more mobile given its peripheral location. We used the *Thermotoga* RecG protein for our experiments in order to correspond to the crystal structure (Singleton et al., 2001). The spin label [1-oxy-2,2,5,5-tetramethyl-pyrolline-3-methyl]-methanethiosulfonate (MTSL) was introduced at positions Glu144, Asn469, and Glu634, which were chosen on the basis of their surface exposed locations. After substitution of native cysteine residues to serine, non-native cysteines were introduced pairwise to produce E144C-E634C (pair 1), N469C-E634C (pair 2), and E144C-N469C (pair 3) mutants necessary for thiol conjugation of MTSL (**Figure 2.4a**). We verified that neither the Cys mutations nor the spin-labels affected the DNA dependent ATPase activity of the protein (**Figure 2.7a,b**). Continuous wave (CW) spectra of each MTSL-RecG protein were consistent with surface exposed sites (**Figure 2.7c**).

DEER data were collected in the absence and presence of a DNA fork similar to that crystallized but containing a 30-nucleotide parental duplex region (**Figure 2.4b**), long enough to span the motor domain (**Figure 2.3b**). In the absence of DNA, the distance distributions were consistent with those predicted from the crystal structures. The DEER traces for pairs 1 and 2 exhibited a significant change upon addition of DNA that are described by an ~10 Å increase in the center of the distance distribution and a decrease in the disorder as judged by a decrease in the width of the distance distribution (**Figure 2.4c**). This shift is consistent with the conformation change shown in **Figure 2.3c,** whereby the C-lobe moves away or rotates relative to both the N-lobe and

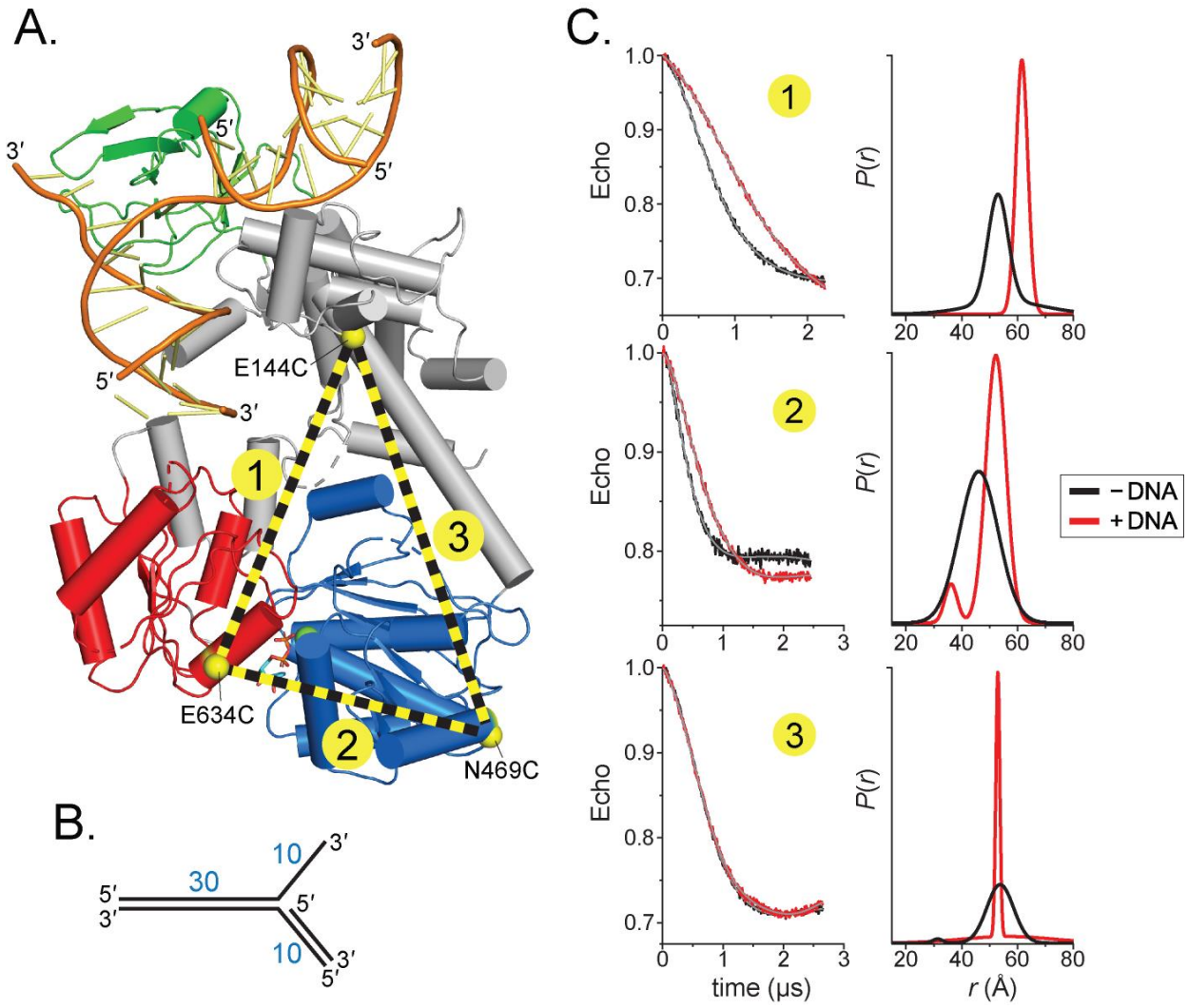

Figure 2.4 RecG changes conformation upon binding DNA. A. Cα carbons of MTSL-labeled cysteines are shown as yellow spheres and labeled on the RecG/DNA crystal structure (PDB ID 1GM5). MTSL pairs 1 (E144-E634), 2 (N469-E634), and 3 (E144-N469) are shown as yellow-black dashed lines. **B.** Schematic of the DNA fork used in electron paramagnetic resonance (EPR) experiments. **C.** Double electron-electron resonance (DEER) data for MTSL pairs 1, 2, and 3 in the absence (black) and presence (red) of DNA. **Left**, pairwise time domain data. **Right**, individual fits of the DEER data shown as a probability distribution (*P*) as a function of interatomic distance (*r*).

the linker. In contrast, the DEER traces for pair 3 were nearly identical in the absence and presence of DNA. The resultant pair 3 distance distributions were not identical, but did not indicate any shift in the median distance, suggesting that the N-lobe does not move

away upon addition of DNA. Taken together, the DEER measurements provide evidence for a RecG conformational change upon binding to a model replication fork and are consistent with the rotation of the ATPase domain predicted from our model (**Figure 2.3**).

Mutation of the TRG Motif Attenuates RecG Conformational Changes Upon DNA Binding

To gain additional insight into how RecG's motor domain engages DNA, we carried out a mutational analysis of residues predicted from our model to bind DNA. The parental DNA duplex is predicted to contact both N- and C-lobes of the ATPase domain and the TRG loop, which is part of the linker connecting the ATPase motor and wedge domains (**Figures 2.3a and 2.5a**). Importantly, the putative DNA binding cleft contains several loops that were disordered in the crystal structure, presumably because of the absence of bound DNA. We thus tested the functional importance of residues within these disordered regions, among others. Residues along the predicted DNA binding cleft, as well as those known to be involved in ATP hydrolysis, were mutated to alanine and the mutant proteins tested for DNA-dependent ATPase and fork reversal activities (**Figures 2.5b and 2.8**). None of the mutants showed a difference in DNA binding affinity relative to wild-type as measured directly using fluorescence polarization or electrophoretic mobility shift assays, consistent with previous mutational analysis of *Escherichia coli* RecG (Mahdi et al., 2003), presumably because tight binding of the wedge domain to the DNA junction masked any potential modest disruption in duplex DNA binding by the motor domain mutants (**Figure 2.10**) (Briggs et al., 2005). Because previous biochemical characterization of RecG has focused on the *E. coli* enzyme, we verified that the fork reversal activities of the *T. maritima* and *E. coli* enzymes are comparable (**Figure 2.9**).

Within the ATPase domain, residues in the N-lobe were found to have the most significant effects on RecG activity. We tested residues within motifs Ic and II, which in SF2 helicases are responsible for DNA binding (motif Ic) and ATP binding and hydrolysis (motif II) (Fairman-Williams et al., 2010, Pyle, 2008, Singleton et al., 2007). Alanine substitution of the conserved Thr478 in motif Ic led to a significant (10-fold) decrease in fork reversal activity without significantly affecting ATPase activity (**Figure 2.5b**), consistent with results from *Mycobacterium tuberculosis* RecG and RNA helicase NS3 (Lin & Kim, 1999, Zegeye, Balasingham et al., 2014). Also consistent with other helicases, mutation of motif II in *T. maritima* RecG (D497A E498A) completely abolished both fork reversal and ATPase activities (**Figure 2.5b**). Residues immediately C-terminal to motif II are conserved across RecG proteins and have been suggested to be important allosteric regulators of DNA-dependent ATP hydrolysis in *E. coli* PriA and RecQ (Windgassen & Keck, 2016, Zittel & Keck, 2005). Our RecG R501A F502A double mutant abrogated ATPase and fork reversal activities, likely because it disrupted the active site. Alanine substitution of Gln506 and Arg507, which were disordered in the RecG structure, had a much weaker effect on ATPase and fork reversal activities (**Figure 2.5b**). Similarly, mutation of residues in the ATPase C-lobe did not have a substantial effect on either ATP hydrolysis or fork reversal. Of the residues we tested, the largest effect was observed from mutation of conserved basic amino acid residues Arg622 and Lys628 within motif IVa (**Figure 2.5b**), which participates in nucleic binding in SF2 helicases and is in close proximity to the DNA backbone in the THFIIH, INO80, and SNF2 structures (Ayala et al., 2018, Eustermann et al., 2018, He et al., 2016, Liu et al., 2017).

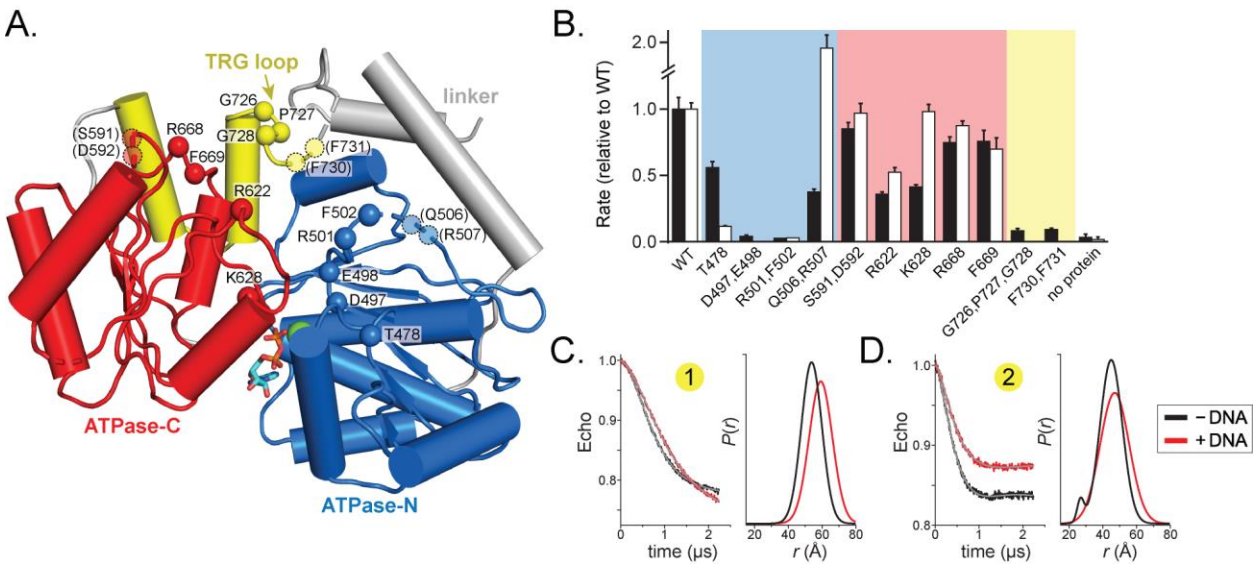

Figure 2.5. Loops within the TRG motif are essential for DNA-dependent ATP hydrolysis and fork reversal activity. A. Structure of the ATPase domain (blue and red) with residues lining the putative DNA binding surface shown as Cα spheres. The TRG hairpin and loop are colored yellow. Dashed lines represent disordered regions in the crystal structure. **B.** Relative DNA-dependent ATP hydrolysis (black bars) and fork reversal activities (white bars) of alanine mutants. Shading corresponds to the location of each mutant in the structure shown in panel a. Raw data and rates are shown in Figure S3. **C,D.** DEER measurements for spin-label pairs 1 **C.** and 2 **D.** in the TRG loop mutant, G726A P727A G728A. Pairwise time domain data and individual fits of the DEER data are shown on the left and right of each panel, respectively.

In contrast to the SF2 motor domain, mutation of the TRG motif had the most severe impact on RecG function. The TRG motif contains a highly conserved loop that was unstructured in the RecG structure and that lies directly in the proposed path of DNA binding (Singleton et al., 2001). Two separate mutants of this loop (G726A P727A G728A and F730A F731A) abrogated fork reversal and ATP hydrolysis (**Figure 2.5b**). Loss of activity by these mutants indicates that the TRG loop is important for binding DNA during translocation, facilitating interdomain movement by the motor during the ATPase cycle, or both. Indeed, the TRG loop lies at the intersection of the two ATPase lobes and the

wedge domain, directly in the proposed path of DNA and near helicase motifs III and VI, which coordinate ATP hydrolysis and translocation (motif III) and facilitate ATP binding and hydrolysis (VI) in other SF2 helicases (Fairman-Williams et al., 2010, Pyle, 2008).

To test the role of the TRG loop in RecG DNA-dependent conformation changes, we used EPR to measure interdomain distances in the dysfunctional TRG loop mutant, G726A P727A G728A. Spin labels were introduced into the mutant in the same location as the wild-type protein. We hypothesized that if the TRG loop mediates DNA binding or the DNA induced conformational change observed in the wild-type protein, then addition of DNA to the mutant would not affect the distance distributions. Indeed, the increase in spin label pair 1 distance upon addition of DNA reduced without the concomitant decrease in disorder compared to wild-type (**Figures 2.5c and 2.7d**). The TRG loop mutation showed an even greater effect on spin label pair 2, from which only a modest shift in distance was observed upon addition of DNA (**Figures 2.5c and 2.7d**). Therefore, we conclude that the loop C-terminal to the TRG motif mediates DNA-induced conformational changes within the motor, and likely couples motor domain dynamics to the fork-binding wedge domain to drive translocation.

Discussion

Coupling of an SF2 motor to a fork recognition domain is a conserved feature in the eukaryotic fork remodelers SMARCAL1, HLTF, and ZRANB3 (Kile et al., 2015, Mason, Rambo et al., 2014, Poole & Cortez, 2017), and thus it is important to understand how the two domains collaborate to drive fork reversal. By extrapolation from ssDNA translocation mechanisms of SF1 and SF2 helicases, the current model for dsDNA

translocation by the fork and chromatin remodelers entails conversion of an open to closed conformation of ATPase lobes upon binding DNA (Durr et al., 2005, Farnung et al., 2017, Lewis, Durr et al., 2008). DNA duplex binding along the interface of the two ATPase lobes places the tracking (3′→5′) strand in contact with motif Ia in the ATPase-N lobe and motif IV in the ATPase C-lobe. Consequently, ATP-induced conformational changes between the two ATPase lobes would drive an inchworm movement of the tracking strand and concomitant rotary motion of the duplex (Hopfner & Michaelis, 2007). As the fork recognition domain keeps the protein anchored to the junction (Briggs et al., 2005), DNA translocation would effectively pull the unwound template strands back into the protein, facilitating their annealing to each other and unwinding from nascent strands as they encounter the junction. This collaboration between motor and fork binding domains is analogous to INO80 chromatin remodeling machinery, which uses the ARP5 subunit to bind both histone and DNA in order to position the INO80 motor to pump DNA into the nucleosome (Ayala et al., 2018, Eustermann et al., 2018). Both mechanisms require an anchor point to grip the substrate to facilitate productive translocation by the motor.

Our EPR results revealed a DNA-induced movement of RecG's ATPase-C lobe relative to the positions of the ATPase-N lobe and the wedge domain. This motion can be modeled by a simple pivoting of the motor at the ATPase-N lobe, or a more complex rotation between the two ATPase lobes. The range of motion that we observe between RecG's two ATPase lobes is not as dramatic as that observed in fluorescence resonance energy transfer studies of an archaeal homolog of Rad54, a related SNF2-like dsDNA translocase (Lewis et al., 2008). Although we cannot say with certainty the nature of the

open and closed conformations of the motor domain from our distance measurements, the two ATPase lobes in the ADP-bound crystal structure are already well-positioned to accommodate dsDNA in a catalytic orientation. The motion of the motor with respect to the wedge that we observe is more striking, since it is clear that the relative positions of the motor and wedge in the crystal structure cannot support a contiguous parental DNA duplex without a rotation of the motor or a sharp bend in the helical axis of the DNA. The latter is unlikely since coupling motor activity to fork stabilization by the wedge domain would place tension on the DNA segment between the two domains. Moreover, the position of the motor domain observed in the crystal structure is constrained by a neighboring protein molecule in the crystal that pushes the motor closer to the wedge. Thus, our data supports a conformational transition from a more compact state in the absence of DNA to a more extended state upon engaging a fork.

Our mutational analysis of the relatively unstructured DNA binding surface of the ATPase domain is consistent with and extends the previous studies showing the TRG motif to be essential for RecG function (Mahdi et al., 2003). The previous mutational analysis focused on the helical hairpin itself, but it is the loop extending from the C-terminal end of the helical hairpin that resides in the path of the DNA and at the intersection of the motor and wedge domains, and that is likely the mechanical element directly responsible for DNA translocation. It was hypothesized that an ATP induced conformational change in the TRG helical hairpin, propagated through motif VI, would restructure the TRG loop to act as a lever or ratchet to mechanically move or stabilize the DNA in a new conformation (Mahdi et al., 2003). This TRG loop is highly conserved among RecG and Mfd orthologs, with the consensus sequence

G(P/A/V)GdΦΦGxxQ(S/T)G (where Φ is a hydrophobic residue). Mutation of the invariant glutamine (Q640) in *E. coli* RecG demonstrated that the TRG loop was essential for RecG activity *in vivo* (Mahdi et al., 2003). We now show by mutation of the GPG and ΦΦ residues in the *T. maritima* enzyme that this loop is essential for ATPase and fork reversal activities. More importantly, we found that disruption of the GPG sequence curtailed the range of DNA-induced interdomain motion, implying that this loop region is important for coupling motor and wedge domains. We hypothesize based on our DEER distance measurements that the TRG motif loop is required to stabilize an activated conformation of the ATPase domains upon DNA binding to promote ATP hydrolysis (Mahdi et al., 2003), similar to the postulated role of the brace helix in the chromatin remodelers (Ayala et al., 2018, Eustermann et al., 2018, Farnung et al., 2017, Liu et al., 2017, Yan, Wang et al., 2016). In those structures, the brace helix spans the two ATPase lobes and likely stabilizes a closed conformation through interaction of hydrophobic residues on the brace helix and the ATPase N-lobe. It may be that the conserved hydrophobic residues in the TRG loop that are essential for RecG activity may help to organize the two ATPase lobes in a similar manner.

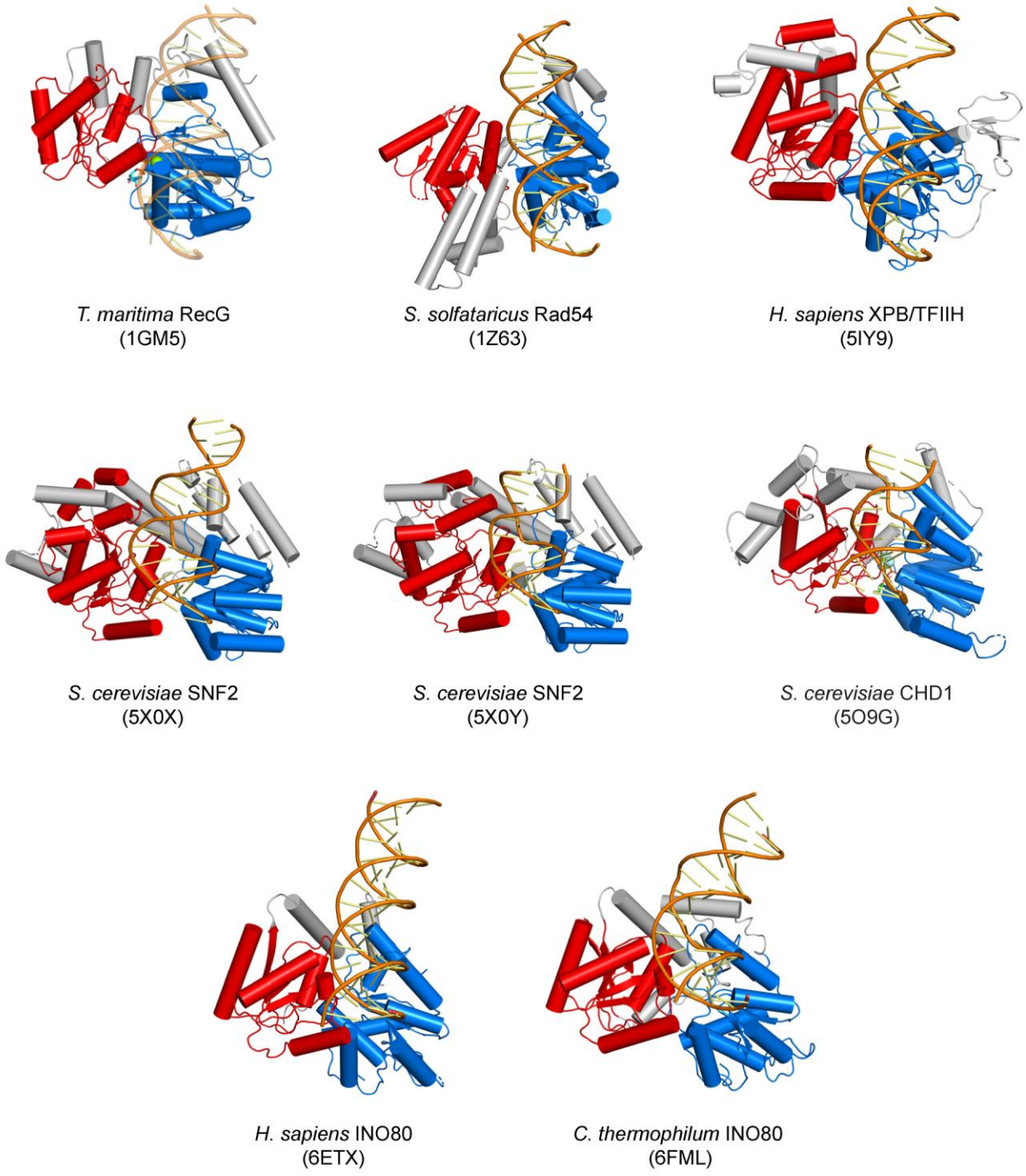

Figure 2.6 Duplex DNA binding by SF2 family remodelers. ATPase motor domains and the region of bound duplex DNA are shown from each structure. ATPase-N and –C subdomains are colored blue and red, respectively. Structures are aligned by their ATPase-N lobes. PDB ID codes are shown in parentheses below each structure. DNA bound to RecG is modeled from the XPB/TFIIH structure.

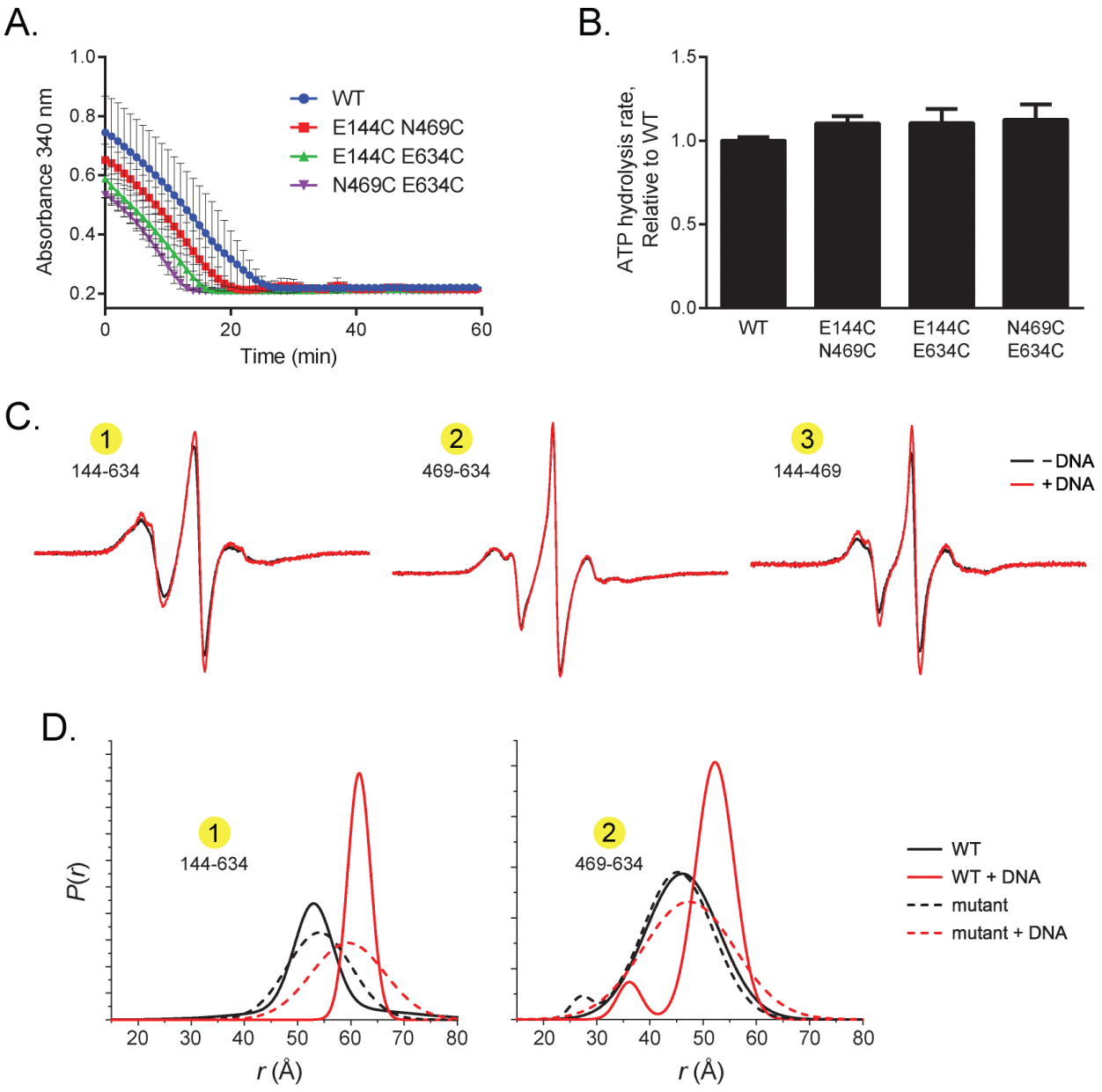

Figure 2.7 Activity of MTSL-labeled RecG proteins. A. Raw ATPase data from an NADH coupled assay of spin-labeled mutants. **B.** Relative ATPase activities of spin-label mutants relative to wild-type RecG, determined from slopes in panel A. **C.** Overlayed CW spectra for MTSL pairs 1 (E144-E634), 2 (N469-E634), and 3 (E144-N469) in the absence (black) and presence of DNA (red). **D.** Probability distributions for MTSL pairs 1 (E144-E634, *left*) and 2 (N469-E634, *right*) in wild-type (solid lines) and the G726A P727A G728A TRG loop mutant (dashed lines). Distributions for protein alone are black and RecG-DNA are red.

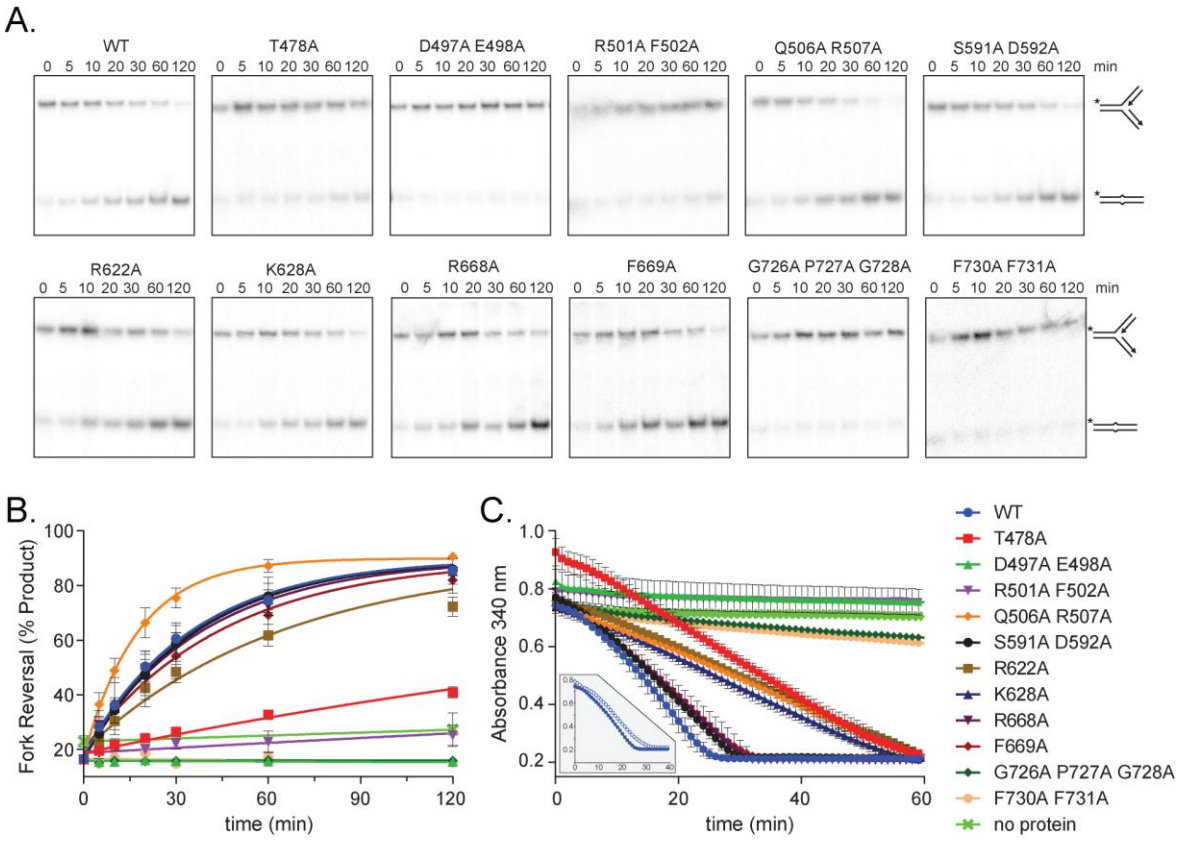

D.

	ATP hydrolysis (min^{-1})	Fork reversal ($\times 10^{-2}$ min^{-1})
WT	242 ± 21	2.9 ± 0.1
T478A	135 ± 11	0.3 ± 0.02
D497A E498A	10 ± 2	n.d.
R501A F502A	7 ± 2	0.09 ± 0.02
Q506A R507A	91 ± 5	5.6 ± 0.3
S591A D592A	206 ± 11	2.8 ± 0.2
R622A	87 ± 4	1.5 ± 0.1
K628A	100 ± 4	2.8 ± 0.2
R668A	181 ± 10	2.6 ± 0.1
F669A	183 ± 20	2.2 ± 0.2
G726A P727A G728A	20 ± 4	n.d.
F730A F731A	23 ± 2	n.d.
no protein	8 ± 6	0.06 ± 0.05

Figure 2.8 Fork reversal and ATP hydrolysis data from TmRecG-His$_6$ mutants. Shown is the raw data used to generate the relative rates in Figure 2.5b. **A.** Representative native PAGE fork reversal data. Lanes are time points in minutes. **B.** Quantitation of fork reversal data from three independent experiments (average ± S.D.). **C.** ATPase activity for WT protein incubated with the immobile Holliday junction used in all ATPase experiments (solid circles) and a reversible fork used in fork reversal assays (open circles). The corresponding rates are 240 min^{-1} (HJ) and 222 min^{-1} (fork). **D.** Rates extracted from data shown in panels B and C.

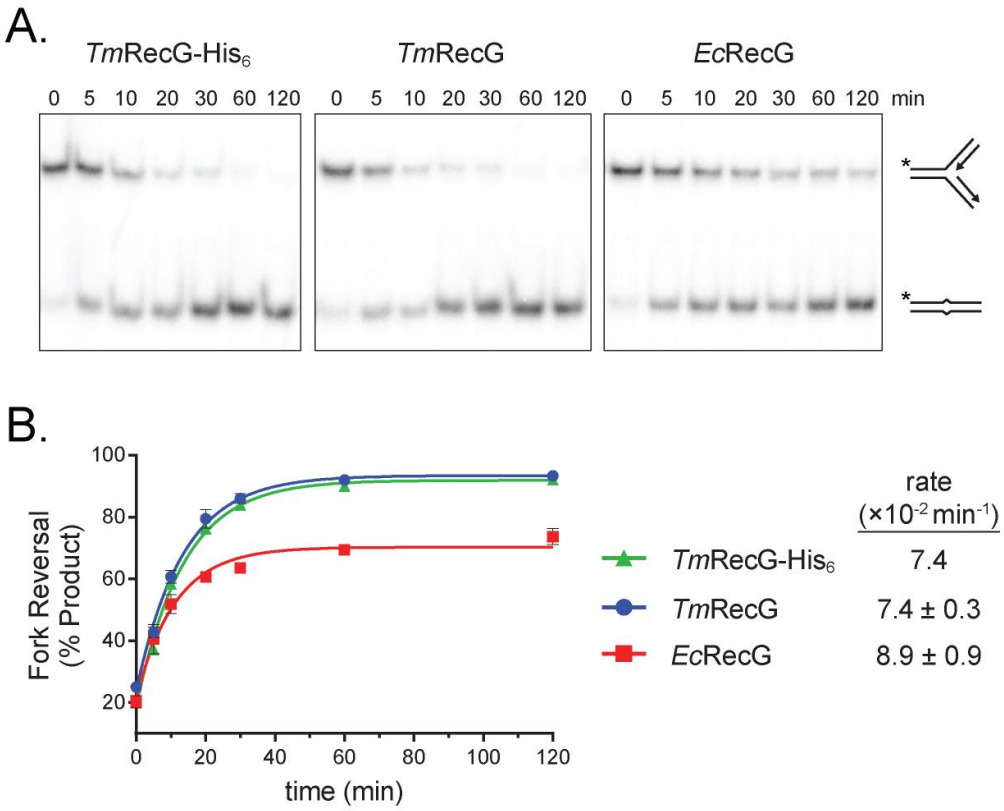

Figure 2.9 The C-terminal His-tag does not affect RecG activity. A. Representative native PAGE fork reversal data for a *T. maritima* RecG variant with or without a 3C protease-cleavable C-terminal His_6 tag, compared to wild-type *E. coli* RecG. Lanes are time points in minutes. **B.** Quantitation of fork reversal data from three independent experiments (average ± S.D.). The *Tm*-RecG-His_6 experiment was performed once. Rates extracted from fits to the data are shown to the right of the legend.

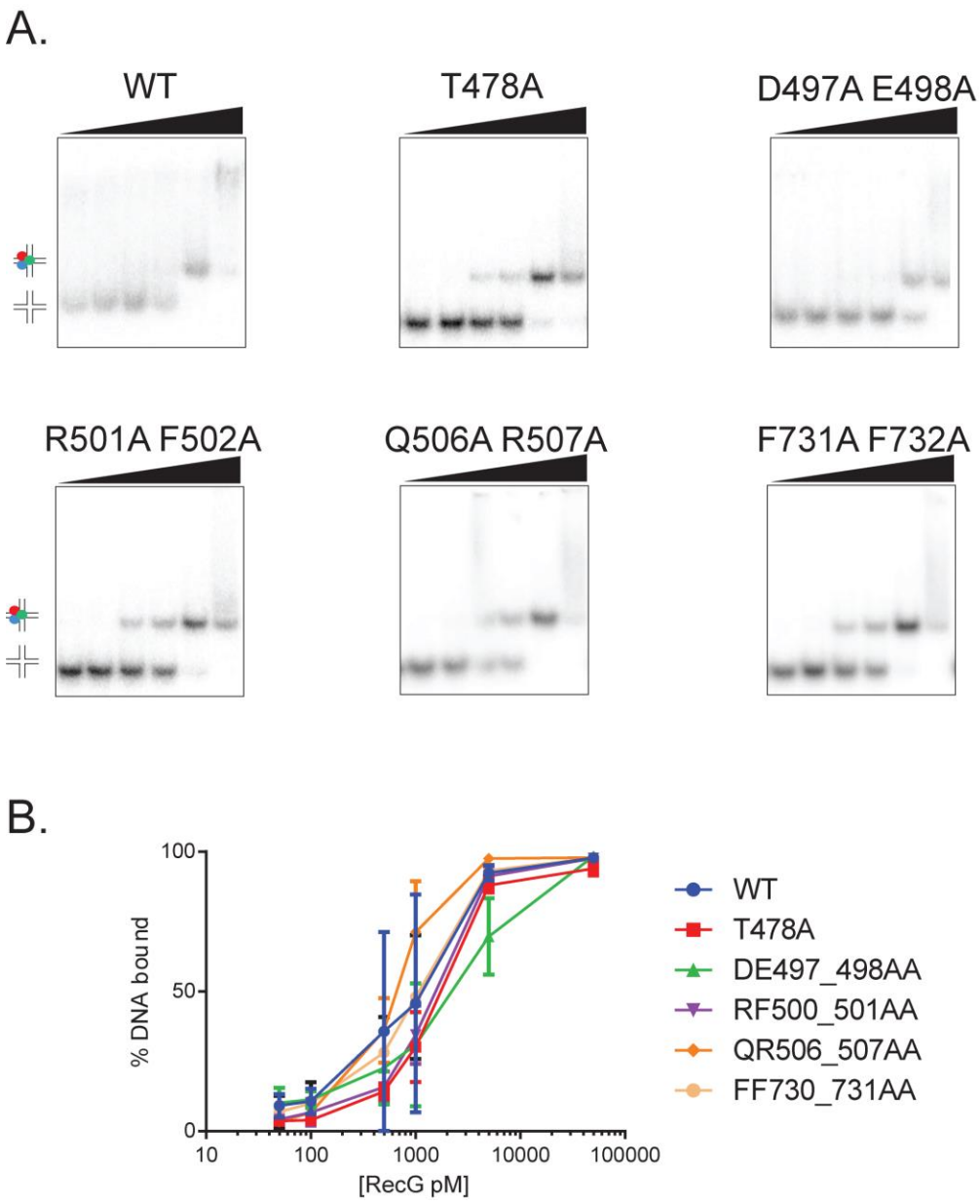

Figure 2.10 Mutations in the RecG motor domain do not reduce RecG DNA binding to Holliday Junctions. A. EMSAs of RecG and alanine mutants binding to 200 pM immobile Holliday junction DNA. Protein-DNA complex and DNA alone indicated by illustrations to the left of the gels. **B.** Quantification of the percent DNA shifted in triplicate (mean and S.D.) plotted on a logarithmic scale.

Materials and Methods

All experiments were carried out using *T. maritima* RecG containing a C-terminal hexahistidine tag (TmRecG-His_6). We verified that addition of the His_6 tag did not affect enzyme activity (**Figure 2.9**).

Protein Purification

TmRecG-His_6 was overexpressed from a pET28a$^+$-*TmrecG* vector (Bianco, Pottinger et al., 2017) in *E. coli* Tuner (DE3) cells at 37 °C for 3 hr in LB medium supplemented with 100 µg/mL kanamycin and 500 µM isopropyl β-D-1 thiogalactopyranoside (IPTG). Cells were lysed by sonication in buffer containing 50 mM Tris pH 7.5, 600 mM NaCl, 20% glycerol (v/v), 1 mM dithiothrietol (DTT), 1 mM phenylmethylsulfonyl fluoride, 0.5 µg/ml leupeptin, and 0.5 µg/ml aprotinin. The lysate was clarified by centrifugation at 50,000 x g at 4 °C for 45 min. RecG-His_6 was purified by Ni-NTA agarose affinity chromatography in buffer containing 50 mM Tris pH 7.5, 600 mM NaCl, 25 mM imidazole, 5% glycerol, and 1 mM tris(2-carboxyethyl)phosphine (TCEP) and eluted in buffer containing 50 mM Tris pH 7.5, 600 mM NaCl, 250 mM imidazole, 5% glycerol, 1 mM TCEP. RecG-His_6-containing fractions were subjected to heparin sepharose chromatography using a 0.1-1 M NaCl gradient in buffer containing 50 mM Tris pH 7.5, 100 mM NaCl, and 15% glycerol.

To test the effect of the C-terminal His_6-tag, we generated a cleavable pET-28a/RecG-3C-His_6 construct in which the His_6-tag could be removed with Rhinovirus 3C protease. Q5 mutagenesis kit (New England Biolabs) was used to replace the sequence K^{776}LIEVG^{781}*KLAAALE* (non-native residues italicized) in the pET28a$^+$-*TmrecG* vector

with the 3C recognition sequence LEVLFQGP. Proteolytic cleavage generates a 781-residue protein with I^{775}*LEVLFQ* sequence at the C-terminus. RecG-3C-His_6 protein was overexpressed and purified the same as TmRecG-His_6. The His_6-tag was removed by a 16-hr incubation with 3C protease after elution from the Ni-NTA column.

E. coli RecG was purified from a pGS772-RecG expression plasmid (Lloyd & Sharples, 1993) obtained from Dr. Piero Bianco as previously described (Betous et al., 2013), with an added heparin-sepharose purification step at the end.

Mutant RecG expression vectors were generated using the Q5 mutagenesis kit (New England Biolabs) and sequence verified prior to use. All mutant proteins were overexpressed the same as wild type protein. Alanine mutants were purified by Ni-NTA affinity chromatography, flash frozen, and stored at -80 °C in buffer containing 50 mM Tris pH 7.5, 600 mM NaCl, 250 mM imidazole, 5% glycerol (v/v), and 1 mM DTT. To prepare cysteine mutants for spin-labeling, all five native cysteines in RecG were first mutated to serine to generate a Cys-less RecG, which was then used to generate three separate double mutants (E144C N469C, E144C E634C, and N469C E634C). Cysteine mutant proteins were purified using Ni-NTA and heparin chromatography and stored at -80 °C in buffer containing 50 mM Tris pH 7.5, 600 mM NaCl, and 10% glycerol (v/v). Spin-labeling was carried out by incubating cysteine mutants with a 20-fold molar excess of MTSL for 2 hr at room temperature, followed by addition of another 20-fold molar excess of MTSL and incubation for 2 hr at room temperature and then overnight at 4 °C. Excess MTSL was removed using a HiTrap sephadex G-25 desalting column (GE Healthcare) in buffer containing 50 mM Tris pH 7.5, 500 mM NaCl, and 10% (v/v) glycerol.

EPR

Spin-labeled TmRecG-3C-His_6 protein was buffer exchanged using Amicon Ultra 15 mL centrifugal units 30 kDa MWCO (Millipore) into buffer containing 50 mM Tris pH 7.5, 100 mM NaCl, and 30% (w/w) glycerol. Fork DNA was prepared by annealing strands F1/F2/F3 (Table 1) in SSC buffer (15 mM sodium citrate pH 7.0 and 150 mM NaCl). A two-fold molar excess of DNA was added to 25-50 µM protein and the complex flash frozen in liquid nitrogen. DEER experiments were performed at 83 K on a Bruker 580 pulsed EPR spectrometer at Q-band frequency (33.5 GHz) using a standard four-pulse protocol (Jeschke, 2012). Analysis of the DEER data to determine $P(r)$ distance distributions was carried out in homemade software running in MATLAB (Mishra, Verhalen et al., 2014, Stein, Beth et al., 2015).

ATPase Assay

TmRecG-His_6 proteins were dialyzed against reaction buffer (50 mM Tris pH 7.5, 50 mM NaCl, and 5 mM $MgCl_2$) prior to use. An immobile Holliday junction with 30-bp arms was prepared by annealing the oligodeoxynucleotides J1/J2/J3/J4 (Table 1) in SSC buffer. ATPase reactions (100 µL) were carried out in reaction buffer and contained 50 nM TmRecG-His_6, 100 nM DNA, 1 mM ATP, 3 mM phosphoenol pyruvate (PEP), 437 µM nicotinamide adenine dinucleotide, 15.75-24.5 units/mL L-lactate dehydrogenase, 10.5-17.5 units/mL pyruvate kinase, and 1 mM DTT. Absorbance at 340 nm was monitored at 25 °C in 96-well plates using a Biotek Synergy H1 hybrid multimode microplate reader. Absorbance was recorded every 60 sec for 1 hr.

Table 1. Oligodeoxynucleotides used in this study.[1]

EPR
F1-(^{32}P)GGTCAGTCCTGTCTTCGGCAAAGCTCCATGATCATTGGCA
F2-CGCCGGGCCGCATGGAGCTTTGCCGAAGACAGGACTGACC
F3-CGGCCCGGCG
ATPase
J1-GGGTGAACCTGCAGGTGGGCCAGCTCCATGATCATTGGCAATCGTCAAGCTTTATGCCGT
J2-CGATGGACACGTCTTATGTGTGCAGTGCTCGCATGGAGCTGGCCCACCTGCAGGTTCACCC
J3-CATGTAGCGGCTGGCGTCTTAAAGATGTCCCGAGCACTGCACACATAAGACGTGTCCATCG
J4-ACGGCATAAAGCTTGACGATTGCCAATGATGGACATCTTTAAGACGCCAGCCGCTACATG
Fork Reversal[2]
F48-ACGCTGCCGAATTCTACCAGTGCCTTGCTAGGACATCTTTGCCCACCTGCAGGTTCACCC
F50-GGGTGAACCTGCAGGTGGGCAAAGATGTCC
F52-GGGTGAACCTGCAGGTGGGCAAAGATGTCCCAGCAAGGCACTGGTAGAATTCGGCAGCGTC
F53-GGACATCTTTGCCCACCTGCAGGTTCACCC

[1] Colors denote homologous regions. [2] Mismatch (underlined) placed at the junction to prevent spontaneous branch migration.

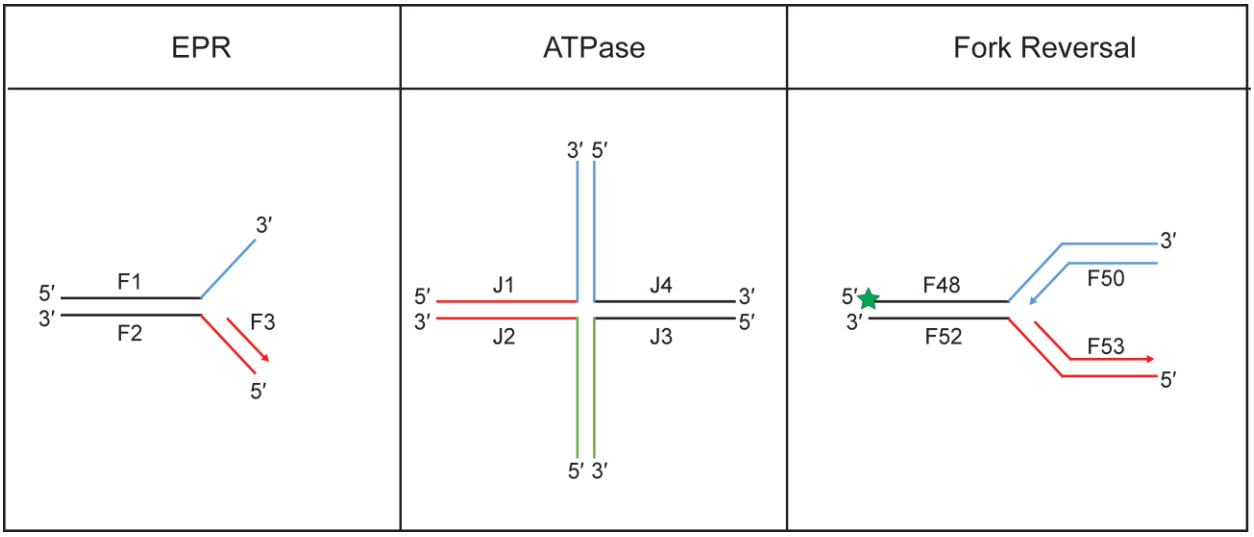

Figure 2.11 Oligodeoxynucleotide substrates used in this study. DNA strands listed in table 2.1 were annealed as described in materials and methods to produce the substrates depicted. Colors demonstrate homologous regions. Fork reversal substrates were 5′ labeled with ^{32}P (green star).

Fork Reversal Activity

Fork reversal activity was measured as previously described (Mason et al., 2014) with minor modifications. Reactions were performed in reaction buffer and contained 200 pM RecG and 1 nM ^{32}P-labeled DNA fork substrate (Table 1). Reactions were quenched at various times (0, 5, 10, 20, 30, 60, and 120 min) by adding proteinase K (Sigma-Aldrich) to a final concentration of 1 mg/mL and incubating for 10 min. Reactions were brought to 5% glycerol (v/v) and 0.1% bromophenol blue prior to electrophroesis on an 8% non-denaturing polyacrylamide gel at 5 W for 3 hr. Gels were exposed overnight to a phosphor plate and bands quantified by autoradiography using a Typhoon Trio and ImageQuant software (GE Healthcare).

CHAPTER III

DNA REPLICATION FORK REMODELING PROTEINS ZRANB3 AND SMARCAL1 ARE SENSITIVE TO BULKY LEADING STRAND DNA LESIONS

Introduction

In order to replicate the genome all domains of life employ a multiprotein complex called the replisome to open the parental DNA molecule and synthesize two new daughter DNA molecules. The replisome must complete this process both accurately and completely to avoid cell death or genome instability. Myriad impediments to the replisome exist including bound proteins, nucleobase modifications, and transcription conflicts (Zeman & Cimprich, 2014). These impediments to the replisome trigger a cascade of DNA repair pathways involving many proteins to restore proper DNA replication. One pathway that is employed to protect stalled replication forks is the fork reversal pathway (Bhat & Cortez, 2018). Fork reversal requires that the two parental strands of DNA are re-annealed while simultaneously the nascent strands anneal to form a four-way DNA junction referred to as a chicken foot structure or Holliday junction (Higgins et al., 1976). Holliday junctions are a substrate for multiple DNA repair pathways such as BER, NER, MMR, HR, or template switching. All of the aforementioned DNA repair pathways allow for error-free bypass of DNA lesions or other impediments to replication. Treatment of cells with various DNA damaging agents results in an elevated number of reversed replication forks caused by seemingly different mechanisms (Kolinjivadi et al., 2017, Sogo et al., 2002, Taglialatela et al., 2017, Vujanovic et al., 2017, Zellweger et al., 2015). Fork

stalling events must then be restored and replication restarted or replicated through by an adjacent replisome to preserve genome stability.

In eukaryotes there are three proteins—SMARCAL1, ZRANB3, and HLTF—that catalyze fork reversal efficiently *in vitro* and *in vivo* (Poole & Cortez, 2017). Each fork remodeling protein likely has a distinct cellular function and each catalyzes fork reversal to minimize genome instability. SMARCAL1 and ZRANB3 are members of the SMARCAL1-like subfamily of SNF2 translocases (Flaus et al., 2006). SMARCAL1 preserves genome stability in response to DNA replication stress and unlike the other SNF2-family fork remodelers acts to protect the replication of telomeres (Bansbach et al., 2009, Ciccia et al., 2009, Poole, Zhao et al., 2015, Postow, Woo et al., 2009, Yuan, Ghosal et al., 2009). SMARCAL1 contains a Replication Protein A (RPA) binding motif (RBM), two HARP domains, and a SF2 ATPase domain. Biallelic mutations in SMARCAL1 result in the human disease Schimke Imunno-osseus Dysplasia (SIOD) (Boerkoel et al., 2002). SMARCAL1 is recruited to sites of DNA replication stress by RPA where it is then able to reverse a stalled replication fork to protect the replication fork and preserve genome stability (Bansbach et al., 2009, Ciccia et al., 2009, Kolinjivadi et al., 2017, Taglialatela et al., 2017). SMARCAL1 is able to reverse forks *in vitro* with leading or lagging strand gaps but is inhibited when RPA is bound to the lagging parental stand and stimulated when RPA is bound to the leading parental strand (Betous et al., 2013). Stimulation of SMARCAL1 fork reversal activity by RPA bound to the leading strand fits a proposed model where stalled replication forks generate excess ssDNA that is immediately bound by RPA which might then require fork reversal to protect the stalled fork.

ZRANB3 is a 1079 amino acid protein that is recruited to stalled replication forks through its interactions with polyubiquitinated PCNA (Ciccia et al., 2012, Vujanovic et al., 2017). Loss of ZRANB3 function has been observed in human endometrial cancers (Lawrence et al., 2014). Like SMARCAL1, ZRANB3 reverses stalled replication forks during various forms of replication stress (Vujanovic et al., 2017). Unlike SMARCAL1, ZRANB3 is inhibited by RPA bound to the leading strand and there is no apparent effect on fork reversal activity when RPA is bound to the lagging strand (Betous et al., 2013). The substrate recognition domain of ZRANB3 is a HARP-like domain that binds dsDNA/ssDNA junctions similar to the HARP domains of SMARCAL1 (Badu-Nkansah et al., 2016). ZRANB3 also contains an HNH endonuclease domain that cleaves the dsDNA portion of dsDNA/ssDNA junctions when the junction cannot be remodeled (Badu-Nkansah et al., 2016, Sebesta et al., 2017, Weston et al., 2012).

HLTF is a member of the Rad5/16 subfamily of SNF2 translocases. HLTF is similar to ZRANB3 as it is believed to be a tumor suppressor and loss of function mutations are found in certain cancers. Indirect evidence exists for HLTF-mediated fork reversal in BRCA-1-deficient cells after replication stress. MRE11-dependent nuclease activity at stalled replication forks is rescued by the removal of HLTF, SMARCAL1, and ZRANB3. SNF2-family fork remodelers generate reversed replication forks that are degraded by MRE11 especially in BRCA1-deficient and BRCA2-dficient cell lines (Taglialatela et al., 2017). In addition to the SNF2 ATPase domain, HLTF contains a substrate recognition domain (HIRAN) that binds 3′ OH and an E3 ubiquitin ligase (RING) domain that is essential for the role of HLTF in polyubiquitinating PCNA upon certain forms of replication stress. Unlike the SMARCAL1-like family fork remodelers HLTF fork reversal activity is

not impeded or enhanced by RPA on either leading or lagging strand. HLTF fork reversal is so robust that it does not require the HIRAN domain to reverse a stalled replication fork (Chavez et al., 2018). Since HLTF does not require its substrate recognition domain to perform fork reversal it might have different fork reversal mechanisms than the SMARCAL1-like fork remodelers. Based on triplex displacement assays HLTF is thought to translocate 3′-5′ using the lagging parental strand as a tracking strand although both strands are required for translocation (Blastyak 2009). The tracking strand of ZRANB3 and SMARCAL1 is currently unknown and might further illuminate the cellular function of these fork-remodeling proteins.

Despite the importance of ZRANB3, SMARCAL1, and HLTF in the DNA damage response their mechanisms of dsDNA translocation and fork reversal are not known. Recent cryo EM structures of chromatin remodelers, which are evolutionarily related to SNF2-family fork remodelers, suggest that dsDNA translocation uses the lagging template strand for tracking and the leading template strand as a guide strand. The current model also suggests that SNF2 dsDNA translocases move along the minor groove of dsDNA and use a 1 bp step size to track along the phosphate backbones. Determining a mechanism of dsDNA translocation for the SNF2-family fork remodelers will require further structural studies, however, currently we can use biochemical approaches to gain insight into mechanisms used for ATP-dependent dsDNA translocation and fork reversal.

The diversity of cellular functions that have been identified for HLTF, ZRANB3, and SMARCAL1 might suggest different mechanisms of fork reversal or differences in DNA substrate preferences. Since these proteins are all activated by replication stress and are

required for genome stability it is plausible that each protein responds differently to different forms of DNA damage or is active at a particular step in the fork reversal pathway. To identify differences in the mechanisms of fork reversal by HLTF, ZRANB3, and SMARCAL1, we incorporated various DNA lesions into model DNA replication fork substrates and tested fork reversal activity on each substrate.

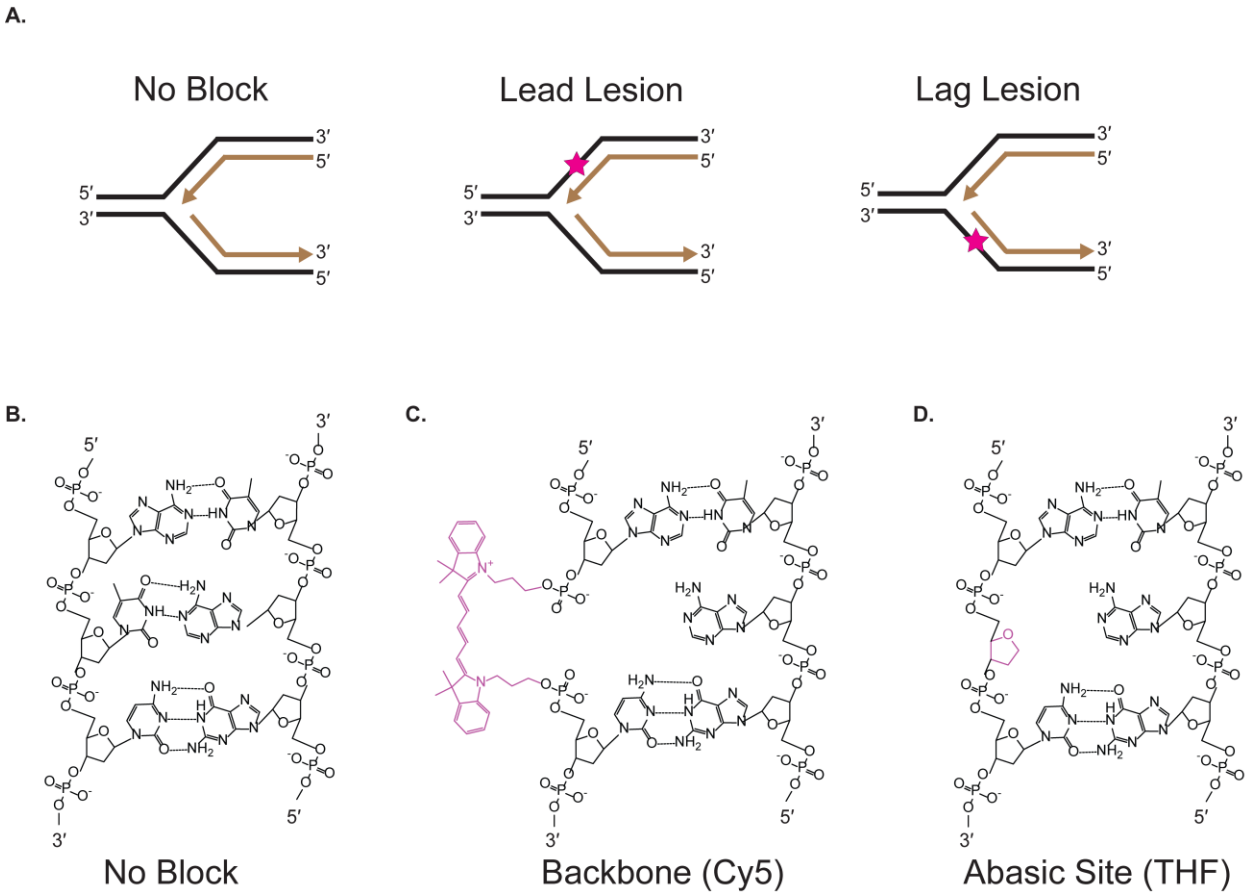

Figure 3.1 Lesions used to test fork reversal activity of the SNF2-family fork remodelers. A. Cartoon schematic of annealed fork DNA used for fork reversal activity assays. The template strands (black) are annealed to the nascent strand (brown) and the reversed products are quantified using native gels. Lesions (**C.** or **D.**) (magenta star) are incorporated on either the leading template strand or lagging template strand. **B.** Unmodified DNA with Watson-Crick base pairing. **C.** DNA containing an internal Cy5 lesion that replaces a single thymidine base. **D.** DNA containing a single THF lesion.

DNA translocation polarity and binding of helicases and translocases has been studied using diverse modifications to the DNA bases generally with larger adducts extending into the minor groove (Buechner, Heil et al., 2014, Pugh, Honda et al., 2008, Rudolf, Rouillon et al., 2010). Alternatively some DNA backbone specific modifications have been used to characterize the activity of DNA helicases and translocases such as polyglycol linkers, phosphorothiates, and reverse polarity DNA. It is important to note that reverse polarity DNA forms a duplex lacking major and minor groove dimensions and the minor groove is important for the translocation of SF2 ATPases like Werner and Bloom (Brosh, Karow et al., 2000). Interestingly, some DNA backbone modifications have been found *in vivo* and determining what effect they have on DNA processing enzymes such as helicases and translocases is important for understanding possible roles in carcinogenesis (Suhasini & Brosh, 2010). Modification of the phosphodiester backbone to form phosphotriesters has been observed in mice treated with n-nitrosodimethylamine (NDMA) and causes kidney and liver cancer (Shooter, 1978). NDMA is classified as a probable human carcinogen and is present in various meat products, water systems, tobacco smoke, and some alcoholic beverages (Najm & Trussell, 2001). Humans are exposed to various nitrosamines and so it is important for human health to understand how DNA processing enzymes respond to phosphotriester linkages. Base modifications have been used to attach streptavidin or fluorescent reporters to DNA to create a roadblock to translocation. One drawback to this approach is that the modifications typically sit in the major groove of the DNA and all structures of SNF2 proteins bound to dsDNA using cryo-EM and X-ray crystallography have demonstrated that the SNF2 motor domains contact the minor groove of DNA. Since a majority of contacts to dsDNA are

through the phosphate backbone in the existing structures of SNF2 proteins bound to dsDNA we sought to modify the backbone of the DNA substrates used in our assays as well as test substrates containing non-bulky lesions known to stall replication such as an AP site mimetic.

Results

SMARCAL1-Like Subfamily dsDNA Translocases are Distantly Related SNF2 dsDNA Tranlocases

SNF2-family chromatin remodelers all appear to engage with dsDNA in a similar manner. SNF2-family fork remodelers SMARCAL1, ZRANB3, and HLTF are evolutionarily related to the chromatin remodelers and it is likely that a mechanism of dsDNA translocation is similar across the SNF2 family. Applying structural data from chromatin remodelers, we know that leading template strand lesions would be present on the guide strand that is in contact with motif IIa and motif Vb while lagging template strand lesions would be present in the tracking strand that is in contact with motifs Ia, Ic, IV, and V. What is interesting is that in SMARCAL1 and ZRANB3, a divergent subfamily of the SNF2 family, the motifs that contact the dsDNA in cryo-EM structures of chromatin remodelers have noticeably different sequences. SMARCAL1 and ZRANB3 motifs IIa, IV, and Vb are highly conserved across vertebrate species but contain sequences unlike other SNF2 dsDNA translocases (**Figure 3.2**). Even HLTF maintains the sequences observed in other SNF2 ATPases in the motifs used to contact the duplex DNA. To determine if sequence differences between the SMARCAL1-like subfamily and other SNF2 ATPases holds any relevance we tested the fork reversal activity of ZRANB3 and

SMARCAL1 and compared it to the activity of HLTF when presented with varying DNA lesions.

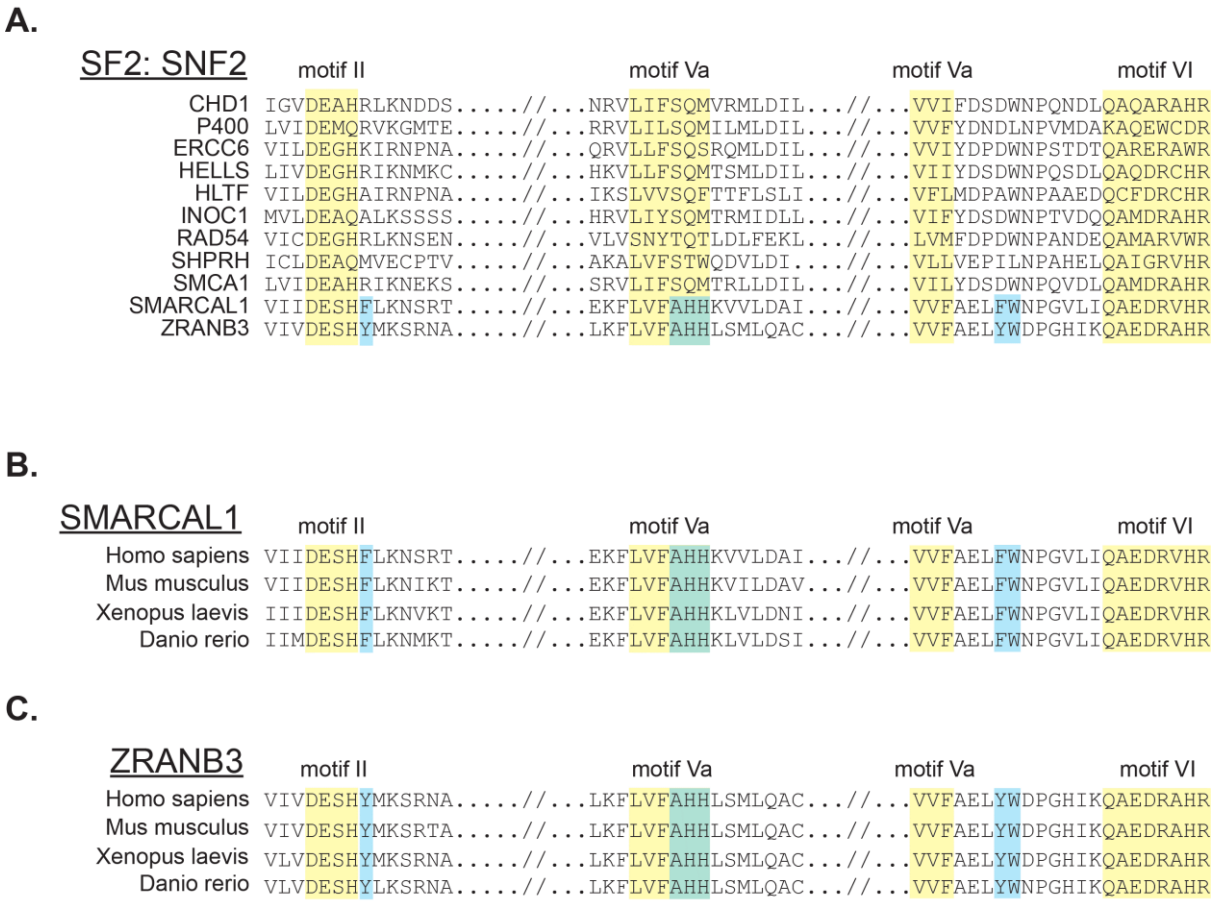

Figure 3.2 Sequence alignments of conserved SNF2 ATPase motifs known to contact nucleic acid. A. Sequence alignment of conserved human SNF2 ATPase motifs (yellow) and adjacent sequences known to contact DNA (blue). ZRANB3 and SMARCAL1 have different amino acid sequences in regions known to contact DNA relative to other SNF2 ATPases (blue). **B.** SMARCAL1 and **C.** ZRANB3 contain divergent sequences adjacent to conserved SNF2 ATPase motifs that are conserved in vertebrates (blue).

ZRANB3 and SMARCAL1 Fork Reversal Activity is Blocked by Leading Template Strand Cy5 Lesions

ZRANB3 and SMARCAL1 are members of the most distantly related subfamily of SNF2 proteins. Evidence from DNA footprinting assays has demonstrated that SMARCAL1 preferentially protects the leading template strand of a model replication fork from benzonase mediated DNAse activity (Betous 2013). In the same study it was revealed that ZRANB3 fork reversal activity is blocked by leading strand RPA on a stalled replication fork. Therefore there is evidence that both of these distantly related SNF2 motor proteins engage with the leading strand of DNA replication forks differently than other known fork remodeling enzymes (Blastyak, Hajdu et al., 2010, Manosas et al., 2013, Manosas, Perumal et al., 2012). We performed fork reversal assays to investigate whether SMARCAL1 and ZRANB3 are impeded disproportionately by modifications to one template DNA strand over the other. Since the current model for translocation by SF2 ATPases requires translocation along the phosphate backbone of DNA we sought to place a bulky lesion between adjacent phosphates of the same DNA strand. In order to test distortions to the DNA backbone we incorporated a Cy5 molecule internally between two phosphate groups of the DNA leaving a 1 base gap in the duplex with a bulky fluorescent reporter protruding from the phosphodiester backbone (**Figure 3.1**). In agreement with previous results HLTF does not demonstrate a strong preference for Cy5 lesions in either strand suggesting a robust motor domain able to overcome impediments (**Figure 3.3**). Surprisingly ZRANB3 fork reversal activity is blocked by a Cy5 lesion in the leading template strand and not the lagging template strand (**Figure 3.3**). SMARCAL1 shares the same phenotype as ZRANB3 but to a lesser extent when encountering Cy5

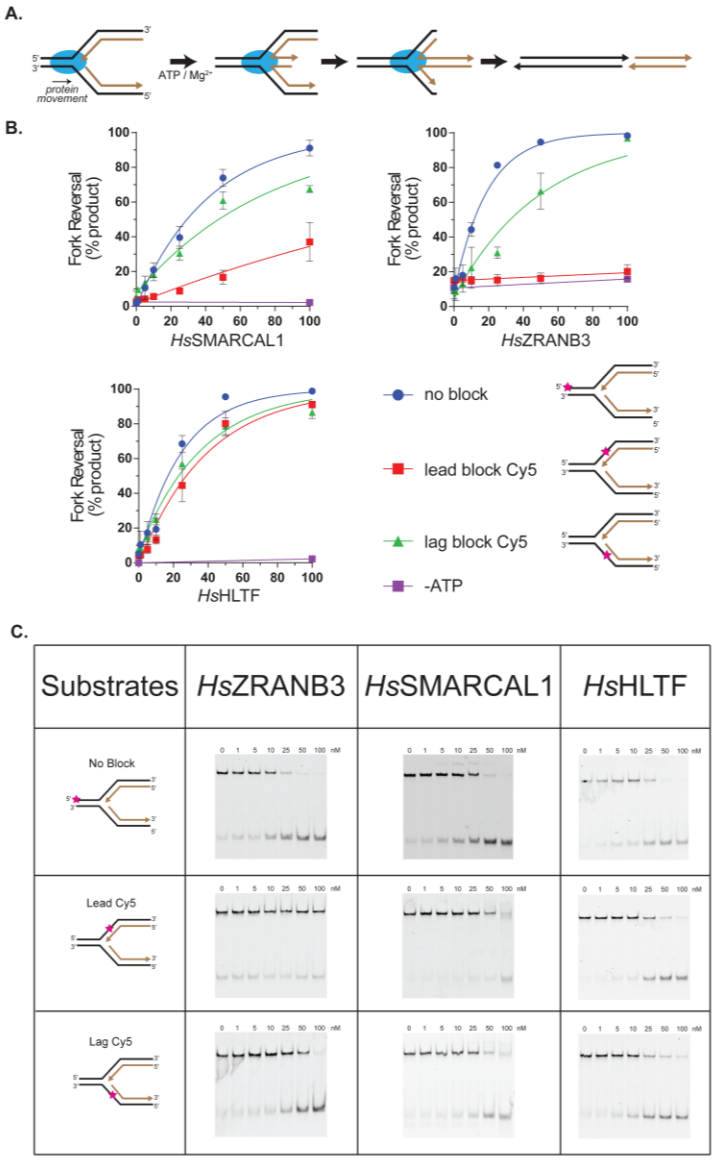

Figure 3.3 Bulky leading template strand lesions block ZRANB3 and SMARCAL1 fork reversal activity. A. Schematic of DNA replication fork reversal by a fork remodeling protein (blue) requiring ATP and Mg2+ for activity on a model DNA replication fork 5′ Cy5 labeled (magenta star) with template strands (black) and nascent strands (brown). **B.** Quantification of fork reversal assays performed in triplicate (mean and S.D.) for HsHLTF, HsSMARCAL1, and HsZRANB3 with the three DNA fork substrates shown on the right (magenta star depicts the location of a Cy5 lesion). **C.** Representative native gels for fork reversal assays performed with ZRANB3, SMARCAL1, or HLTF on an unmodified DNA fork, a leading Cy5 lesion containing fork, and a lagging Cy5 lesion containing DNA fork. DNA substrates used in fork reversal activity assays are on the left with the Cy5 location labeled by a star (magenta). Fork reversal activity assays were performed in triplicate with increasing concentrations of ZRANB3, SMARCAL1, or HLTF (0, 1, 5, 10, 25, 50, 100 nM) at 37°C for 30 minutes. One representative gel is shown for each DNA fork substrate.

lesions in the leading template strand (**Figure 3.3**). It is interesting that neither enzyme is overwhelmingly impeded by Cy5 modification on the lagging template strand (**Figure 3.3**). Another robust fork remodeler, RecG, found in bacteria was also tested for fork reversal activity against Cy5 lesions. RecG like HLTF was not impeded by Cy5 lesions in either template strand. The activity of RecG further demonstrates that some fork remodelers are sensitive to DNA backbone modifications while others are not.

SNF2-Family Fork Remodelers are Not Impeded by THF Lesions

Having tested modifications to the backbone we sought to investigate whether an abasic site that is known to stall DNA polymerases would have an effect on the fork reversal activity of SNF2-family fork remodeling proteins (Haracska, Unk et al., 2001). Since the backbone is unimpeded by this substrate modification it might be that the duplex distortion or recognition by a substrate recognition domain might account for any differences seen in the fork reversal activity assays. Neither HLTF nor ZRANB3 were impeded by a THF lesion present in the leading template strand or lagging template strand (**Figure 3.4**) suggesting that the mechanism of fork reversal is not reliant on contact with the nucleobases of the template DNA. Unexpectedly SMARCAL1 fork reversal activity was slightly enhanced by the presence of a THF modification in the lagging template strand (**Figure 3.4**). The enhancement of SMARCAL1 fork reversal activity could be due to substrate recognition by the HARP domains or the mechanism of translocation by the ATPase domain.

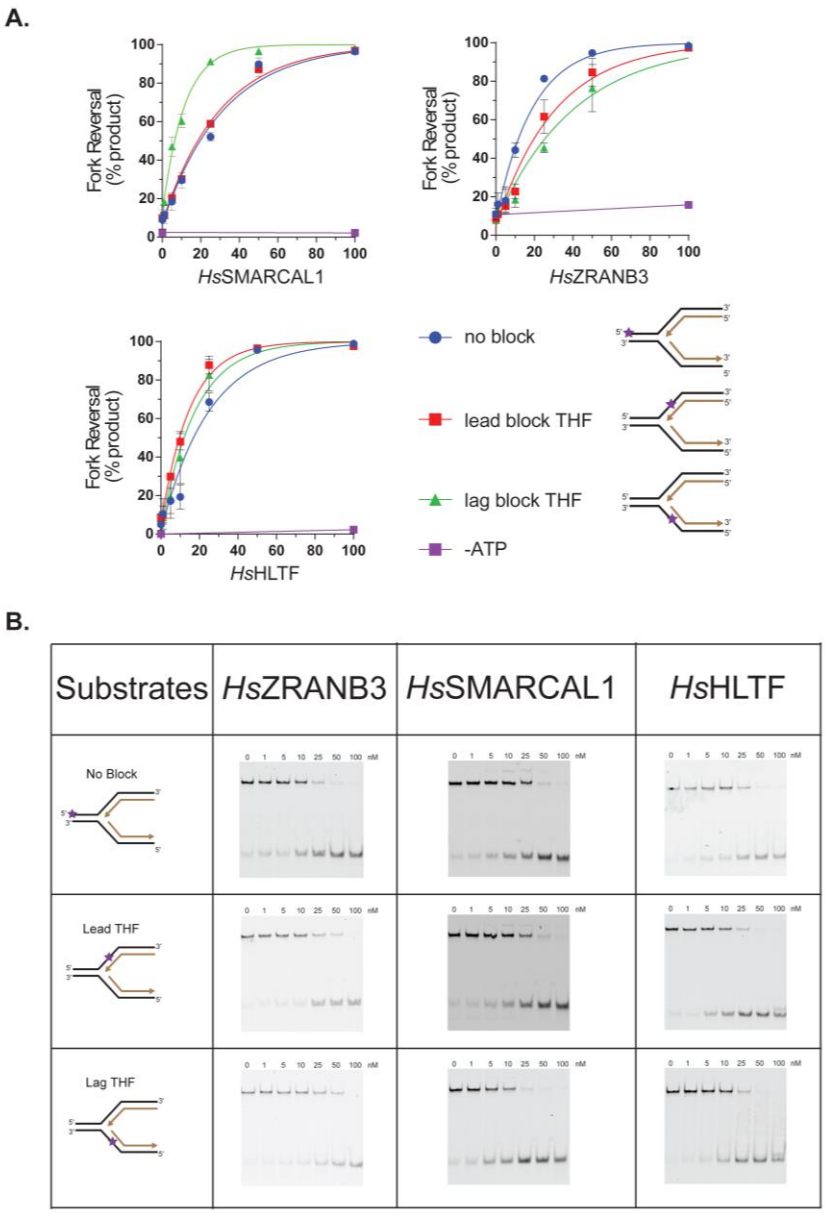

Figure 3.4 THF lesions do not inhibit the SNF2-family fork remodelers. A. Quantification of fork reversal assays performed in triplicate (mean and S.D.) for HsHLTF, HsSMARCAL1, and HsZRANB3 with the three DNA fork substrates shown on the right (purple star depicts the location of a THF lesion). **B.** Representative native gels for fork reversal assays performed with ZRANB3, SMARCAL1, or HLTF on an unmodified DNA fork, a leading THF lesion containing fork, and a lagging THF lesion containing DNA fork. DNA substrates used in fork reversal activity assays are on the left with the THF lesion location labeled by a star (purple). Fork reversal activity assays were performed in triplicate with increasing concentrations of ZRANB3, SMARCAL1, or HLTF (0, 1, 5, 10, 25, 50, 100 nM) at 37°C for 30 minutes. One representative gel is shown for each DNA fork substrate.

Discussion

Presently, all SF2 motors that translocate on dsDNA have a 3′-5′ polarity for the tracking strand. Here we show that fork reversal by ZRANB3 and SMARCAL1 is blocked when a Cy5 lesion is present on the leading template strand rather than the lagging template strand of fork reversal activity assay DNA substrates. Our data suggests that ZRANB3 and SMARCAL1 might translocate on dsDNA with a 5′-3′ polarity or that accessory domains are inhibited by bulky leading strand lesions. If ZRANB3 and SMARCAL1 translocate with a 5′-3′ polarity they would require a new model for dsDNA translocation. If a substrate recognition domain is responsible for the phenotype observed then it would suggest that the substrate recognition domains dictate the context of fork reversal for ZRANB3 and SMARCAL1. Our findings suggest that despite similarities the fork remodeling enzymes ZRANB3, SMARCAL1, and HLTF have different mechanisms of fork reversal and translocation that may diversify cellular function.

Previous DNA footprinting assays have revealed that SMARCAL1 protects the parental leading strand from nuclease activity (betous 2013), which suggests a mechanism whereby SMARCAL1 tracks along the leading parental duplex. Since ZRANB3 is part of the same distantly related subfamily of SNF2 motors as SMARCAL1 (Flaus et al., 2006) it is reasonable to propose that the motor domain of ZRANB3 might share a mechanism of dsDNA translocation with SMARCAL1. Sequence alignments of all SF2 motors demonstrate that SMARCAL1 and ZRANB3 contain highly conserved sequences at motifs IIa, IV, and Vb that are known to interact with DNA. The sequences near DNA binding motifs are strikingly different and conserved when compared to all other SNF2 proteins including HLTF (Fairman-Williams et al., 2010).

Alternatively the substrate recognition domains of SMARCAL1 or ZRANB3 could dictate the fork reversal substrate preferences observed. ZRANB3 contains an HNH endonuclease domain that cleaves the backbone on the leading strand of a fork junction (Sebesta et al., 2017). Since ZRANB3 is blocked by a leading template strand Cy5 lesion but not a lagging template strand Cy5 lesion this might suggest that the HARP-like SRD or the HNH endonuclease domain of ZRANB3 have direct interactions with the leading strand phosphate backbone and that modification of the DNA backbone sterically hinders association with the DNA fork. Previous work that demonstrates ZRANB3 fork reversal activity inhibition by leading strand RPA also supports this hypothesis although the phenotype resulting from translocation block of the motor domain still cannot be ruled out in either case (**Figure 3.5**). Polyubiquitinated PCNA is essential for the recruitment of ZRANB3 to stalled replication forks and the fork reversal activity of the enzyme *in vivo* so it remains an open question as to how the presence of PCNA or polyubiquitinated PCNA would alter the fork reversal mechanism of ZRANB3 (Ciccia et al., 2012, Vujanovic et al., 2017).

In SMARCAL1 it is plausible that the two HARP domains dimerize like the structurally similar PUR repeats to bind either side of a fork ssDNA junction and that one binding site is more important for interaction with the fork (Betous et al., 2012, Graebsch, Roche et al., 2009). If the HARP domains must associate with ssDNA at the junction then bulky lesions could alter the fork reversal mechanism in SMARCAL1.

Finally the DNA constructs used in the study might have an effect on the fork reversal assays. Placement of the damage 5 bp from the DNA junction ensures that the enzyme must bypass the modification in some way and that spontaneous branch

migration after initiation of fork reversal past the A:C mismatch is not masking any effect of the modification on fork reversal. It is worth noting however that based on studies of the bacterial fork remodeler RecG the dsDNA is expected to extend 20-25 bp from the junction into the motor (Tanaka & Masai, 2006). Therefore by the time the SRD is at the end of the fork reversal substrate the motor domain has just reached the position of the lesion (**Figure 3.5**). Testing longer substrates might rule this interpretation out, however, where the SRD sits in relation to the ATPase domain for SNF2-family fork remodelers remains speculative and might be more similar to the bacteriophage fork remodeler UvsW where the SRD, a HARP domain like that of SMARCAL1, is located directly on the ATPase domain.

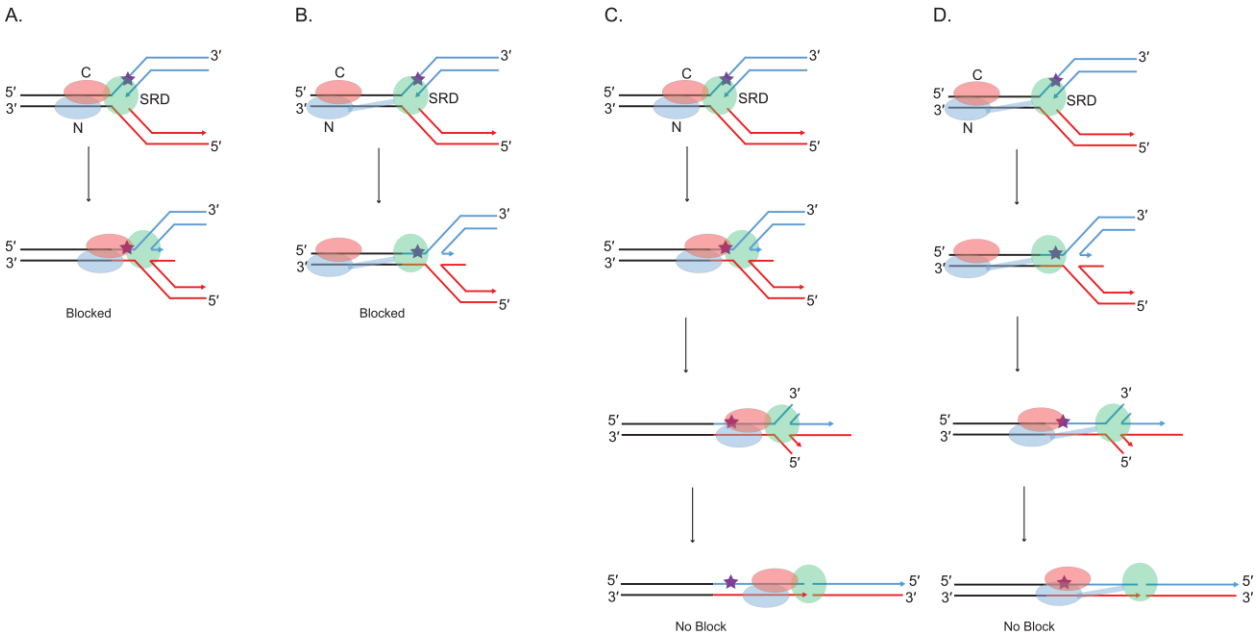

Figure 3.5 Models for leading template strand blocks to SNF2-family fork remodelers. A. Model fork remodeler with N (blue) and C (red) ATPase domains and SRD (green). Model for a fork remodeler ATPase domain blocked by DNA damage (purple star). **B.** Model for a fork remodeler SRD blocked by DNA damage. **C.** and **D.** Model for an extended or compact fork remodeler completing fork reversal and bypassing DNA damage.

Materials and Methods

Protein Purification

His_6-SMARCAL1 was cloned into pFastBac-HTb vector (Invitrogen) and expressed in bacolovirus-infected Hi5 insect cells. Cells were harvested and centrifuged at 1000xg. Pellets were stored at -80°C. Cell pellets were thawed and lysed using a dounce homogenizer in buffer (20 mM HEPES pH 7.6, 300 mM NaCl, 2 mM $MgCl_2$, 0.5 mM TCEP, 20% glycerol, 0.2 mM PMSF, and 10 mM Imidazole) and protein purified by Ni-NTA affinity chromatography, eluting with buffer (20 mM HEPES pH 7.6, 50 mM NaCl, 2 mM $MgCl_2$, 0.5 mM TCEP, 20% glycerol, 0.2 mM PMSF, and 250 mM Imidazole). Protein was then purified over a Superdex S200 size exclusion column (GE Healthcare) in buffer (20 mM HEPES pH 7.6, 20% glycerol, 200 mM NaCl, 2 mM $MgCl_2$, and 0.5 mM TCEP), concentrated using an Amicon-Ultra 30-kDa concentrator and stored at -80°C.

FLAG-ZRANB3 was cloned into pFastBac-HTb vector (Invitrogen) and expressed in bacolovirus-infected Hi5 insect cells. Cells were harvested and centrifuged at 1000xg. Pellets were stored at -80°C. Cell pellets were thawed and lysed using a dounce homogenizer in buffer (20 mM HEPES pH 7.6, 500 mM KCl, 1.5 mM $MgCl_2$, 1 mM DTT, 0.2 mM EDTA, 20% glycerol, 0.2 mM PMSF, 0.01% NP-40 (v/v), 1 ug/uL leupeptin, 1 ug/uL aprotonin, and 1 ug/uL pepstatin) and protein purified by FLAGM2 affinity chromatography (sigma), eluting with buffer (20 mM HEPES pH 7.6, 100 mM KCl, 1.5 mM $MgCl_2$, 1 mM DTT, 0.2 mM EDTA, 20% glycerol, 0.2 mM PMSF, 0.01% NP-40 (v/v), 250 mg/mL FLAG peptide). Protein was buffer exchanged into buffer (20 mM HEPES pH 7.6, 100 mM KCl, 1.5 mM $MgCl_2$, 1 mM DTT, 0.2 mM EDTA, 20% glycerol, 0.2 mM PMSF,

0.01% NP-40 (v/v), 1 ug/uL leupeptin, 1 ug/uL aprotonin, and 1 ug/uL pepstatin), concentrated using an Amicon-Ultra 30-kDa concentrator, and stored at -80°C. His_6-MBP-HLTF was purified as previously described (Chavez *et al*, 2018).

Fork Reversal Activity

Fork reversal activity was measured as previously described (Mason 2014) with minor modifications. Fork reversal activity assays containing *Hs*SMARCAL1 were performed at 37 °C in buffer containing 40mM HEPES pH 7.6, 20mM KCl, 5mM MgCl, 2mM ATP, 1mM TCEP, 100 ug/mL BSA and 5 nM DNA fork substrate. Reactions with varying concentration of *Hs*SMARCAL1 (0, 1, 5, 10, 25, 50, 100 nM) were quenched after 30 minutes by adding proteinase K (Sigma-Aldrich, St. Louis, MO, USA) to a final concentration of 1 mg/mL and incubating for 10 minutes.

Fork reversal activity assays containing *Hs*HLTF were performed at 37 °C in buffer containing 40mM Tris pH 7.6, 50mM NaCl, 5mM MgCl, 2mM ATP, 1mM TCEP, 100 ug/mL BSA and 5 nM DNA fork substrate. Reactions with varying concentration of *Hs*HLTF (0, 1, 5, 10, 25, 50, 100 nM) were quenched after 30 minutes by adding proteinase K (Sigma-Aldrich, St. Louis, MO, USA) to a final concentration of 1 mg/mL and incubating for 10 minutes.

Fork reversal activity assays containing *Ec*RecG were performed at 37 °C in buffer containing 20mM Tris pH 7.5, 50mM NaCl, 5mM MgCl, 2mM ATP, 100 ug/mL BSA and 5 nM DNA fork substrate. Reactions with varying concentration of *Ec*RecG (0, 10, 50, 100, 250, 500, 1000 pM) were quenched after 30 minutes by adding proteinase K (Sigma-Aldrich, St. Louis, MO, USA) to a final concentration of 1 mg/mL and incubating for 10 minutes.

Fork reversal activity assays containing *Hs*ZRANB3 were performed at 37 °C in buffer containing 40mM Tris pH 7.5, 100 KCl, 5mM MgCl2, 2mM ATP, 100 ug/mL BSA and 5 nM DNA fork substrate. Reactions with varying concentration of *Hs*ZRANB3 (0, 1, 5, 10, 25, 50, 100 nM) were quenched after 30 minutes by adding proteinase K (Sigma-Aldrich, St. Louis, MO, USA) to a final concentration of 1 mg/mL and incubating for 10 minutes.

Reactions were brought to 5% glycerol (v/v) prior to electrophoresis on an 8% non-denaturing polyacrylamide gel at 5W for 2.5h. Gels were fluorimaged at 635 nm excitation and 670 nm emission wavelengths on a Typhoon Trio variable mode imager. Band intensities were quantified with GelAnalyzer and data were plotted using GraphPad Prism 6.

Fork Reversal		
F48	-	ACGCTGCCGAATTCTACCAGTGCCTTGCTAGGACATCTTTGCCCACCTGCAGGTTCACCC
F48Cy5	-	Cy5ACGCTGCCGAATTCTACCAGTGCCTTGCTAGGACATCTTTGCCCACCTGCAGGTTCACCC
F48Cy5block	-	ACGCTGCCGAATTCTACCAGTGCCTTGCTAGGACA**Cy5**CTTTGCCCACCTGCAGGTTCACCC
F48Cy5THF	-	Cy5ACGCTGCCGAATTCTACCAGTGCCTTGCTAGGACA**THF**CTTTGCCCACCTGCAGGTTCACCC
F50	-	GGGTGAACCTGCAGGTGGGCAAAGATGTCC
F52	-	GGGTGAACCTGCAGGTGGGCAAAGATGTCCCAGCAAGGCACTGGTAGAATTCGGCAGCGTC
F52Cy5	-	GGGTGAACCTGCAGGTGGGCAAAGATGTCCCAGCAAGGCACTGGTAGAATTCGGCAGCGTCCy5
F52Cy5block	-	GGGTGAACCTGCAGGTGGGCAAAGA**Cy5**GTCCCAGCAAGGCACTGGTAGAATTCGGCAGCGTC
F52Cy5THF	-	GGGTGAACCTGCAGGTGGGCAAAGA**THF**GTCCCAGCAAGGCACTGGTAGAATTCGGCAGCGTCCy5
F53	-	GGACATCTTTGCCCACCTGCAGGTTCACCC

Colors denote homologous regions

Bold denote internal modification

Mismatch (underlined) placed at the junction to prevent spontaneous brandch migration

Table 3.1 Oligodeoxynucleotides used in this study.

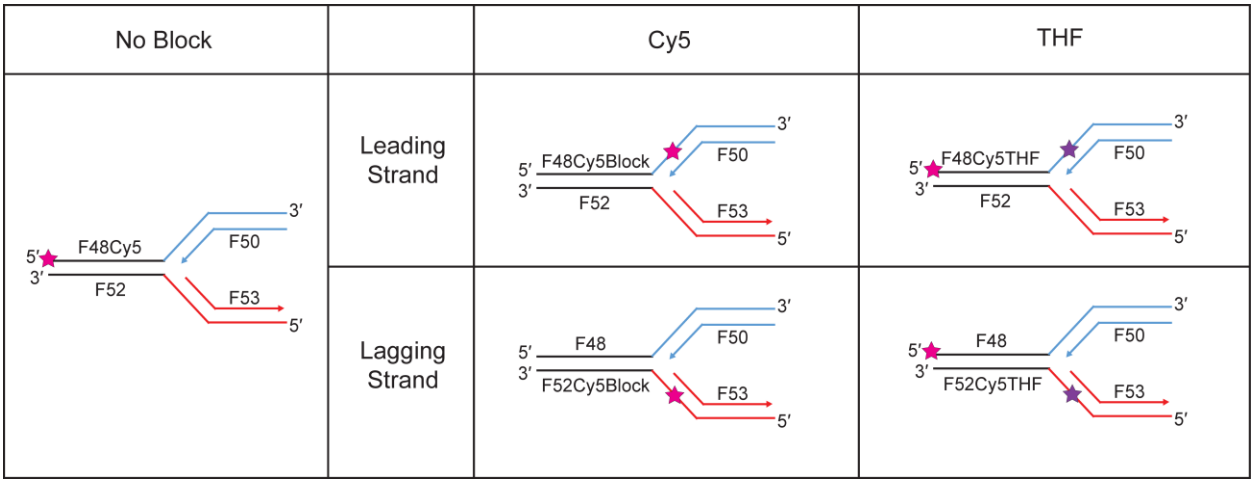

Figure 3.6 Fork DNA substrates used in this study. DNA strands listed in table 3.1 were annealed as described to produce the substrates depicted. Colors demonstrate homologous regions. Fork reversal substrates are 5′ labeled with Cy5 (pink star). Fork reversal substrates containing a modification, THF (purple star) or Cy5 (pink star), in the leading or lagging strand 5 bp from the fork junction were synthesized by IDT.

CHAPTER IV

DISCUSSION AND FUTURE DIRECTIONS

Summary of Work

DNA replication fork reversal pathways are critical for genome integrity. Understanding the mechanisms required for effective fork reversal and identifying what proteins are necessary in the pathway are essential to understanding the biology of DNA replication and DNA repair. A deeper understanding of the fork reversal pathway also has implications for improving human health. Defects in replication fork reversal manifest in human diseases such as SIOD and cancer. Recent studies of fork reversal pathways using cancer cell lines treated with replication stress have demonstrated that the SNF2-family fork remodelers actively reverse stalled replication forks *in vivo*. In bacteria the replication fork reversal pathway protects genome stability. RecG regulates replication restart and replication termination to prevent over-replication of the genome. In this dissertation I have described how the prokaryotic fork remodeling protein RecG is activated by a conformational change upon binding a model DNA replication fork substrate. I have also described how the eukaryotic SNF2-family fork remodelers respond to different DNA lesions that mimic DNA damage encountered during replication. However, there are still many lingering questions surrounding how the RecG ATPase domain binds dsDNA and how the SNF2 fork remodeling proteins work in a concerted fashion to achieve a like response. In this chapter I will address several outstanding

questions about the mechanisms of fork reversal by dsDNA translocases and discuss several models generated from my work.

DNA-Dependent Conformational Changes are Critical for Activation of SF2 ATPase Motors

Since fork remodeling enzymes are integral to the DNA damage response during replication in eukaryotes and critical for genome stability in prokaryotes, it is becoming increasingly important to determine mechanisms for the activation and activity of this class of proteins. The work described in chapter II demonstrated that the prokaryotic fork remodeler RecG undergoes a conformational change upon binding to a model replication fork. Activity assays and DEER experiments performed on RecG containing TRG loop mutations demonstrated that inability to undergo DNA-dependent conformational changes leads to loss of RecG activity. Distance distributions obtained from DEER experiments suggest that WT RecG and RecG TRG loop mutants have similar conformations in the absence of DNA. Therefore our data suggests that TRG loop mutants disrupt a DNA-dependent conformational change and not the conformation of the protein alone. We propose that the conformational change observed upon RecG binding to a model replication fork is a reorganization of the ATPase domains to prepare the motor domain for the first step of translocation. The work presented in chapter II is supported by evidence of DNA-dependent conformational changes observed in other SF2 ATPases although we are the first to report this mechanism in a fork remodeling enzyme.

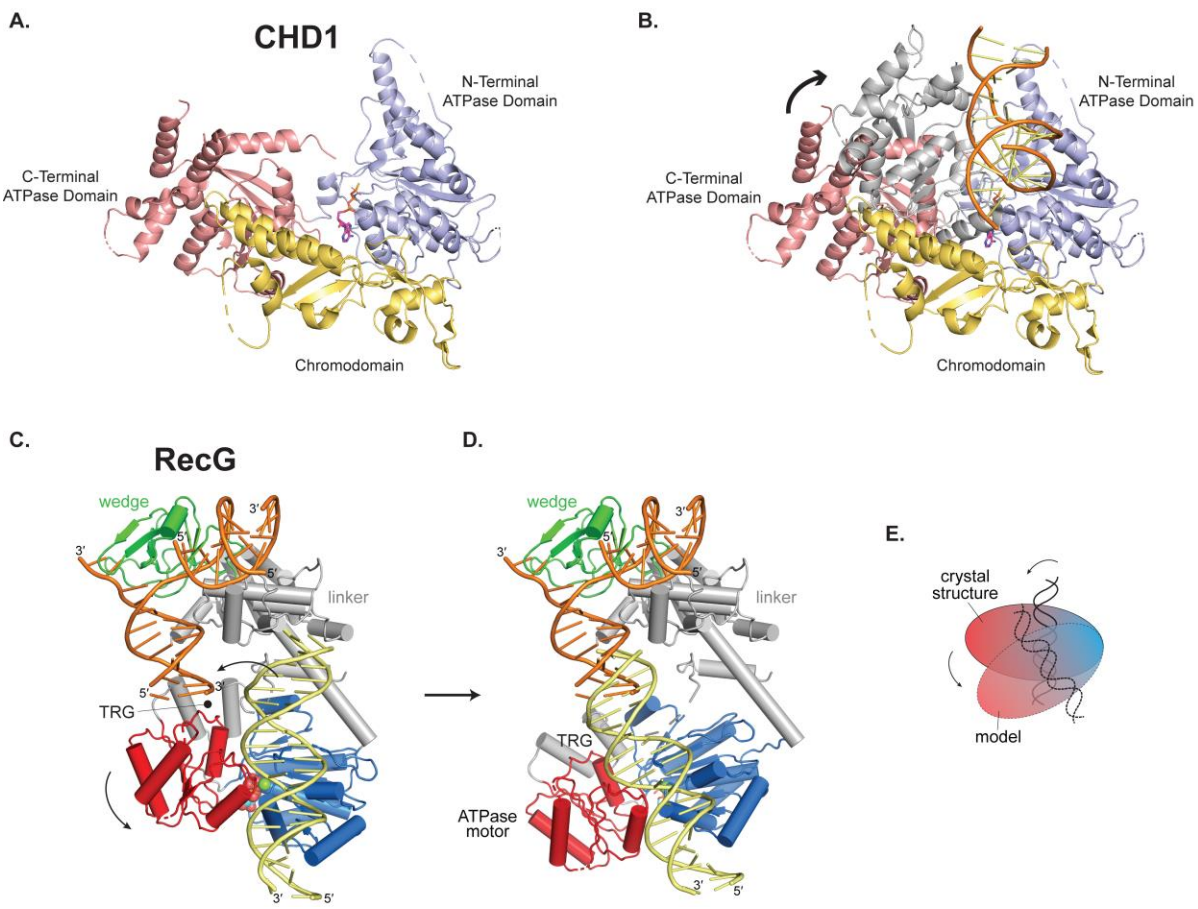

Figure 4.1 CHD1 and RecG require DNA-dependent conformational changes for activation. A. Crystal structure of the CHD1 ATPase domain without DNA (PDB ID: 3MWY) ATPase N-terminal domain blue, ATPase C-terminal domain (red), chromodomain (yellow). **B.** CHD1 crystal structure superimposed on the cryo-EM structure of CHD1 (grey) (PDB ID: 5O9G) bound to dsDNA. The curved black arrow denotes the rotation of the C-terminal ATPase domain of CHD1 necessary to bind dsDNA. (**C.** and **D.** from **Figure 2.3**) **C.** The RecG/DNA crystal structure (PDB ID 1GM5). The wedge domain is colored green, the linker domain is grey, and the ATPase motor is blue (N-lobe) and red (C-lobe). Parental DNA (yellow) was modeled by superposition of the XPB-ATPase and its bound DNA from the TFIIH complex (PDB ID 5IY9) onto the RecG-ATPase domain. The curved black arrow denotes the rotation of the motor domain necessary to align the helical axis of the modeled DNA to that of the crystal structure. **D.** Model of RecG bound to parental DNA after 30° rotation of the RecG motor and its accompanying DNA. **E.** Schematic of the rotation of the motor domain needed to bring parental duplex into alignment with the fork.

DNA-dependent conformational changes required to activate the chromatin remodeling SNF2 ATPase CHD1 have been observed using both structural and biophysical approaches (Farnung et al., 2017, Sundaramoorthy, Hughes et al., 2018). The first structure determined for the CHD1 ATPase domain was in the absence of DNA. In the original crystal structure of CHD1 the autoinhibitory chromodomains of the protein were bound to the cleft between the ATPase domains where DNA is now known to bind (Hauk, McKnight et al., 2010). This work also demonstrated that mutation of the chromodomains deregulated the ATPase activation of the protein by nucleosomal DNA. A conformational change is required for removal of the autoinhibitory chromodomains allowing CHD1 to bind DNA and become activated (**Figure 4.1**). Interestingly DEER experiments were also used to characterize conformational changes that occur between the ATPase domain and the chromodomains upon alterations in nucleotide bound state (Sundaramoorthy et al., 2018). The addition of ADP-BeF_3 to CHD1 leads to a change in the distance distribution between the chromodomains and ATPase domains and suggests that forming the nucleotide bound state requires removal of the chromodomains and rearrangement of the ATPase domains. Recent publication of cryo-EM structures of CHD1 revealed that upon DNA binding the chromodomains of CHD1 must undergo a conformational change to allow for the ATPase domains to bind dsDNA on the nucleosome (Farnung et al., 2017, Smolle, 2018, Sundaramoorthy et al., 2018). The C-terminal ATPase domain swivels during this DNA binding event similar to what we observe in RecG (**Figure 4.1**). This alteration in the ATPase domain conformation to bind DNA prepares the motor domain for its first translocation step.

Another striking example of a conformational change induced by DNA binding in SF2 ATPases comes from work on the SNF2-family ATPase and homologous recombination protein Rad54. Rad54 is an important protein in multiple DNA repair pathways as loss of Rad54 in yeast leads to hypersensitivity to IR and other DSB inducing agents (Game & Mortimer, 1974). Like other SNF2-family members Rad54 ATPase activity is stimulated by dsDNA and the protein lacks helicase activity (Petukhova, Stratton et al., 1998). Rad54 has a highly dynamic range of conformations between the two SNF2 ATPase domains that have been observed in two different crystal structures of the protein (Durr, Flaus et al., 2006, Durr et al., 2005, Thoma, Czyzewski et al., 2005). In one structure the C-terminal ATPase domain of Rad54 is rotated 180° from what would be expected of a SF2 ATPase in a nucleotide bound state whereas another structure shows the two ATPase domains in what appears to be a catalytically competent conformation forming the ATP binding pocket but in the absence of DNA. These two structures likely represent snapshots of conformations present *in vivo* but are potentially trapped in two different states by crystallographic packing.

Large conformational changes in Rad54 are supported by FRET studies. FRET efficiency was monitored for Rad54 upon binding to a DNA substrate in the presence or absence of various nucleotides. In the presence of DNA there is high FRET efficiency between the labeled Rad54 ATPase domains, which is expected in a model of a closed ATPase conformation (Lewis et al., 2008). Without DNA, Rad54 exhibits two-fold to three-fold lower FRET efficiency between the two ATPase domains suggesting a more open conformation. These observations demonstrate that DNA-dependent conformational changes are essential for dsDNA translocases involved in different aspects of biology

such as chromatin remodeling and homologous recombination. Our observations that RecG undergoes a conformational change upon DNA binding, which is essential to activation of the enzyme, is the first for a SF2 fork remodeler. These similarities suggest that other mechanisms important for dsDNA translocation in SF2 ATPases are shared across proteins involved in different aspects of nucleic acid metabolism.

In Chapter II we hypothesized that within RecG the importance of the TRG loop might be to stabilize the two ATPase domains in an activated conformation. Interestingly cryo-EM structures of SNF2 support this hypothesis in that the region of SNF2 analogous to the TRG loop in RecG forms a packing interaction between the two ATPase domains in an activated state of the enzyme bound to the nucleosome (Eustermann et al., 2018, Li, Xia et al., 2019, Liu et al., 2017). The helix known to bridge the two ATPase domains in closed conformations of SNF2 chromatin remodelers has been referred to as the brace helix (Eustermann et al., 2018). Recent structural and biochemical work on SNF2, ISWI, INO80, and CHD1 support this hypothesis, however, our work on RecG is the first to identify this stabilizing role between ATPase domains in a fork remodeler.

Summary of DEER Technique

Electron paramagnetic resonance spectroscopy (EPR) is a method used to study materials that contain free electrons (Brustolon et al., 2009). The more commonly used method of nuclear magnetic resonance (NMR) relies on the excitation of nuclei in a magnetic field using electromagnetic radiation. EPR is analogous to NMR but instead relies on excitement of electron spins rather than nuclear spins. Appropriate electromagnetic radiation frequencies change the spin state of a free electron when the

sample is present in a magnetic field. In the presence of a magnetic field paramagnetic materials form induced magnetic fields (Brustolon et al., 2009). Furthermore, a free electron will have a spin I=1/2 or I=-1/2 in the presence of a magnetic field.

The magnetic field from one paramagnetic center can influence the magnetic field of another in the same sample. Dipolar coupling refers to the influence of the spin state of one paramagnetic center on another through space. The EPR technique double electron-electron resonance (DEER) takes advantage of the dipolar coupling between electron spins in a sample (Jeschke, 2012). S-(1-oxyl-2,2,5,5-tetramethyl-2,5-dihydro-1H-pyrrol-3-yl)methyl methanesulfonothioate (MTSL) is a commonly used spin-label for 4-pulsed DEER experiments with proteins. MTSL has a nitroxide functional group with a free electron and a thiosulfonate ester functional group used to covalently attach the spin-label to cysteines within a protein.

In a 4-pulsed DEER experiment a pulse sequence produces an echo (Jeschke, 2012). The amplitude of the echo is monitored as the timing of the pump pulse is changed. The amplitude of the echo decays faster when there is more dipolar coupling between the two spin labels. When there is less dipolar coupling between spin labels, meaning the spin labels are farther apart, the echo decay is slower. The echo decays are then converted from the time domain to the frequency domain by a Fourier transform and then from the frequency domain into distance distributions (**Figure 2.4** and **Figure 2.5**).

Might SNF2-Family Fork Remodelers Translocate on dsDNA with a Mechanism Similar to that Observed in Chromatin Remodelers?

Chromatin remodeling enzymes require an active SNF2 ATPase domain to move nucleosomes or eject nucleosomes on DNA. The motor domains of chromatin remodelers have been studied in more detail than the motor domains of fork remodelers and a mechanism for dsDNA translocation has been proposed by several groups based on cryo-EM structures of the ATPase domain bound to the nucleosome. Structures of SNF2, ISWI, and CHD1 chromatin remodelers bound to nucleosomes have recently been determined in the presence and absence of the transition state mimetic ADP-BeF_3 (Farnung et al., 2017, Li et al., 2019, Yan, Wu et al., 2019). These structures have resulted in the proposal of a mechanism of dsDNA translocation by SNF2 family ATPases. The current model of dsDNA translocation by SNF2 ATPases involves a single base pair step size tracking along the phosphate backbone in a 3′-5′ direction on one strand of the DNA duplex while making secondary interactions with the opposing DNA duplex strand that is commonly referred to as the guide strand in the literature (**Figure 4.2**).

Cryo-EM structures of the chromatin remodelers SNF2 and then CHD1 were a major step in our understanding of dsDNA translocation by SF2 ATPases because the structures revealed how the ATPase domains contact dsDNA. Work on SNF2 and CHD1 is now supported by cryo-EM structures of the chromatin remodelers SWR1, ISWI, and INO80 (Aramayo, Willhoft et al., 2018, Ayala et al., 2018, Li et al., 2019, Liu et al., 2017, Willhoft, Ghoneim et al., 2018, Yan et al., 2019). All of the available cryo-EM structures demonstrate similar contacts to the dsDNA through conserved ATPase motifs including some that are specific to the SNF2 family. Each cryo-EM structure independently

demonstrated that motifs 1a, 1c, IV, IVa, V, and Va are involved in interactions with the tracking strand of dsDNA (**Figure 1.5**). The structures also revealed interactions with the guide strand of the dsDNA by motifs IIa and Vb. Most contacts to the nucleic acid are formed by hydrogen bonds with the phosphate backbone as has been determined for many SF2 helicases such as DinG, VASA, Lhr, and Hel308 (Buttner, Nehring et al., 2007, Cheng & Wigley, 2018, Ejaz, Ordonez et al., 2018, Kim, Morgenstern et al., 1998). The interactions to the guide strand of dsDNA by motif IIa and motif Vb are novel for SF2 translocases. Interestingly these novel contacts made with the guide strand are through a conserved tryptophan in motif Vb that sits in the minor groove and interacts with the phosphate backbone as well as a conserved arginine present in motif IIa.

Work on the CHD1 protein by both the Cramer and Owen-Hughes labs has demonstrated that without ADP-BeF_3 present the C-terminal ATPase domain remains in a partially open conformation and that the presence of ADP-BeF_3 closes the N-terminal and C-terminal ATPase domains tightly on DNA (Farnung et al., 2017, Sundaramoorthy et al., 2018). Structural data demonstrating an open and closed conformation of the ATPase domains with and without ADP-BeF_3 was reproduced in subsequent cryo-EM structures of SNF2 and ISWI (Li et al., 2019, Yan et al., 2019).

In chapter III, I determined that SMARCAL1 and ZRANB3 have divergent sequences in motifs used to contact both the tracking strand and guide strand of dsDNA when compared to other SNF2 dsDNA translocases including HLTF. I generated homology models of the ATPase domains of ZRANB3 and SMARCAL1 using the program SWISS-MODEL to demonstrate where regions of sequence variation occur in the ATPase domain (**Figure 4.2**). Specifically motif IIa and motif Vb contain aromatic residues that

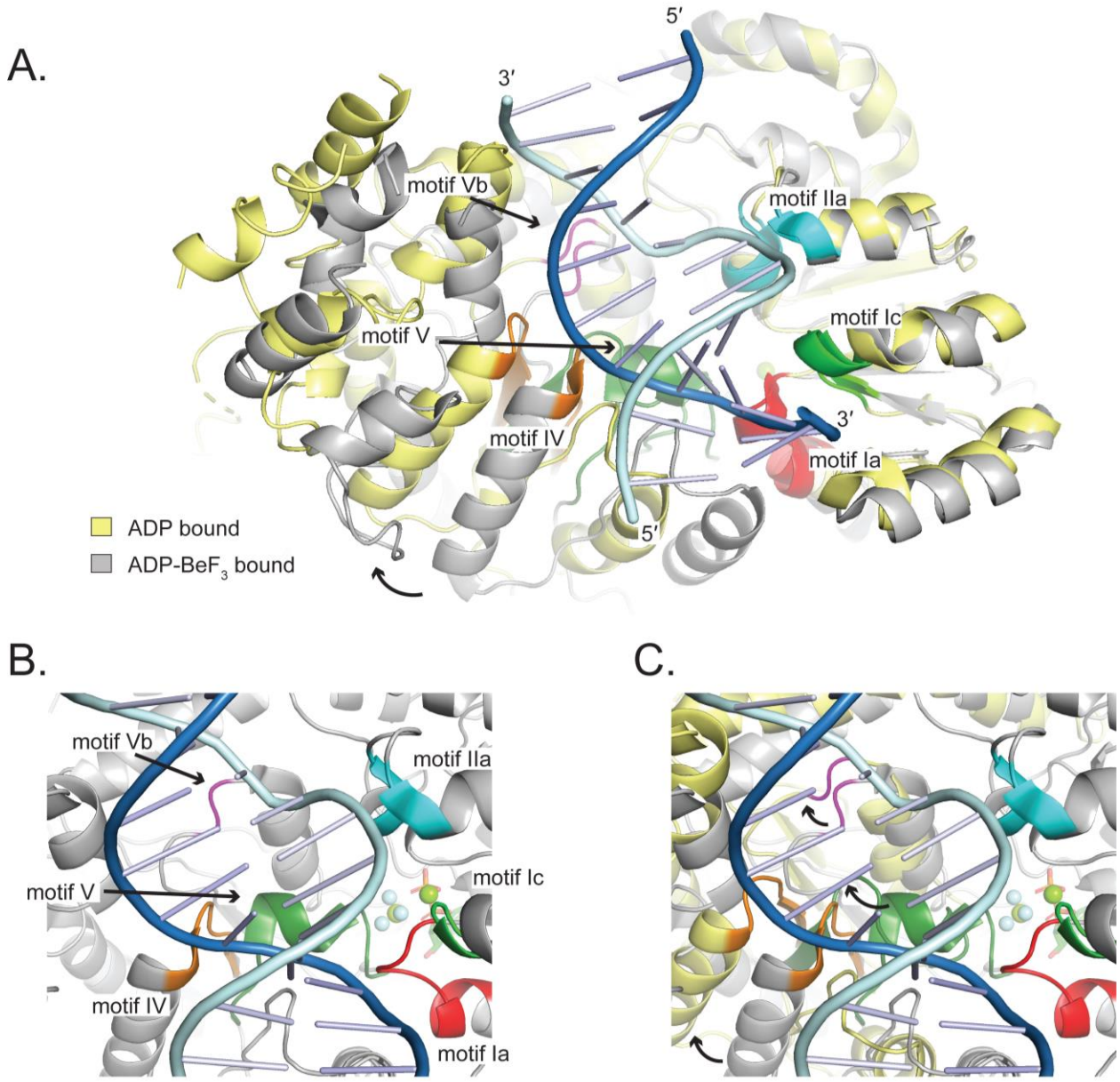

Figure 4.2 Model of dsDNA translocation revealed by SNF2. A. Overlay of SNF2 cryo-EM structures bound to dsDNA in a closed conformation with ADP-BeF_3 (grey) (PDB ID 5Z3T) or in an open conformation with ADP (yellow) (PDB ID 5Z3O). Nucleic acid binding motifs are labeled with motif Ia (red), motif Ic (green), motif IIa (cyan), motif IV (orange), motif V (dark green), and motif Vb (magenta). Duplex DNA with the tracking strand (dark blue) and the guide strand (light blue). **B.** Close up view of motifs contacting the tracking strand and guide strand of dsDNA in the closed conformation with ADP-BeF_3 bound. **C.** Close up view of conformational changes observed in ATPase C-terminal domain nucleic acid binding motifs (black arrows) induced by ATP hydrolysis.

might engage with the minor groove of dsDNA or the phosphate backbone. Sequence differences found in motifs that contact the guide strand of the dsDNA might explain why SMARCAL1 and ZRANB3 are more sensitive to Cy5 lesions in the backbone of the leading template DNA strand of DNA forks used in fork reversal activity assays. A steric

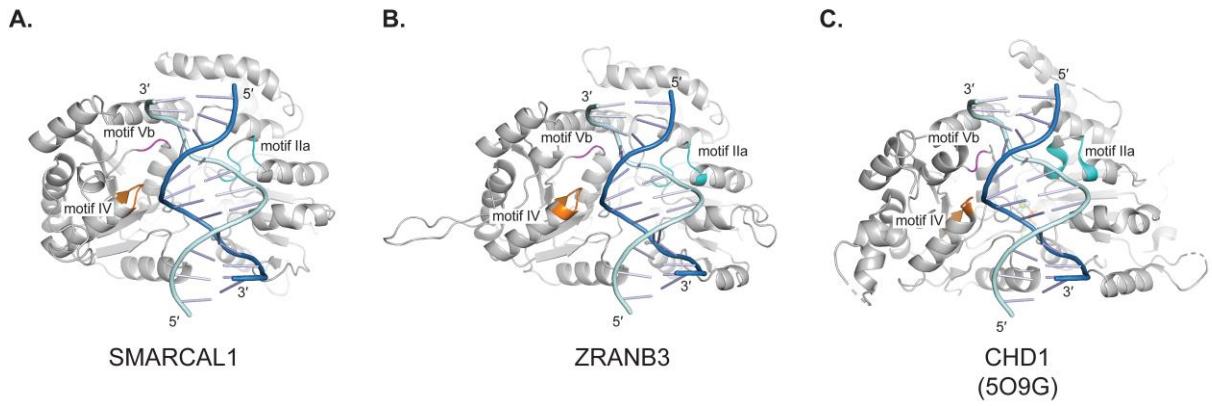

Figure 4.3 Homology models of SMARCAL1 and ZRANB3 bound to dsDNA.
A. Homology model of SMARCAL1 generated by SWISS-MODEL using INO80 bound to dsDNA in the nucleosome complex as a template (PDB ID 6FML). Duplex DNA with tracking strand (dark blue) and guide strand (light blue) bound to SMARCAL1 was modeled by superposition of SMARCAL1 homology model on CHD1 bound to dsDNA and ADP-BeF_3 (PDB ID 5O9G). DNA binding motifs IIa (cyan), IV (orange), and Vb (magenta) are divergent in SMARCAL1 and ZRANB3. **B.** Homology model of ZRANB3 generated by SWISS-MODEL using INO80 bound to dsDNA in the nucleosome complex as a template. Duplex DNA with tracking strand (dark blue) and guide strand (light blue) bound to SMARCAL1 was modeled by superposition of ZRANB3 homology model on CHD1 bound to dsDNA and ADP-BeF_3 (PDB ID 5O9G). **C.** CHD1 bound to dsDNA and ADP-BeF_3 (PDB ID 5O9G).

clash with the Cy5 lesion might inhibit SMARCAL1 or ZRANB3 from passing the location of the lesion because of an increase in aromatic residues found in these motifs. It will be interesting to test whether mutating these divergent sequences in SMARCAL1 and ZRANB3 to those found in HLTF might alleviate the phenotype that we observed in our

fork reversal activity assays. Currently those protein constructs are being generated for future experiments testing the importance of these motifs in SMARCAL1-like fork remodelers.

Substrate Recognition Domains Provide Direction Across SF2 dsDNA Translocases

Determining a mechanism of dsDNA translocation by SF2 ATPases is critical to our understanding of fork reversal, however, it is apparent that anchoring translocation to substrate binding domains provides direction to translocation. Anchoring dsDNA translocation by the use of a substrate recognition domain is a common theme in SF2 dsDNA translocases. In the INO80 complex the ARP5 protein has been characterized both structurally and biochemically as anchoring the ATPase motor to the nucleosome. By anchoring the motor domain to a fixed point, torque can be generated allowing INO80 to push DNA into the nucleosome dyad in a productive and directional mechanism (Ayala et al., 2018, Eustermann et al., 2018). The structure of RecG and characterization of substrate recognition domains found in the SNF2-family fork remodelers suggest that the fork remodelers anchor their motors to the fork junction by the same means and provide directionality. It is plausible to propose a model where the SRD generates the anchor point for the motor domain to generate productive and directional dsDNA translocation analogous to the mechanism observed in INO80. Other chromatin remodelers such as SNF2, ISWI, and CHD1 possess auxiliary domains to bind specific positions in nucleosomal DNA or the nucleosome itself to provide direction to translocation (Farnung et al., 2017, Li et al., 2019, Yan et al., 2019).

Other SF2 ATPases that bind to a specific substrate to provide direction to dsDNA translocation are the transcription-coupled repair proteins Mfd and CSB which bind to stalled RNA polymerases in prokaryotes and eukaryotes, respectively. Although Mfd is a RecG-like ATPase, and CSB is a SNF2 ATPase they are functional orthologs that couple binding of stalled RNA polymerases to dsDNA translocation. The observation of this anchoring mechanism in dsDNA translocases with relatively divergent motor domains suggests a common mechanism for providing direction to dsDNA translocases.

In RecG the wedge domain is essential for binding dsDNA/ssDNA junctions and has been previously characterized (Briggs et al., 2005). The wedge domain is an OB-fold and the substrate recognition domain for RecG. The crystal structure of RecG bound to a DNA junction demonstrates how the wedge domain recognizes both the branch point of a fork and the lagging dsDNA (Singleton et al., 2001). The wedge domain might orient the RecG ATPase domain onto the template dsDNA of a fork for productive translocation. Similarly the HIRAN domain of HLTF, the HARP domains of SMARCAL1, and the HARP-like domain of ZRANB3 are essential for efficient fork reversal activity *in vitro* (Badu-Nkansah et al., 2016, Betous et al., 2012, Kile et al., 2015). It will be interesting to determine how the substrate recognition domains contribute to the translocation mechanisms of the SNF2-family fork remodelers as more biochemical, biophysical, and structural approaches are applied to studying this important class of proteins.

In Vitro and *In Vivo* Data for SNF2-Family Fork Remodelers

In order to understand the fork reversal pathway it is critical to understand what substrates each of the SNF2-family fork remodelers is most active on and which

substrates are inhibitory to the fork reversal reaction. Pulling all of the available *in vitro* and *in vivo* fork reversal data together will shape a clearer view of the specific functions of each SNF2-family fork remodeler. The SNF2-family fork remodelers are required for maintaining genome stability after treatment with many types of replication stress, which I will expand upon in this section.

Removal of HLTF, SMARCAL1, or ZRANB3 results in increased genome instability upon replication stress. Interestingly, SMARCAL1-deficient cells also show levels of genome instability even without the presence of replication stress suggesting some basal function of SMARCAL1. Treatment with different challenges to replication revealed that SMARCAL1-deficient cells are sensitive to hydroxyurea (HU), aphidicolin, mitomycin C (MMC), ionizing radiation (IR), and camptothecin (Cpt) (Poole & Cortez, 2017). Importantly SMARCAL1-deficient cells treated with camptothecin and depleted of ZRANB3 demonstrated increased sensitivity suggesting independent activity of the two fork remodelers (Ciccia et al., 2012). Among the treatments that caused sensitivity in SMARCAL1-deficient cells, only MMC alkylates the template DNA to form monoadducts or crosslinks that might form a physical barrier to translocation. The other treatments that lead to sensitivity in SMARCAL1-deficient cells cause slowing of replication through inhibition of polymerases, reduced dNTP pools, or steric hindrance of replication progression by trapping topoisomerase. Therefore the role of SMARCAL1 under these inducers of replication stress would be to reverse the stalled replication fork to promote fork protection until conditions favorable to restart replication. In the case of MMC, other alkylating agents, or other covalent modifications to the template DNA the replisome

components would be physically blocked by DNA damage that, depending on the pathway, might require TLS or a fork remodeling enzyme to traverse the lesion.

HLTF-deficient cells are prone to increased mutagenesis after UV exposure and a role has been suggested for regulating the error-free bypass of UV-induced lesions and also regulating replication speeds (Lin et al., 2011). HLTF-deficient cells have also been shown to have sensitivity to MMS and HU treatments. In chapter III, HLTF fork reversal activity was assessed using replication forks with DNA modifications. None of the substrates tested in fork reversal activity assays has altered HLTF fork reversal dramatically from an unmodified replication fork suggesting that HLTF can perform fork reversal on a wide range of DNA structures unlike SMARCAL1 and ZRANB3.

Previous work on the regulation of SMARCAL1 fork reversal activity by RPA demonstrated that SMARCAL1 fork reversal activity is enhanced when RPA is bound to the leading template strand but inhibited when RPA is present on the lagging template strand. In chapter III, I demonstrated that fork reversal activity of SMARCAL1 is only abrogated by a bulky backbone Cy5 modification on the leading strand of the replication fork. There is slightly reduced fork reversal activity when the Cy5 modification is present in the lagging template strand. When THF is introduced into the leading and lagging template strands, only the lagging template strand THF minimally enhances the fork reversal activity of SMARCAL1. It will be important to determine in future studies if SMARCAL1 relies on interactions with RPA to bypass bulky lesions in the leading template strand.

The current *in vitro* data suggests that SMARCAL1 might not be able to translocate past a bulky DNA modification on the leading template strand efficiently and therefore

decrease fork reversal activity. It appears that SMARCAL1-deficient cells are not hypersensitive to UV radiation that might produce bulky CPD lesions but they are hypersensitive to MMC that would produce bulky DNA modifications. It is possible that NER and or other fork reversal mechanisms are more involved in the recognition and repair of CPD lesions that cause fork reversal. U2OS cells exposed to UV radiation have an increase in the frequency of reversed forks observed by cryo-EM but, interestingly, when ZRANB3 is removed the percentage of reversed forks is reduced to levels observed in untreated cells (Vujanovic et al., 2017). ZRANB3 does colocalize with PCNA after UV exposure in a dose dependent manner suggesting some response to UV exposure that is regulated by ZRANB3. ZRANB3 is responsible for the majority of fork reversal observed after UV radiation but ZRANB3-deificient 293T cells do not appear to be hyper-sensitive to UV radiation. The lack of sensitivity to UV exposure in ZRANB3-deficient cells might be explained by repair through TLS pathways or HLTF regulated template switching since HLTF-deficient cells do exhibit hypersensitivity to UV exposure.

Similar to SMARCAL1-deficient cells, ZRANB3-deficient cells are hypersensitive to treatment with HU, MMC, MMS, Cisplatin, and Cpt (Ciccia et al., 2012, Poole & Cortez, 2017, Weston et al., 2012, Yuan, Ghosal et al., 2012). ZRANB3-deficient cells also have increased fork stalling and recombination by sister chromatid exchanges (SCE). In Chapter III, I determined that ZRANB3 was blocked completely by leading template strand Cy5 lesions. It will be interesting to determine if the presence of PCNA or polyubiquitinated PCNA stimulates the fork reversal activity of ZRANB3 allowing for bypass of bulky leading strand lesions or if this sensitivity to bulky lesions in the leading template strand is a mechanism for sensing DNA damage that might require the

endonuclease activity of ZRANB3 to resume replication. Whether the sensitivity of ZRANB3 and SMARCAL1 to leading template damage plays any significant role in cells that must bypass bulky lesions during replication remains speculative but future studies might illuminate this potential function. It will be interesting to determine how active each SNF2-family fork remodeler is in relation to the others in the replication fork reversal pathway upon treatment with various agents of replication stress. For now it seems that the generation of excess ssDNA at the fork increases the activity of the SNF2-family fork remodelers.

Remaining Questions for the Field of DNA Replication Fork Reversal

To fully understand how fork remodeling enzymes alter our picture of DNA replication during replication stress it will be important for the field to identify what the replisome does during fork reversal and fork protection. It might be possible that the MCM helicase switches to a dsDNA diffusive mode that is facilitated by the presence of MCM10 as suggested by *in vitro* work from the O'Donnell lab (Wasserman, Schauer et al., 2019). This would allow for the replisome to clear the way for fork reversal and fork protection pathways while maintaining the replisome components near the replication fork for a switch back to replication restart also possibly facilitated by MCM10 and the various mechanisms that regulate MCM10 function such as ubiquitination and phosphorylation.

Another open question in our understanding of the fork reversal mechanism is how the fork remodeling enzymes are effected by DNA damage that creates bulky lesions such as polyaromatic hydrocarbons, phosphotriester linkages, and DNA-protein crosslinks. These types of lesions are impediments to replication that might result in fork

reversal. Testing the effect bulky lesions have on the SNF2-family fork remodelers will expand our understanding of the mechanisms of dsDNA translocation and fork reversal.

It will be interesting to see how the field of DNA replication grows as we continue to characterize the proteins required for fork reversal and fork protection pathways and identify new proteins in the pathway.

REFERENCES

Abd Wahab S, Choi M, Bianco PR (2013) Characterization of the ATPase activity of RecG and RuvAB proteins on model fork structures reveals insight into stalled DNA replication fork repair. *J Biol Chem* 288: 26397-409

Achar YJ, Balogh D, Haracska L (2011) Coordinated protein and DNA remodeling by human HLTF on stalled replication fork. *Proc Natl Acad Sci U S A* 108: 14073-8

Aguilera A, Garcia-Muse T (2012) R loops: from transcription byproducts to threats to genome stability. *Mol Cell* 46: 115-24

Alzu A, Bermejo R, Begnis M, Lucca C, Piccini D, Carotenuto W, Saponaro M, Brambati A, Cocito A, Foiani M, Liberi G (2012) Senataxin associates with replication forks to protect fork integrity across RNA-polymerase-II-transcribed genes. *Cell* 151: 835-846

Aramayo RJ, Willhoft O, Ayala R, Bythell-Douglas R, Wigley DB, Zhang X (2018) Cryo-EM structures of the human INO80 chromatin-remodeling complex. *Nat Struct Mol Biol* 25: 37-44

Atkinson J, McGlynn P (2009) Replication fork reversal and the maintenance of genome stability. *Nucleic Acids Res* 37: 3475-92

Ayala R, Willhoft O, Aramayo RJ, Wilkinson M, McCormack EA, Ocloo L, Wigley DB, Zhang X (2018) Structure and regulation of the human INO80-nucleosome complex. *Nature* 556: 391-395

Azeroglu B, Leach DRF (2017) RecG controls DNA amplification at double-strand breaks and arrested replication forks. *FEBS Lett* 591: 1101-1113

Azeroglu B, Mawer JS, Cockram CA, White MA, Hasan AM, Filatenkova M, Leach DR (2016) RecG Directs DNA Synthesis during Double-Strand Break Repair. *PLoS Genet* 12: e1005799

Badu-Nkansah A, Mason AC, Eichman BF, Cortez D (2016) Identification of a Substrate Recognition Domain in the Replication Stress Response Protein Zinc Finger Ran-binding Domain-containing Protein 3 (ZRANB3). *J Biol Chem* 291: 8251-7

Ball HL, Myers JS, Cortez D (2005) ATRIP binding to replication protein A-single-stranded DNA promotes ATR-ATRIP localization but is dispensable for Chk1 phosphorylation. *Mol Biol Cell* 16: 2372-81

Bansbach CE, Betous R, Lovejoy CA, Glick GG, Cortez D (2009) The annealing helicase SMARCAL1 maintains genome integrity at stalled replication forks. *Genes Dev* 23: 2405-14

Baradaran-Heravi A, Cho KS, Tolhuis B, Sanyal M, Morozova O, Morimoto M, Elizondo LI, Bridgewater D, Lubieniecka J, Beirnes K, Myung C, Leung D, Fam HK, Choi K, Huang Y, Dionis KY, Zonana J, Keller K, Stenzel P, Mayfield C et al. (2012) Penetrance of biallelic SMARCAL1 mutations is associated with environmental and genetic disturbances of gene expression. *Hum Mol Genet* 21: 2572-87

Bass TE, Luzwick JW, Kavanaugh G, Carroll C, Dungrawala H, Glick GG, Feldkamp MD, Putney R, Chazin WJ, Cortez D (2016) ETAA1 acts at stalled replication forks to maintain genome integrity. *Nat Cell Biol* 18: 1185-1195

Beck H, Nahse-Kumpf V, Larsen MS, O'Hanlon KA, Patzke S, Holmberg C, Mejlvang J, Groth A, Nielsen O, Syljuasen RG, Sorensen CS (2012) Cyclin-dependent kinase

suppression by WEE1 kinase protects the genome through control of replication initiation and nucleotide consumption. *Mol Cell Biol* 32: 4226-36

Bermejo R, Lai MS, Foiani M (2012) Preventing replication stress to maintain genome stability: resolving conflicts between replication and transcription. *Mol Cell* 45: 710-8

Berti M, Vindigni A (2016) Replication stress: getting back on track. *Nat Struct Mol Biol* 23: 103-9

Betous R, Couch FB, Mason AC, Eichman BF, Manosas M, Cortez D (2013) Substrate-selective repair and restart of replication forks by DNA translocases. *Cell Rep* 3: 1958-69

Betous R, Mason AC, Rambo RP, Bansbach CE, Badu-Nkansah A, Sirbu BM, Eichman BF, Cortez D (2012) SMARCAL1 catalyzes fork regression and Holliday junction migration to maintain genome stability during DNA replication. *Genes Dev* 26: 151-62

Bhat KP, Betous R, Cortez D (2015) High-affinity DNA-binding domains of replication protein A (RPA) direct SMARCAL1-dependent replication fork remodeling. *J Biol Chem* 290: 4110-7

Bhat KP, Cortez D (2018) RPA and RAD51: fork reversal, fork protection, and genome stability. *Nat Struct Mol Biol* 25: 446-453

Bhat KP, Krishnamoorthy A, Dungrawala H, Garcin EB, Modesti M, Cortez D (2018) RADX Modulates RAD51 Activity to Control Replication Fork Protection. *Cell Rep* 24: 538-545

Bianco PR (2015) I came to a fork in the DNA and there was RecG. *Prog Biophys Mol Biol* 117: 166-173

Bianco PR, Pottinger S, Tan HY, Nguyenduc T, Rex K, Varshney U (2017) The IDL of E. coli SSB links ssDNA and protein binding by mediating protein-protein interactions. *Protein Sci* 26: 227-241

Bizard AH, Hickson ID (2014) The dissolution of double Holliday junctions. *Cold Spring Harb Perspect Biol* 6: a016477

Blastyak A, Hajdu I, Unk I, Haracska L (2010) Role of double-stranded DNA translocase activity of human HLTF in replication of damaged DNA. *Mol Cell Biol* 30: 684-93

Bochkareva E, Kaustov L, Ayed A, Yi GS, Lu Y, Pineda-Lucena A, Liao JC, Okorokov AL, Milner J, Arrowsmith CH, Bochkarev A (2005) Single-stranded DNA mimicry in the p53 transactivation domain interaction with replication protein A. *Proc Natl Acad Sci U S A* 102: 15412-7

Bochman ML, Paeschke K, Zakian VA (2012) DNA secondary structures: stability and function of G-quadruplex structures. *Nat Rev Genet* 13: 770-80

Boerkoel CF, Takashima H, John J, Yan J, Stankiewicz P, Rosenbarker L, Andre JL, Bogdanovic R, Burguet A, Cockfield S, Cordeiro I, Frund S, Illies F, Joseph M, Kaitila I, Lama G, Loirat C, McLeod DR, Milford DV, Petty EM et al. (2002) Mutant chromatin remodeling protein SMARCAL1 causes Schimke immuno-osseous dysplasia. *Nat Genet* 30: 215-20

Boutros R, Dozier C, Ducommun B (2006) The when and wheres of CDC25 phosphatases. *Curr Opin Cell Biol* 18: 185-91

Briggs GS, Mahdi AA, Wen Q, Lloyd RG (2005) DNA binding by the substrate specificity (wedge) domain of RecG helicase suggests a role in processivity. *J Biol Chem* 280: 13921-7

Brosh RM, Jr., Karow JK, White EJ, Shaw ND, Hickson ID, Bohr VA (2000) Potent inhibition of werner and bloom helicases by DNA minor groove binding drugs. *Nucleic Acids Res* 28: 2420-30

Brustolon, M (2009) Electron paramagnetic resonance: a practitioner's toolkit. John Wiley & Sons.

Buechner CN, Heil K, Michels G, Carell T, Kisker C, Tessmer I (2014) Strand-specific recognition of DNA damages by XPD provides insights into nucleotide excision repair substrate versatility. *J Biol Chem* 289: 3613-24

Bugreev DV, Rossi MJ, Mazin AV (2011) Cooperation of RAD51 and RAD54 in regression of a model replication fork. *Nucleic Acids Res* 39: 2153-64

Buttner K, Nehring S, Hopfner KP (2007) Structural basis for DNA duplex separation by a superfamily-2 helicase. *Nat Struct Mol Biol* 14: 647-52

Byun TS, Pacek M, Yee MC, Walter JC, Cimprich KA (2005) Functional uncoupling of MCM helicase and DNA polymerase activities activates the ATR-dependent checkpoint. *Genes Dev* 19: 1040-52

Chambers AL, Smith AJ, Savery NJ (2003) A DNA translocation motif in the bacterial transcription--repair coupling factor, Mfd. *Nucleic Acids Res* 31: 6409-18

Chavez DA, Greer BH, Eichman BF (2018) The HIRAN domain of helicase-like transcription factor positions the DNA translocase motor to drive efficient DNA fork regression. *J Biol Chem* 293: 8484-8494

Cheng K, Wigley DB (2018) DNA translocation mechanism of an XPD family helicase. *Elife* 7

Ciccia A, Bredemeyer AL, Sowa ME, Terret ME, Jallepalli PV, Harper JW, Elledge SJ (2009) The SIOD disorder protein SMARCAL1 is an RPA-interacting protein involved in replication fork restart. *Genes Dev* 23: 2415-25

Ciccia A, Elledge SJ (2010) The DNA damage response: making it safe to play with knives. *Mol Cell* 40: 179-204

Ciccia A, Nimonkar AV, Hu Y, Hajdu I, Achar YJ, Izhar L, Petit SA, Adamson B, Yoon JC, Kowalczykowski SC, Livingston DM, Haracska L, Elledge SJ (2012) Polyubiquitinated PCNA recruits the ZRANB3 translocase to maintain genomic integrity after replication stress. *Mol Cell* 47: 396-409

Cimprich KA, Cortez D (2008) ATR: an essential regulator of genome integrity. *Nat Rev Mol Cell Biol* 9: 616-27

Clewing JM, Antalfy BC, Lucke T, Najafian B, Marwedel KM, Hori A, Powel RM, Do AF, Najera L, SantaCruz K, Hicks MJ, Armstrong DL, Boerkoel CF (2007) Schimke immuno-osseous dysplasia: a clinicopathological correlation. *J Med Genet* 44: 122-30

Cortez D (2015) Preventing replication fork collapse to maintain genome integrity. *DNA Repair (Amst)* 32: 149-57

Couch FB, Bansbach CE, Driscoll R, Luzwick JW, Glick GG, Betous R, Carroll CM, Jung SY, Qin J, Cimprich KA, Cortez D (2013) ATR phosphorylates SMARCAL1 to prevent replication fork collapse. *Genes Dev* 27: 1610-23

Courcelle J, Donaldson JR, Chow KH, Courcelle CT (2003) DNA damage-induced replication fork regression and processing in Escherichia coli. *Science* 299: 1064-7

Courcelle J, Hanawalt PC (2003) RecA-dependent recovery of arrested DNA replication forks. *Annu Rev Genet* 37: 611-46

Cox MM, Goodman MF, Kreuzer KN, Sherratt DJ, Sandler SJ, Marians KJ (2000) The importance of repairing stalled replication forks. *Nature* 404: 37-41

Dalgaard JZ (2012) Causes and consequences of ribonucleotide incorporation into nuclear DNA. *Trends Genet* 28: 592-7

De Piccoli G, Katou Y, Itoh T, Nakato R, Shirahige K, Labib K (2012) Replisome stability at defective DNA replication forks is independent of S phase checkpoint kinases. *Mol Cell* 45: 696-704

Deaconescu AM, Chambers AL, Smith AJ, Nickels BE, Hochschild A, Savery NJ, Darst SA (2006) Structural basis for bacterial transcription-coupled DNA repair. *Cell* 124: 507-20

Deaconescu AM, Savery N, Darst SA (2007) The bacterial transcription repair coupling factor. *Curr Opin Struct Biol* 17: 96-102

Dekel B, Metsuyanim S, Goldstein N, Pode-Shakked N, Kovalski Y, Cohen Y, Davidovits M, Anikster Y (2008) Schimke immuno-osseous dysplasia: expression of SMARCAL1 in blood and kidney provides novel insight into disease phenotype. *Pediatr Res* 63: 398-403

Dimitrova DS, Gilbert DM (2000) Temporally coordinated assembly and disassembly of replication factories in the absence of DNA synthesis. *Nat Cell Biol* 2: 686-94

Dungrawala H, Bhat KP, Le Meur R, Chazin WJ, Ding X, Sharan SK, Wessel SR, Sathe AA, Zhao R, Cortez D (2017) RADX Promotes Genome Stability and Modulates Chemosensitivity by Regulating RAD51 at Replication Forks. *Mol Cell* 67: 374-386 e5

Dungrawala H, Rose KL, Bhat KP, Mohni KN, Glick GG, Couch FB, Cortez D (2015) The Replication Checkpoint Prevents Two Types of Fork Collapse without Regulating Replisome Stability. *Mol Cell* 59: 998-1010

Durr H, Flaus A, Owen-Hughes T, Hopfner KP (2006) Snf2 family ATPases and DExx box helicases: differences and unifying concepts from high-resolution crystal structures. *Nucleic Acids Res* 34: 4160-7

Durr H, Korner C, Muller M, Hickmann V, Hopfner KP (2005) X-ray structures of the Sulfolobus solfataricus SWI2/SNF2 ATPase core and its complex with DNA. *Cell* 121: 363-73

Ejaz A, Ordonez H, Jacewicz A, Ferrao R, Shuman S (2018) Structure of mycobacterial 3 '-to-5 ' RNA: DNA helicase Lhr bound to a ssDNA tracking strand highlights distinctive features of a novel family of bacterial helicases. *Nucleic Acids Research* 46: 442-455

Eustermann S, Schall K, Kostrewa D, Lakomek K, Strauss M, Moldt M, Hopfner KP (2018) Structural basis for ATP-dependent chromatin remodelling by the INO80 complex. *Nature* 556: 386-390

Fairman-Williams ME, Guenther UP, Jankowsky E (2010) SF1 and SF2 helicases: family matters. *Curr Opin Struct Biol* 20: 313-24

Fairman ME, Maroney PA, Wang W, Bowers HA, Gollnick P, Nilsen TW, Jankowsky E (2004) Protein displacement by DExH/D "RNA helicases" without duplex unwinding. *Science* 304: 730-4

Farnung L, Vos SM, Wigge C, Cramer P (2017) Nucleosome-Chd1 structure and implications for chromatin remodelling. *Nature* 550: 539-542

Firman K, Szczelkun MD (2000) Measuring motion on DNA by the type I restriction endonuclease EcoR124I using triplex displacement. *EMBO J* 19: 2094-102

Flaus A, Martin DM, Barton GJ, Owen-Hughes T (2006) Identification of multiple distinct Snf2 subfamilies with conserved structural motifs. *Nucleic Acids Res* 34: 2887-905

Fugger K, Mistrik M, Neelsen KJ, Yao Q, Zellweger R, Kousholt AN, Haahr P, Chu WK, Bartek J, Lopes M, Hickson ID, Sorensen CS (2015) FBH1 Catalyzes Regression of Stalled Replication Forks. *Cell Rep* 10: 1749-1757

Fujiwara Y, Tatsumi M (1976) Replicative bypass repair of ultraviolet damage to DNA of mammalian cells: caffeine sensitive and caffeine resistant mechanisms. *Mutat Res* 37: 91-110

Furnari B, Rhind N, Russell P (1997) Cdc25 mitotic inducer targeted by chk1 DNA damage checkpoint kinase. *Science* 277: 1495-7

Gaidutsik I, Sedman T, Sillamaa S, Sedman J (2016) Irc3 is a mitochondrial DNA branch migration enzyme. *Sci Rep* 6: 26414

Game JC, Mortimer RK (1974) A genetic study of x-ray sensitive mutants in yeast. *Mutat Res* 24: 281-92

Gari K, Decaillet C, Delannoy M, Wu L, Constantinou A (2008a) Remodeling of DNA replication structures by the branch point translocase FANCM. *Proc Natl Acad Sci U S A* 105: 16107-12

Gari K, Decaillet C, Stasiak AZ, Stasiak A, Constantinou A (2008b) The Fanconi anemia protein FANCM can promote branch migration of Holliday junctions and replication forks. *Mol Cell* 29: 141-8

Gibb B, Ye LF, Gergoudis SC, Kwon Y, Niu H, Sung P, Greene EC (2014) Concentration-dependent exchange of replication protein A on single-stranded DNA revealed by single-molecule imaging. *PLoS One* 9: e87922

Graebsch A, Roche S, Niessing D (2009) X-ray structure of Pur-alpha reveals a Whirly-like fold and an unusual nucleic-acid binding surface. *Proc Natl Acad Sci U S A* 106: 18521-6

Gregg AV, McGlynn P, Jaktaji RP, Lloyd RG (2002) Direct rescue of stalled DNA replication forks via the combined action of PriA and RecG helicase activities. *Mol Cell* 9: 241-51

Guilliam TA, Brissett NC, Ehlinger A, Keen BA, Kolesar P, Taylor EM, Bailey LJ, Lindsay HD, Chazin WJ, Doherty AJ (2017) Molecular basis for PrimPol recruitment to replication forks by RPA. *Nat Commun* 8: 15222

Gupta S, Yeeles JT, Marians KJ (2014a) Regression of replication forks stalled by leading-strand template damage: I. Both RecG and RuvAB catalyze regression, but RuvC cleaves the holliday junctions formed by RecG preferentially. *J Biol Chem* 289: 28376-87

Gupta S, Yeeles JT, Marians KJ (2014b) Regression of replication forks stalled by leading-strand template damage: II. Regression by RecA is inhibited by SSB. *J Biol Chem* 289: 28388-98

Haracska L, Unk I, Johnson RE, Johansson E, Burgers PMJ, Prakash S, Prakash L (2001) Roles of yeast DNA polymerases delta and zeta and of Rev1 in the bypass of abasic sites. *Genes & Development* 15: 945-954

Hashimoto Y, Ray Chaudhuri A, Lopes M, Costanzo V (2010) Rad51 protects nascent DNA from Mre11-dependent degradation and promotes continuous DNA synthesis. *Nat Struct Mol Biol* 17: 1305-11

Hauk G, McKnight JN, Nodelman IM, Bowman GD (2010) The chromodomains of the Chd1 chromatin remodeler regulate DNA access to the ATPase motor. *Mol Cell* 39: 711-23

He Y, Yan C, Fang J, Inouye C, Tjian R, Ivanov I, Nogales E (2016) Near-atomic resolution visualization of human transcription promoter opening. *Nature* 533: 359-65

Helmrich A, Ballarino M, Nudler E, Tora L (2013) Transcription-replication encounters, consequences and genomic instability. *Nat Struct Mol Biol* 20: 412-8

Higgins NP, Kato K, Strauss B (1976) A model for replication repair in mammalian cells. *J Mol Biol* 101: 417-25

Hilario J, Amitani I, Baskin RJ, Kowalczykowski SC (2009) Direct imaging of human Rad51 nucleoprotein dynamics on individual DNA molecules. *Proc Natl Acad Sci U S A* 106: 361-8

Hishiki A, Hara K, Ikegaya Y, Yokoyama H, Shimizu T, Sato M, Hashimoto H (2015) Structure of a Novel DNA-binding Domain of Helicase-like Transcription Factor (HLTF) and Its Functional Implication in DNA Damage Tolerance. *J Biol Chem* 290: 13215-23

Hopfner KP, Michaelis J (2007) Mechanisms of nucleic acid translocases: lessons from structural biology and single-molecule biophysics. *Curr Opin Struct Biol* 17: 87-95

Huang C, Gu S, Yu P, Yu F, Feng C, Gao N, Du J (2010) Deficiency of smarcal1 causes cell cycle arrest and developmental abnormalities in zebrafish. *Dev Biol* 339: 89-100

Huertas P, Aguilera A (2003) Cotranscriptionally formed DNA:RNA hybrids mediate transcription elongation impairment and transcription-associated recombination. *Mol Cell* 12: 711-21

Jaskelioff M, Van Komen S, Krebs JE, Sung P, Peterson CL (2003) Rad54p is a chromatin remodeling enzyme required for heteroduplex DNA joint formation with chromatin. *J Biol Chem* 278: 9212-8

Jeschke G (2012) DEER distance measurements on proteins. *Annu Rev Phys Chem* 63: 419-46

Jiang Y, Lucas I, Young DJ, Davis EM, Karrison T, Rest JS, Le Beau MM (2009) Common fragile sites are characterized by histone hypoacetylation. *Hum Mol Genet* 18: 4501-12

Kile AC, Chavez DA, Bacal J, Eldirany S, Korzhnev DM, Bezsonova I, Eichman BF, Cimprich KA (2015) HLTF's Ancient HIRAN Domain Binds 3' DNA Ends to Drive Replication Fork Reversal. *Mol Cell* 58: 1090-100

Kim C, Paulus BF, Wold MS (1994) Interactions of human replication protein A with oligonucleotides. *Biochemistry* 33: 14197-206

Kim JC, Mirkin SM (2013) The balancing act of DNA repeat expansions. *Curr Opin Genet Dev* 23: 280-8

Kim JL, Morgenstern KA, Griffith JP, Dwyer MD, Thomson JA, Murcko MA, Lin C, Caron PR (1998) Hepatitis C virus NS3 RNA helicase domain with a bound oligonucleotide: the crystal structure provides insights into the mode of unwinding. *Structure* 6: 89-100

Klein HL (2008) The consequences of Rad51 overexpression for normal and tumor cells. *DNA Repair (Amst)* 7: 686-93

Kolinjivadi AM, Sannino V, De Antoni A, Zadorozhny K, Kilkenny M, Techer H, Baldi G, Shen R, Ciccia A, Pellegrini L, Krejci L, Costanzo V (2017) Smarcal1-Mediated Fork Reversal Triggers Mre11-Dependent Degradation of Nascent DNA in the Absence of Brca2 and Stable Rad51 Nucleofilaments. *Mol Cell* 67: 867-881 e7

Kowalczykowski SC (2000) Initiation of genetic recombination and recombination-dependent replication. *Trends Biochem Sci* 25: 156-65

Kowalczykowski SC (2015) An Overview of the Molecular Mechanisms of Recombinational DNA Repair. *Cold Spring Harb Perspect Biol* 7

Kumagai A, Lee J, Yoo HY, Dunphy WG (2006) TopBP1 activates the ATR-ATRIP complex. *Cell* 124: 943-55

Lama G, Marrone N, Majorana M, Cirillo F, Salsano ME, Rinaldi MM (1995) Spondyloepiphyseal dysplasia tarda and nephrotic syndrome in three siblings. *Pediatr Nephrol* 9: 19-23

Lambert S, Carr AM (2013) Impediments to replication fork movement: stabilisation, reactivation and genome instability. *Chromosoma* 122: 33-45

Lawrence MS, Stojanov P, Mermel CH, Robinson JT, Garraway LA, Golub TR, Meyerson M, Gabriel SB, Lander ES, Getz G (2014) Discovery and saturation analysis of cancer genes across 21 tumour types. *Nature* 505: 495-501

Lazzaro F, Novarina D, Amara F, Watt DL, Stone JE, Costanzo V, Burgers PM, Kunkel TA, Plevani P, Muzi-Falconi M (2012) RNase H and postreplication repair protect cells from ribonucleotides incorporated in DNA. *Mol Cell* 45: 99-110

Levy O, Ptacin JL, Pease PJ, Gore J, Eisen MB, Bustamante C, Cozzarelli NR (2005) Identification of oligonucleotide sequences that direct the movement of the Escherichia coli FtsK translocase. *Proc Natl Acad Sci U S A* 102: 17618-23

Lewis R, Durr H, Hopfner KP, Michaelis J (2008) Conformational changes of a Swi2/Snf2 ATPase during its mechano-chemical cycle. *Nucleic Acids Res* 36: 1881-90

Li M, Xia X, Tian Y, Jia Q, Liu X, Lu Y, Li M, Li X, Chen Z (2019) Mechanism of DNA translocation underlying chromatin remodelling by Snf2. *Nature* 567: 409-413

Lin C, Kim JL (1999) Structure-based mutagenesis study of hepatitis C virus NS3 helicase. *J Virol* 73: 8798-807

Lin JR, Zeman MK, Chen JY, Yee MC, Cimprich KA (2011) SHPRH and HLTF act in a damage-specific manner to coordinate different forms of postreplication repair and prevent mutagenesis. *Mol Cell* 42: 237-49

Lindahl T, Barnes DE (2000) Repair of endogenous DNA damage. *Cold Spring Harb Symp Quant Biol* 65: 127-33

Liu Q, Guntuku S, Cui XS, Matsuoka S, Cortez D, Tamai K, Luo G, Carattini-Rivera S, DeMayo F, Bradley A, Donehower LA, Elledge SJ (2000) Chk1 is an essential kinase that is regulated by Atr and required for the G(2)/M DNA damage checkpoint. *Genes Dev* 14: 1448-59

Liu X, Li M, Xia X, Li X, Chen Z (2017) Mechanism of chromatin remodelling revealed by the Snf2-nucleosome structure. *Nature* 544: 440-445

Lloyd RG (1991) Conjugational recombination in resolvase-deficient ruvC mutants of Escherichia coli K-12 depends on recG. *J Bacteriol* 173: 5414-8

Lloyd RG, Buckman C (1991) Genetic analysis of the recG locus of Escherichia coli K-12 and of its role in recombination and DNA repair. *J Bacteriol* 173: 1004-11

Lloyd RG, Rudolph CJ (2016) 25 years on and no end in sight: a perspective on the role of RecG protein. *Curr Genet* 62: 827-840

Lloyd RG, Sharples GJ (1993) Dissociation of synthetic Holliday junctions by E. coli RecG protein. *EMBO J* 12: 17-22

Lopez-Girona A, Tanaka K, Chen XB, Baber BA, McGowan CH, Russell P (2001) Serine-345 is required for Rad3-dependent phosphorylation and function of checkpoint kinase Chk1 in fission yeast. *Proc Natl Acad Sci U S A* 98: 11289-94

Lou S, Lamfers P, McGuire N, Boerkoel CF (2002) Longevity in Schimke immuno-osseous dysplasia. *J Med Genet* 39: 922-5

Lucke T, Billing H, Sloan EA, Boerkoel CF, Franke D, Zimmering M, Ehrich JH, Das AM (2005) Schimke-immuno-osseous dysplasia: new mutation with weak genotype-phenotype correlation in siblings. *Am J Med Genet A* 135: 202-5

Machwe A, Karale R, Xu X, Liu Y, Orren DK (2011) The Werner and Bloom syndrome proteins help resolve replication blockage by converting (regressed) holliday junctions to functional replication forks. *Biochemistry* 50: 6774-88

Machwe A, Xiao L, Groden J, Orren DK (2006) The Werner and Bloom syndrome proteins catalyze regression of a model replication fork. *Biochemistry* 45: 13939-46

Mahdi AA, Briggs GS, Sharples GJ, Wen Q, Lloyd RG (2003) A model for dsDNA translocation revealed by a structural motif common to RecG and Mfd proteins. *EMBO J* 22: 724-34

Mahdi AA, Lloyd RG (1989) Identification of the recR locus of Escherichia coli K-12 and analysis of its role in recombination and DNA repair. *Mol Gen Genet* 216: 503-10

Manosas M, Perumal SK, Bianco PR, Ritort F, Benkovic SJ, Croquette V (2013) RecG and UvsW catalyse robust DNA rewinding critical for stalled DNA replication fork rescue. *Nat Commun* 4: 2368

Manosas M, Perumal SK, Croquette V, Benkovic SJ (2012) Direct observation of stalled fork restart via fork regression in the T4 replication system. *Science* 338: 1217-20

Marians KJ (2018) Lesion Bypass and the Reactivation of Stalled Replication Forks. *Annu Rev Biochem* 87: 217-238

Mason AC, Rambo RP, Greer B, Pritchett M, Tainer JA, Cortez D, Eichman BF (2014) A structure-specific nucleic acid-binding domain conserved among DNA repair proteins. *Proc Natl Acad Sci U S A* 111: 7618-23

McGlynn P, Lloyd RG (2001) Rescue of stalled replication forks by RecG: simultaneous translocation on the leading and lagging strand templates supports an active DNA

unwinding model of fork reversal and Holliday junction formation. *Proc Natl Acad Sci U S A* 98: 8227-34

McGlynn P, Lloyd RG (2002) Genome stability and the processing of damaged replication forks by RecG. *Trends Genet* 18: 413-9

McHaourab HS, Steed PR, Kazmier K (2011) Toward the fourth dimension of membrane protein structure: insight into dynamics from spin-labeling EPR spectroscopy. *Structure (London, England : 1993)* 19: 1549-61

McMurray CT (2010) Mechanisms of trinucleotide repeat instability during human development. *Nat Rev Genet* 11: 786-99

Mer G, Bochkarev A, Gupta R, Bochkareva E, Frappier L, Ingles CJ, Edwards AM, Chazin WJ (2000) Structural basis for the recognition of DNA repair proteins UNG2, XPA, and RAD52 by replication factor RPA. *Cell* 103: 449-56

Merrick CJ, Jackson D, Diffley JF (2004) Visualization of altered replication dynamics after DNA damage in human cells. *J Biol Chem* 279: 20067-75

Michel B, Sandler SJ (2017) Replication Restart in Bacteria. *J Bacteriol* 199

Midgley-Smith SL, Dimude JU, Taylor T, Forrester NM, Upton AL, Lloyd RG, Rudolph CJ (2018a) Chromosomal over-replication in Escherichia coli recG cells is triggered by replication fork fusion and amplified if replichore symmetry is disturbed. *Nucleic Acids Res* 46: 7701-7715

Midgley-Smith SL, Dimude JU, Taylor T, Forrester NM, Upton AL, Lloyd RG, Rudolph CJ (2018b) Chromosomal over-replication in Escherichia coli recG cells is triggered by replication fork fusion and amplified if replichore symmetry is disturbed. *Nucleic Acids Res*

Mishra S, Verhalen B, Stein RA, Wen PC, Tajkhorshid E, McHaourab HS (2014) Conformational dynamics of the nucleotide binding domains and the power stroke of a heterodimeric ABC transporter. *Elife* 3: e02740

Morimoto M, Choi K, Boerkoel CF, Cho KS (2016) Chromatin changes in SMARCAL1 deficiency: A hypothesis for the gene expression alterations of Schimke immuno-osseous dysplasia. *Nucleus* 7: 560-571

Morimoto M, Myung C, Beirnes K, Choi K, Asakura Y, Bokenkamp A, Bonneau D, Brugnara M, Charrow J, Colin E, Davis A, Deschenes G, Gentile M, Giordano M, Gormley AK, Govender R, Joseph M, Keller K, Lerut E, Levtchenko E et al. (2016) Increased Wnt and Notch signaling: a clue to the renal disease in Schimke immuno-osseous dysplasia? *Orphanet J Rare Dis* 11: 149

Morimoto M, Yu Z, Stenzel P, Clewing JM, Najafian B, Mayfield C, Hendson G, Weinkauf JG, Gormley AK, Parham DM, Ponniah U, Andre JL, Asakura Y, Basiratnia M, Bogdanovic R, Bokenkamp A, Bonneau D, Buck A, Charrow J, Cochat P et al. (2012) Reduced elastogenesis: a clue to the arteriosclerosis and emphysematous changes in Schimke immuno-osseous dysplasia? *Orphanet J Rare Dis* 7: 70

Motegi A, Liaw HJ, Lee KY, Roest HP, Maas A, Wu X, Moinova H, Markowitz SD, Ding H, Hoeijmakers JH, Myung K (2008) Polyubiquitination of proliferating cell nuclear antigen by HLTF and SHPRH prevents genomic instability from stalled replication forks. *Proc Natl Acad Sci U S A* 105: 12411-6

Najm I, Trussell RR (2001) NDMA formation in water and wastewater. *J Am Water Works Ass* 93: 92-99

Nam EA, Cortez D (2011) ATR signalling: more than meeting at the fork. *Biochem J* 436: 527-36

Neelsen KJ, Lopes M (2015) Replication fork reversal in eukaryotes: from dead end to dynamic response. *Nat Rev Mol Cell Biol* 16: 207-20

Nick McElhinny SA, Kumar D, Clark AB, Watt DL, Watts BE, Lundstrom EB, Johansson E, Chabes A, Kunkel TA (2010) Genome instability due to ribonucleotide incorporation into DNA. *Nat Chem Biol* 6: 774-81

Opresko PL, Sowd G, Wang H (2009) The Werner syndrome helicase/exonuclease processes mobile D-loops through branch migration and degradation. *PLoS One* 4: e4825

Paeschke K, Bochman ML, Garcia PD, Cejka P, Friedman KL, Kowalczykowski SC, Zakian VA (2013) Pif1 family helicases suppress genome instability at G-quadruplex motifs. *Nature* 497: 458-62

Park JS, Marr MT, Roberts JW (2002) E. coli Transcription repair coupling factor (Mfd protein) rescues arrested complexes by promoting forward translocation. *Cell* 109: 757-67

Peng CY, Graves PR, Thoma RS, Wu Z, Shaw AS, Piwnica-Worms H (1997) Mitotic and G2 checkpoint control: regulation of 14-3-3 protein binding by phosphorylation of Cdc25C on serine-216. *Science* 277: 1501-5

Petukhova G, Stratton S, Sung P (1998) Catalysis of homologous DNA pairing by yeast Rad51 and Rad54 proteins. *Nature* 393: 91-4

Pokhrel N, Caldwell CC, Corless EI, Tillison EA, Tibbs J, Jocic N, Tabei SMA, Wold MS, Spies M, Antony E (2019) Dynamics and selective remodeling of the DNA-binding domains of RPA. *Nat Struct Mol Biol* 26: 129-136

Poole LA, Cortez D (2017) Functions of SMARCAL1, ZRANB3, and HLTF in maintaining genome stability. *Crit Rev Biochem Mol Biol* 52: 696-714

Poole LA, Zhao R, Glick GG, Lovejoy CA, Eischen CM, Cortez D (2015) SMARCAL1 maintains telomere integrity during DNA replication. *Proc Natl Acad Sci U S A* 112: 14864-9

Postow L, Woo EM, Chait BT, Funabiki H (2009) Identification of SMARCAL1 as a component of the DNA damage response. *J Biol Chem* 284: 35951-61

Prado F, Aguilera A (2005) Partial depletion of histone H4 increases homologous recombination-mediated genetic instability. *Mol Cell Biol* 25: 1526-36

Pugh RA, Honda M, Leesley H, Thomas A, Lin Y, Nilges MJ, Cann IK, Spies M (2008) The iron-containing domain is essential in Rad3 helicases for coupling of ATP hydrolysis to DNA translocation and for targeting the helicase to the single-stranded DNA-double-stranded DNA junction. *J Biol Chem* 283: 1732-43

Pyle AM (2008) Translocation and unwinding mechanisms of RNA and DNA helicases. *Annu Rev Biophys* 37: 317-36

Richardson C, Stark JM, Ommundsen M, Jasin M (2004) Rad51 overexpression promotes alternative double-strand break repair pathways and genome instability. *Oncogene* 23: 546-53

Rudolf J, Rouillon C, Schwarz-Linek U, White MF (2010) The helicase XPD unwinds bubble structures and is not stalled by DNA lesions removed by the nucleotide excision repair pathway. *Nucleic Acids Res* 38: 931-41

Rudolph CJ, Upton AL, Briggs GS, Lloyd RG (2010) Is RecG a general guardian of the bacterial genome? *DNA Repair (Amst)* 9: 210-23

Rudolph CJ, Upton AL, Lloyd RG (2009) Replication fork collisions cause pathological chromosomal amplification in cells lacking RecG DNA translocase. *Mol Microbiol* 74: 940-55

Rudolph CJ, Upton AL, Stockum A, Nieduszynski CA, Lloyd RG (2013) Avoiding chromosome pathology when replication forks collide. *Nature* 500: 608-11

Saikrishnan K, Powell B, Cook NJ, Webb MR, Wigley DB (2009) Mechanistic basis of 5'-3' translocation in SF1B helicases. *Cell* 137: 849-59

Saldivar JC, Hamperl S, Bocek MJ, Chung M, Bass TE, Cisneros-Soberanis F, Samejima K, Xie L, Paulson JR, Earnshaw WC, Cortez D, Meyer T, Cimprich KA (2018) An intrinsic S/G2 checkpoint enforced by ATR. *Science* 361: 806-810

Sanchez Y, Wong C, Thoma RS, Richman R, Wu Z, Piwnica-Worms H, Elledge SJ (1997) Conservation of the Chk1 checkpoint pathway in mammals: linkage of DNA damage to Cdk regulation through Cdc25. *Science* 277: 1497-501

Sanyal M, Morimoto M, Baradaran-Heravi A, Choi K, Kambham N, Jensen K, Dutt S, Dionis-Petersen KY, Liu LX, Felix K, Mayfield C, Dekel B, Bokenkamp A, Fryssira H, Guillen-Navarro E, Lama G, Brugnara M, Lucke T, Olney AH, Hunley TE et al. (2015) Lack of IL7Ralpha expression in T cells is a hallmark of T-cell

immunodeficiency in Schimke immuno-osseous dysplasia (SIOD). *Clin Immunol* 161: 355-65

Sarin S, Javidan A, Boivin F, Alexopoulou I, Lukic D, Svajger B, Chu S, Baradaran-Heravi A, Boerkoel CF, Rosenblum ND, Bridgewater D (2015) Insights into the renal pathogenesis in Schimke immuno-osseous dysplasia: A renal histological characterization and expression analysis. *J Histochem Cytochem* 63: 32-44

Saugar I, Ortiz-Bazan MA, Tercero JA (2014) Tolerating DNA damage during eukaryotic chromosome replication. *Exp Cell Res* 329: 170-7

Savery NJ (2007) The molecular mechanism of transcription-coupled DNA repair. *Trends Microbiol* 15: 326-33

Schlacher K, Christ N, Siaud N, Egashira A, Wu H, Jasin M (2011) Double-strand break repair-independent role for BRCA2 in blocking stalled replication fork degradation by MRE11. *Cell* 145: 529-42

Sebesta M, Cooper CDO, Ariza A, Carnie CJ, Ahel D (2017) Structural insights into the function of ZRANB3 in replication stress response. *Nat Commun* 8: 15847

Sharma T, Bansal R, Haokip DT, Goel I, Muthuswami R (2015) SMARCAL1 Negatively Regulates C-Myc Transcription By Altering The Conformation Of The Promoter Region. *Sci Rep* 5: 17910

Shooter KV (1978) DNA phosphotriesters as indicators of cumulative carcinogen-induced damage. *Nature* 274: 612-4

Singleton MR, Dillingham MS, Wigley DB (2007) Structure and mechanism of helicases and nucleic acid translocases. *Annu Rev Biochem* 76: 23-50

Singleton MR, Scaife S, Wigley DB (2001) Structural analysis of DNA replication fork reversal by RecG. *Cell* 107: 79-89

Smolle MM (2018) Chd1 bends over backward to remodel. *Nat Struct Mol Biol* 25: 2-3

Sogo JM, Lopes M, Foiani M (2002) Fork reversal and ssDNA accumulation at stalled replication forks owing to checkpoint defects. *Science* 297: 599-602

Sorensen CS, Syljuasen RG (2012) Safeguarding genome integrity: the checkpoint kinases ATR, CHK1 and WEE1 restrain CDK activity during normal DNA replication. *Nucleic Acids Res* 40: 477-86

Sparks JL, Chon H, Cerritelli SM, Kunkel TA, Johansson E, Crouch RJ, Burgers PM (2012) RNase H2-initiated ribonucleotide excision repair. *Mol Cell* 47: 980-6

Stanley LK, Seidel R, van der Scheer C, Dekker NH, Szczelkun MD, Dekker C (2006) When a helicase is not a helicase: dsDNA tracking by the motor protein EcoR124I. *EMBO J* 25: 2230-9

Stasiak A, Egelman EH (1994) Structure and function of RecA-DNA complexes. *Experientia* 50: 192-203

Stein RA, Beth AH, Hustedt EJ (2015) A Straightforward Approach to the Analysis of Double Electron-Electron Resonance Data. *Methods Enzymol* 563: 531-67

Storm PK, Hoekstra WP, de Haan PG, Verhoef C (1971) Genetic recombination in Escherichia coli. IV. Isolation and characterization of recombination-deficiency mutants of Escherichia coli K12. *Mutat Res* 13: 9-17

Suhasini AN, Brosh RM, Jr. (2010) Mechanistic and biological aspects of helicase action on damaged DNA. *Cell Cycle* 9: 2317-29

Sundaramoorthy R, Hughes AL, El-Mkami H, Norman DG, Ferreira H, Owen-Hughes T (2018) Structure of the chromatin remodelling enzyme Chd1 bound to a ubiquitinylated nucleosome. *Elife* 7

Sung P, Prakash L, Matson SW, Prakash S (1987) RAD3 protein of Saccharomyces cerevisiae is a DNA helicase. *Proc Natl Acad Sci U S A* 84: 8951-5

Taglialatela A, Alvarez S, Leuzzi G, Sannino V, Ranjha L, Huang JW, Madubata C, Anand R, Levy B, Rabadan R, Cejka P, Costanzo V, Ciccia A (2017) Restoration of Replication Fork Stability in BRCA1- and BRCA2-Deficient Cells by Inactivation of SNF2-Family Fork Remodelers. *Mol Cell* 68: 414-430 e8

Tanaka S, Diffley JF (2002) Deregulated G1-cyclin expression induces genomic instability by preventing efficient pre-RC formation. *Genes Dev* 16: 2639-49

Tanaka T, Masai H (2006) Stabilization of a stalled replication fork by concerted actions of two helicases. *J Biol Chem* 281: 3484-93

Tatsumi K, Strauss B (1978) Production of DNA bifilarly substituted with bromodeoxyuridine in the first round of synthesis: branch migration during isolation of cellular DNA. *Nucleic Acids Res* 5: 331-47

Tercero JA, Diffley JF (2001) Regulation of DNA replication fork progression through damaged DNA by the Mec1/Rad53 checkpoint. *Nature* 412: 553-7

Theriot CA, Hegde ML, Hazra TK, Mitra S (2010) RPA physically interacts with the human DNA glycosylase NEIL1 to regulate excision of oxidative DNA base damage in primer-template structures. *DNA Repair (Amst)* 9: 643-52

Thoma NH, Czyzewski BK, Alexeev AA, Mazin AV, Kowalczykowski SC, Pavletich NP (2005) Structure of the SWI2/SNF2 chromatin-remodeling domain of eukaryotic Rad54. *Nat Struct Mol Biol* 12: 350-6

Unk I, Hajdu I, Fatyol K, Hurwitz J, Yoon JH, Prakash L, Prakash S, Haracska L (2008) Human HLTF functions as a ubiquitin ligase for proliferating cell nuclear antigen polyubiquitination. *Proc Natl Acad Sci U S A* 105: 3768-73

Vujanovic M, Krietsch J, Raso MC, Terraneo N, Zellweger R, Schmid JA, Taglialatela A, Huang JW, Holland CL, Zwicky K, Herrador R, Jacobs H, Cortez D, Ciccia A, Penengo L, Lopes M (2017) Replication Fork Slowing and Reversal upon DNA Damage Require PCNA Polyubiquitination and ZRANB3 DNA Translocase Activity. *Mol Cell* 67: 882-890 e5

Walworth NC, Bernards R (1996) rad-dependent response of the chk1-encoded protein kinase at the DNA damage checkpoint. *Science* 271: 353-6

Warren GM, Stein RA, McHaourab HS, Eichman BF (2018) Movement of the RecG Motor Domain upon DNA Binding Is Required for Efficient Fork Reversal. *Int J Mol Sci* 19

Wasserman MR, Schauer GD, O'Donnell ME, Liu SX (2019) Replisome Preservation by a Single-Stranded DNA Gate in the CMG Helicase. *Biophysical Journal* 116: 76a-76a

West SC (1997) Processing of recombination intermediates by the RuvABC proteins. *Annu Rev Genet* 31: 213-44

Weston R, Peeters H, Ahel D (2012) ZRANB3 is a structure-specific ATP-dependent endonuclease involved in replication stress response. *Genes Dev* 26: 1558-72

Whitby MC, Ryder L, Lloyd RG (1993) Reverse branch migration of Holliday junctions by RecG protein: a new mechanism for resolution of intermediates in recombination and DNA repair. *Cell* 75: 341-50

Whitehouse I, Stockdale C, Flaus A, Szczelkun MD, Owen-Hughes T (2003) Evidence for DNA translocation by the ISWI chromatin-remodeling enzyme. *Mol Cell Biol* 23: 1935-45

Willhoft O, Ghoneim M, Lin CL, Chua EYD, Wilkinson M, Chaban Y, Ayala R, McCormack EA, Ocloo L, Rueda DS, Wigley DB (2018) Structure and dynamics of the yeast SWR1-nucleosome complex. *Science* 362

Windgassen TA, Keck JL (2016) An aromatic-rich loop couples DNA binding and ATP hydrolysis in the PriA DNA helicase. *Nucleic Acids Res* 44: 9745-9757

Xu X, Vaithiyalingam S, Glick GG, Mordes DA, Chazin WJ, Cortez D (2008) The basic cleft of RPA70N binds multiple checkpoint proteins, including RAD9, to regulate ATR signaling. *Mol Cell Biol* 28: 7345-53

Yan L, Wang L, Tian Y, Xia X, Chen Z (2016) Structure and regulation of the chromatin remodeller ISWI. *Nature* 540: 466-469

Yan L, Wu H, Li X, Gao N, Chen Z (2019) Structures of the ISWI-nucleosome complex reveal a conserved mechanism of chromatin remodeling. *Nat Struct Mol Biol*

Ye X, Franco AA, Santos H, Nelson DM, Kaufman PD, Adams PD (2003) Defective S phase chromatin assembly causes DNA damage, activation of the S phase checkpoint, and S phase arrest. *Mol Cell* 11: 341-51

Yuan J, Ghosal G, Chen J (2009) The annealing helicase HARP protects stalled replication forks. *Genes Dev* 23: 2394-9

Yuan J, Ghosal G, Chen J (2012) The HARP-like domain-containing protein AH2/ZRANB3 binds to PCNA and participates in cellular response to replication stress. *Mol Cell* 47: 410-21

Yuce O, West SC (2013) Senataxin, defective in the neurodegenerative disorder ataxia with oculomotor apraxia 2, lies at the interface of transcription and the DNA damage response. *Mol Cell Biol* 33: 406-17

Zegeye ED, Balasingham SV, Laerdahl JK, Homberset H, Kristiansen PE, Tonjum T (2014) Effects of conserved residues and naturally occurring mutations on Mycobacterium tuberculosis RecG helicase activity. *Microbiology* 160: 217-227

Zellweger R, Dalcher D, Mutreja K, Berti M, Schmid JA, Herrador R, Vindigni A, Lopes M (2015) Rad51-mediated replication fork reversal is a global response to genotoxic treatments in human cells. *J Cell Biol* 208: 563-79

Zeman MK, Cimprich KA (2014) Causes and consequences of replication stress. *Nat Cell Biol* 16: 2-9

Zhao W, Vaithiyalingam S, San Filippo J, Maranon DG, Jimenez-Sainz J, Fontenay GV, Kwon Y, Leung SG, Lu L, Jensen RB, Chazin WJ, Wiese C, Sung P (2015) Promotion of BRCA2-Dependent Homologous Recombination by DSS1 via RPA Targeting and DNA Mimicry. *Mol Cell* 59: 176-87

Zittel MC, Keck JL (2005) Coupling DNA-binding and ATP hydrolysis in Escherichia coli RecQ: role of a highly conserved aromatic-rich sequence. *Nucleic Acids Res* 33: 6982-91

Zou L, Elledge SJ (2003) Sensing DNA damage through ATRIP recognition of RPA-ssDNA complexes. *Science* 300: 1542-8